PB82-234329

Evaluation of Short-Term NO2 Plume Models for Point Sources. Volume 1: Technical Discussion

Systems Applications, Inc.
San Rafael, CA

Prepared for

Environmental Sciences Research Lab.
Research Triangle Park, NC

Dec 81

U.S. Department of Commerce
National Technical Information Service
NTIS

EPA-600/4-81-079

PB82-234329

EVALUATION OF SHORT-TERM NO_2 PLUME MODELS FOR POINT SOURCES
Volume 1. Technical Discussion

by

M. A. Yocke
D. A. Stewart
J. Johnson
R. J. Frost

Systems Applications, Incorporated
950 Northgate Drive
San Rafael, California 94903

Contract No. 68-02-2775

Project Officer

Kenneth L. Schere
Meteorology and Assessment Division
Environmental Sciences Research Laboratory
Research Triangle Park, North Carolina 27711

ENVIRONMENTAL SCIENCES RESEARCH LABORATORY
OFFICE OF RESEARCH AND DEVELOPMENT
U.S. ENVIRONMENTAL PROTECTION AGENCY
RESEARCH TRIANGLE PARK, NORTH CAROLINA 27711

REPRODUCED BY
NATIONAL TECHNICAL
INFORMATION SERVICE
U.S. DEPARTMENT OF COMMERCE
SPRINGFIELD, VA 22161

TYPING GUIDE SHEET
BEGIN FIRST LINE OF TEXT HERE
CENTER OF PAGE
TOP OF IMAGE AREA
DROPPED HEAD BEGIN SECTIONS HERE
9-1/8"
BEGIN LAST LINE OF TEXT
3/8"
PAGE NUMBER
BOTTOM OF IMAGE AREA; OUTSIDE DIMENSION FOR TABLES AND ILLUSTRATIONS
EPA-287 (Cin.)
(4-76)

TECHNICAL REPORT DATA

(Please read Instructions on the reverse before completing)

1. REPORT NO.
EPA-600/4-81-079

2.

3. RECIPIENT'S ACCESSION NO.
PB82 234329

4. TITLE AND SUBTITLE
EVALUATION OF SHORT-TERM NO_2 PLUME MODELS FOR POINT SOURCES
Volume 1. Technical Discussion

5. REPORT DATE
December 1981

6. PERFORMING ORGANIZATION CODE

7. AUTHOR(S)
M.A. Yocke, D.A. Stewart, J. Johnson and R.J. Frost

8. PERFORMING ORGANIZATION REPORT NO.

9. PERFORMING ORGANIZATION NAME AND ADDRESS
Systems Applications, Incorporated
950 Northgate Drive
San Rafael, California 94903

10. PROGRAM ELEMENT NO.
1AA603A AA-050 (FY-79)

11. CONTRACT/GRANT NO.
Contract No. 68-02-2775

12. SPONSORING AGENCY NAME AND ADDRESS
Environmental Sciences Research Laboratory - RTP, NC
Office of Research and Development
U.S. Environmental Protection Agency
Research Triangle Park, NC 27711

13. TYPE OF REPORT AND PERIOD COVERED
Final 8/77 - 7/79

14. SPONSORING AGENCY CODE
EPA/600/09

15. SUPPLEMENTARY NOTES

16. ABSTRACT

Models for predicting short-term NO_2 concentrations are discussed, and several (RPM-II, TCM, OLM, and CNOM) are selected for evaluation. The MISTT data, collected in 1976, were to be used to evaluate the models, but careful scrutiny of the data base revealed certain deficiencies relative to the data needs of the models. These deficiencies preclude a strict evaluation of the performance of the models, but simple fitting techniques were used to compensate for input data deficiencies. The models are shown to perform reasonably well using simple statistical measures of performance. The performance of the models is also evaluated using a "restricted" data base (i.e., one that could be derived from NSW, local, or state agency data sources only), and model performance is shown to be poorer with the "unrestricted" data base.

17. KEY WORDS AND DOCUMENT ANALYSIS

a. DESCRIPTORS	b. IDENTIFIERS/OPEN ENDED TERMS	c. COSATI Field/Group

18. DISTRIBUTION STATEMENT
RELEASE TO PUBLIC

19. SECURITY CLASS *(This Report)*
UNCLASSIFIED

20. SECURITY CLASS *(This page)*
UNCLASSIFIED

21. NO. OF PAGES
194

22. PRICE

EPA Form 2220-1 (9-73)

DISCLAIMER

This report has been reviewed by the Environmental Sciences Research Laboratory, U.S. Environmental Protection Agency, and approved for publication. Approval does not signify that the contents necessarily reflect the views and policies of the U.S. Environmental Protection Agency, nor does mention of trade names or commercial products constitute endorsement or recommendation for use.

ABSTRACT

Models for predicting short-term NO_2 concentrations are discussed, and several (RPM-II, TCM, OLM, and CNOM) are selected for evaluation. The MISTT data, collected in 1976, were to be used to evaluate the models, but careful scrutiny of the data base revealed certain deficiencies relative to the data needs of the models. These deficiencies preclude a strict evaluation of the performance of the models, but simple fitting techniques were used to compensate for input data deficiencies. The models are shown to perform reasonably well using simple statistical measures of performance. The performance of the models is also evaluated using a "restricted" data base (i.e., one that could be derived from NSW, local, or state agency data sources only), and model performance is shown to be poorer with the "unrestricted" data base.

CONTENTS

Abstract iii

List of Illustrations vi

List of Tables viii

I Introduction 1

II Review of Alternative Modeling Approaches 3

- A. Empirico-Mechanistic Models 3
- B. Deterministic-Mechanistic Models 4

III Selection of Models for This Study 22

IV Selection of Case Studies from MISTT Data 24

- A. Selection of 10 Case Study Days 24
- B. Preparation of Model Inputs 26

V Evaluation of RPM-II and Simple Model Performance . . 56

- A. Procedures for the Specification of Input Data . . 56
- B. Model Input with the Unrestricted Data Set 68
- C. Model Input with the Restricted Data Set 68
- D. Results 75
- E. Discussion of Results 75

VI Conclusions 111

VII Recommendations 113

References. 114

Appendices

- A. An Improved Version of the Reactive Plume Model (RPM-II) 117
- B. RPM-I Sensitivity Study 130
- C. A Sensitivity Study of the Reactive Plume Model (RPM-I)--Theoretical Basis and Procedures 154

Preceding page blank

FIGURES

1 Schematic of cell expansion as a function of downwind distance in RPM-II 10

2 Schematic representation of the trajectory model concept. 12

3 Conjoint model schematic: a reactive plume model supplies a boundary condition for an urban grid model 19

4 Conjoint model schematic: a reactive plume model is nested within an urban grid modeling region 20

5 Positions and widths of Labadie plumes on the 10 case study days 28

6 Estimates of the spread of the Labadie plume as a function of altitude and distance from the Labadie power plant. 42

7 Estimated NO_2 photolysis rate constant as a function of solar zenith angle for unpolluted clear skies case. 65

8 Scattergram comparison of concentration values predicted by RPM-II with measured values for unrestricted cases. 88

9 Scattergram comparison of NO_2 concentration values predicted by TCM with measured values for unrestricted cases. 91

10 Scattergram comparison of NO_2 concentration values predicted by OLM with measured values for unrestricted cases. 92

11 Scattergram comparison of NO_2 concentration values predicted by CNOM with measured values for unrestricted cases 93

12 Observed plume profiles for 30 July 1976 95

13 Concentration profiles predicted by RPM-II for 30 July 1976, using the unrestricted data set 97

14 Concentration profiles predicted by RPM-II with reduced hydrocarbons for 30 July 1976 103

15 Concentration profiles predicted by RPM-II with reduced plume dispersion rates for 30 July 1976. 105

TABLES

Number Page

1 Summary of 1976 MISTT Data Base 25

2 Ranges of Labadie Plume Widths and Depths on 5 and 14 July 1976 54

3 Model Input Data for Unrestricted Data Set 69

4 Model Input for Restricted Data Set 74

5 Measured Concentrations and Concentrations Predicted by RPM-II, TCM, OLM, and CNOM for Unrestricted Cases 76

6 Measured Concentrations and Concentrations Predicted by RPM-II, TCM, OLM, and CNOM for Restricted Cases 82

7 Computed Statistical Parameters for RPM-II, TCM, OLM, and CNOM NO_2 Predictions for Unrestricted Cases 86

8 Computed Statistical Parameters for RPM-II, TCM, OLM, and CNOM NO_2 Predictions for Restricted Cases 109

I INTRODUCTION

The burning of fossil fuels by automobiles, power plants, and refineries produces appreciable amounts of oxides of nitrogen (NO_x), which are then released into the atmosphere. Although these emissions consist primarily of relatively harmless nitric oxide (NO), under suitable conditions, such as in the presence of reactive hydrocarbons and sunlight, nitric oxide can be oxidized to form nitrogen dioxide (NO_2). Nitrogen dioxide, a red-brown gas,* is a strong oxidizing agent and, as a consequence, can have potentially harmful effects. According to an epidemiological study carried out by Shy et al. (1970a, 1970b) in Chattanooga, Tennessee, the respiratory performance of children was found to be adversely affected by high NO_2 levels. In fact, long-term exposure to ambient NO_2 concentrations of between 117 and 205 $\mu g/m^3$ was associated with a higher incidence (18 percent higher) of respiratory disease. This study probably forms the basis for the promulgation of the federal primary NO_2 standard, which specifies that the annual average NO_2 concentration is not to exceed 100 $\mu g/m^3$.

Recently, however, there has been some concern about the effect of short-term peak NO_2 concentrations on the frequency and severity of acute respiratory disease. For example, several experimental studies were performed exposing animals to nitrogen dioxide of varying concentration levels and durations and then to viruses or bacteria (Ehrlich, 1966; Coffin et al., 1968, 1972). The results of these studies showed that the magnitude of the short-term peak NO_2 concentration had a significantly greater influence than either the duration or frequency of exposure. These conclusions were also essentially confirmed by epidemiological studies subsequently conducted in Chattanooga, Tennessee (Riggan, 1976), which suggest that repeated short-term exposures of 228 to 815 $\mu g/m^3$ of nitrogen dioxide may contribute to the incidence of acute respiratory disease in the absence of excessive long-period exposure.

---

* The brownish color of urban photochemical smog is attributed to nitrogen dioxide.

In view of the importance of these studies, it is not surprising that the U.S. Environmental Protection Agency (EPA) is giving serious consideration to promulgating short-term NO_2 air quality regulations. Part of this consideration is the review of techniques that can be used to predict short-term (about 1 hour) average, ground-level, NO_2 concentrations. Specific attention is being given to the ability to predict NO_2 impacts due to NO_x emissions from large point sources (e.g., power plants and other large combustion processes).

At the request of the EPA, Systems Applications, Incorporated (SAI) has undertaken a review of models that can be used to predict ground-level NO_2 concentration impacts from point sources and has applied selected models to the Midwest Interstate Sulfur Transformation and Transport (MISTT) data base (a large aerometric and meteorological data base collected near St. Louis) for the purpose of evaluating their performance. The MISTT data base was selected by EPA because the MISTT program involved a large urban and point source monitoring effort that included a significant number of aircraft plume measurements. At the start of this study, the usefulness of the MISTT data base for applying and evaluating NO_2 prediction techniques was unknown, because the data had been designed to characterize plume sulfur and aerosol transport and transformations, not to support reactive plume modeling. The limitations of the MISTT data base relative to the objectives of this study are discussed in Chapter IV.

Chapter II presents a review of pertinent modeling approaches and Chapter III delineates those models selected by application to the MISTT data base. Efforts spent on preparing the MISTT data for this study are covered in Chapter III, along with the selection of case study days. Results of the model applications and evaluations are presented in Chapter V, followed by conclusions in Chapter VI. Computer plots of the MISTT data, which were generated in the data preparation phase of this study, are presented in Volume II of this report (under separate cover).

II REVIEW OF ALTERNATIVE MODELING APPROACHES

A variety of NO_2 estimation techniques--ranging from simple empirico-mechanistic approaches to sophisticated, grid-based, photochemical advection-diffusion models--are available for application to NO_x emissions problems. This chapter discusses several types of techniques and specific examples of each type. The range of applicability of each type of technique is also discussed.

The scope of this study requires that the models to be considered must incorporate at least the following features:

- A state-of-the-art atmospheric chemical transformation mechanism that includes, but is not necessarily limited to, nonmethane hydrocarbons, NO, NO_2, O_3, SO_2, and $SO_4^{=}$.
- A methodology for the treatment of the spatial and temporal variations of wind fields, diffusivity fields, and mixing heights.
- A methodology for the treatment of plume buoyancy and entrainment.
- An efficient and accurate numerical integration technique.

It was also agreed that only currently operational and nonproprietary models would be considered. Furthermore, the extremely large data requirements and heavy computation and data preparation costs of some of the more sophisticated models preclude their application and subsequent evaluation in this study.

A. EMPIRICO-MECHANISTIC MODELS

Empirico-mechanistic models account only for the principal physical and chemical phenomena affecting pollutant concentrations. Important parameters such as wind speed, mixing depth, emissions rates, and chemical reactions are incorporated into a basic one-dimensional, steady-state dispersion equation. Then coefficients or exponents of these parameters in the model equation are determined by statistical correlation of the predictions with many observations. A model of this type was developed by White (1977) to predict ozone in a power plant plume. It assumes photostationarity and conservation of NO_x and oxidant. Dispersion is treated by statistical correlations with observed plume concentration data. Because of the equilibrium among NO, NO_2, and O_3, the model could also be adapted for predicting NO_2 concentrations downwind of a point source. However, such models may not be suitable for application to situations other than those for which they were specifically derived. Moreover, the conservation of NO_x and oxidant assumptions are usually valid only during the first phases (the first 30 to 60 minutes) of plume advection and diffusion, because beyond these times oxidation of NO to NO_2 by hydrocarbons and conversion to nitrates can be important.

B. DETERMINISTIC-MECHANISTIC MODELS

Within the deterministic-mechanistic category of models we include simple equilibrium models, reactive plume models, grid models, and conjoint models. Each technique is discussed in this section.

1. Simple Equilibrium Models

In a fashion similar to the empirico-mechanistic models, the equilibrium models account for only the principal physical and chemical phenomena affecting pollutant concentrations. However, empiricism does not enter the treatment of any processes for a particular site. Rather, the equilibrium relationship among NO, NO_2, and O_3 is used in conjunction with the assumptions of oxidant and NO_x conservation to simplify the chemical kinetics. NO_x conservation is expressed as:

$$\frac{d[NO_2]}{dt} + \frac{d[NO]}{dt} = 0 \quad . \qquad (1)$$

yielding

$$[NO] + [NO_2] = [NO]_{initial} + [NO_2]_{initial} \quad . \tag{2}$$

Similarly, oxidant conservation can be written as follows:

$$\frac{d[NO_2]}{dt} + \frac{d[O_3]}{dt} + \frac{d[O]}{dt} = 0 \tag{3}$$

so,

$$[NO_2] + [O_3] = [NO_2]_{initial} + [O_3]_{initial} \quad . \tag{4}$$

With equations (2) and (4) and the photostationary relationship,

$$[O_3] = \frac{k_1^{*}[NO_2]}{k_3^{\dagger}[NO]} \quad , \tag{5}$$

the two equations

and

$$[NO] + [NO_2] = \alpha[NO_x]_{initial} + (1-\alpha)[NO_x]_{background} \tag{6}$$

$$[NO_2] + [O_3] = \alpha\left\{[NO_2] + [O_3]\right\}_{initial} + (1-\alpha)\left\{[NO_2] + [O_3]\right\}_{background} \tag{7}$$

can be solved for $[NO_2]$ to yield:

$$[NO_2] = \frac{C_2(\alpha) + C_1(\alpha) + k_{13} \pm \left\{\left[C_2(\alpha) + C_1(\alpha) + k_{13}\right]^2 - 4\ C_1(\alpha)\,C_2(\alpha)\right\}^{1/2}}{2} \tag{8}$$

where

---

* k_1 is the NO_2 photolysis rate constant.

† k_3 is the rate constant for the reaction $O_3 + NO \rightarrow NO_2 + O_2$.

$k_{13} = k_1/k_3$,

$C_1(\alpha) = \alpha\{[NO_2] + [O_3]\}_{initial} + (1-\alpha)\{[NO_2] + [O_3]\}_{background}$,

$C_2(\alpha) = \alpha[NO_x]_{initial} + (1-\alpha)[NO_x]_{background}$,

k_1, k_3 = rate constants.

In these equations α is a dilution factor* that can be obtained, for example, through tracer measurements or by assuming that Gaussian dispersion applies.

This treatment, which is commonly called the "conservation of NO_x and oxidant method" (CNOM), has many features similar to the method reported by Richards and Peters (1977). It suffers the limitation that beyond a few kilometers from the source its simplified treatment of chemistry is invalid in hydrocarbon-rich environments. In addition, any deficiencies in the dispersion parameter computations--the Gaussian dispersion relationship, for example, has many known limitations--will be reflected in predicted NO_2 concentrations.

There are even simpler equilibrium models. One such simplification is known as the oxidant limiting method (OLM). The OLM assumes that NO_2 concentrations in the plume are equal to the background O_3 plus some small fraction of the emitted NO concentration, expressed in the relationship:

$$[NO_2] = [O_3]_{background} + \alpha C_3[NO]_{initial} + (1-\alpha)[NO_2]_{background} \quad . \quad (9)$$

The term involving the initial NO concentrations is intended to account for the thermal oxidation of NO to NO_2, which occurs in and near the stack (where C_3 is the percent of emitted NO converted by thermal oxidation to NO_2). The dependence on the background O_3 is an acknowledgement that one NO_2 molecule is formed for every reaction of O_3 and NO molecules and that NO_2

---

* α is defined as the ratio of the plume concentration at some downwind point (minus background or ambient concentration) divided by the initial plume or stack concentration. α can be determined in a number of ways including the use of a standard Gaussian dispersion equation, and does permit treatment of non-homogeneous plume concentration distributions.

thus may be limited by the background O_3 in an NO-rich plume. However, it does not explicitly account for diffusion, entrainment, and the photostationary relationship. Another simplification, called total or partial conversion (TCM or PCM), assumes that all or some fraction of the emitted NO_x is ultimately converted to NO_2; thus,

$$[NO_2] = \alpha \cdot C_4 \cdot [NO_x]_{initial} + (1-\alpha)[NO_2]_{background} \quad , \tag{10}$$

where $C_4 \leq 100$ percent. Obviously, this simplification is valid only at large downwind distances where a large amount of dispersion has occurred.

The TCM, PCM, and OLM suffer the same deficiencies as CNOM; moreover, these methods are further limited by their own, more restrictive, assumptions. However, in many cases they are useful screening procedures. They can be used quickly and inexpensively to obtain an estimate of the magnitude of the potential NO_2 impacts.

2. Reactive Plume Models

Reactive plume models are intended to focus on the chemistry and diffusion of reactive pollutants from individual point sources. They can treat more complex time-varying photochemistry and diffusion than can the simple equilibrium models, and they provide better spatial and temporal resolution of concentration distributions than do grid models, which are discussed later. The most important advantage of reactive plume models is their potential to accommodate large chemical kinetic mechanisms. This capability allows proper consideration of the oxidation of entrained ambient hydrocarbons and NO_x. The basis of the formation of most sophisticated air quality models, including reactive plume models, is the solution of some form of the atmospheric diffusion equation:

$$\frac{\partial c_i}{\partial t} + \frac{\partial (uC_i)}{\partial x} + \frac{\partial (vC_i)}{\partial y} + \frac{\partial (wC_i)}{\partial z} = \frac{\partial}{\partial x} K_H \frac{\partial C_i}{\partial x} + \frac{\partial}{\partial y} K_H \frac{\partial C_i}{\partial y} + \frac{\partial}{\partial z} K_V \frac{\partial C_i}{\partial z} + R_i + S_i \quad , \tag{11}$$

where

C_i = concentration of species i,
u, v, w = wind velocity components along x, y, and z Cartesian coordinate axes,
K_H = horizontal diffusivity,
K_V = vertical diffusivity,
R_i = chemical reaction term,
S_i = emissions term,
t = time.

Of the nonproprietary reactive plume models available for use in predicting NO_2 concentrations, the most notable are DeBower's Reactive Plume Model and SAI's RPM-II. The model developed by DeBower (1976) uses a semi-Lagrangian approach. Advection-diffusion processes are separated from chemical processes in the solution procedure. The plume is assumed to be composed of many "mini-plumes" that advect and diffuse separately. The pollutant concentration at any point is estimated by adding the concentrations at that point in the mini-plumes. Wind and temperature fields must be provided for the model. Diffusivities are assumed to be those specified by Gifford (1961). Virtual plume height information must be supplied for the model. In its most recently published configuration, the model considers only the species NO, NO_2, and O_3 in a photostationary state; conceivably, however, it could be extended to include a state-of-the-art chemical mechanism. It should be mentioned that the fundamental assumption that the plume is composed of numerous "mini-plumes" is of questionable validity, as was noted by DeBower. The problem is that the diffusivity or dispersion rate of the small "mini-plumes" is likely to be much different from that of the overall plume (Csanady, 1973), for diffusivity is a function of plume size. This difference in diffusivity could lead to large errors in the model's treatment of dispersion and entrainment of ambient pollutants into the plume. The magnitudes of the errors that might result from this problem are hard to estimate and no comparisons against field data have been reported.

As a generalization of the single box concept, SAI's RPM-II (Liu, Stewart, and Roth, 1978) considers an array of well mixed reactors or cells across the plume, each of which moves downwind and disperses along the mean-wind trajectory (see Figure 1). The model can accommodate temporally and spatially varying wind speeds, reaction rates, ambient concentration levels, and dispersion or entrainment rates. As currently configured, RPM-II uses a state-of-the-art 68-step Carbon-Bond photochemical reaction mechanism developed by Whitten and Hogo (1977); other mechanisms can be easily substituted for the Carbon-Bond Mechanism if desired. The most severe limitation of a sophisticated reactive plume model like RPM-II is the requirement for valid ambient concentration estimates of reactants along the plume trajectory. These must be measured, predicted or hypothesized. Ambient hydrocarbons are extremely difficult to characterize even by measurement, yet predictions of plume NO_2 are very sensitive to hydrocarbons. The user has several alternative methods for estimating ambient concentrations:

> Allow RPM-II to compute its own time-varying ambient concentrations based on:
  - Sunlight intensity.
  - An initial mix of ambient pollutants (an option included in the RPM-II computer model).

> Use a regional scale photochemical grid model (discussed below) to compute ambient concentrations.

> Use best available measurements of temporal ambient concentration levels.

Like most other operational dispersion models, RPM-II is also limited by the user's ability to properly specify wind speeds and dispersion rates, especially in complex terrain applications. But despite such limitations, sophisticated reactive plume models like RPM-II are clearly technically superior to either the empirico-mechanistic or equilibrium approaches to NO_2 estimation that were discussed above. Furthermore, reactive plume

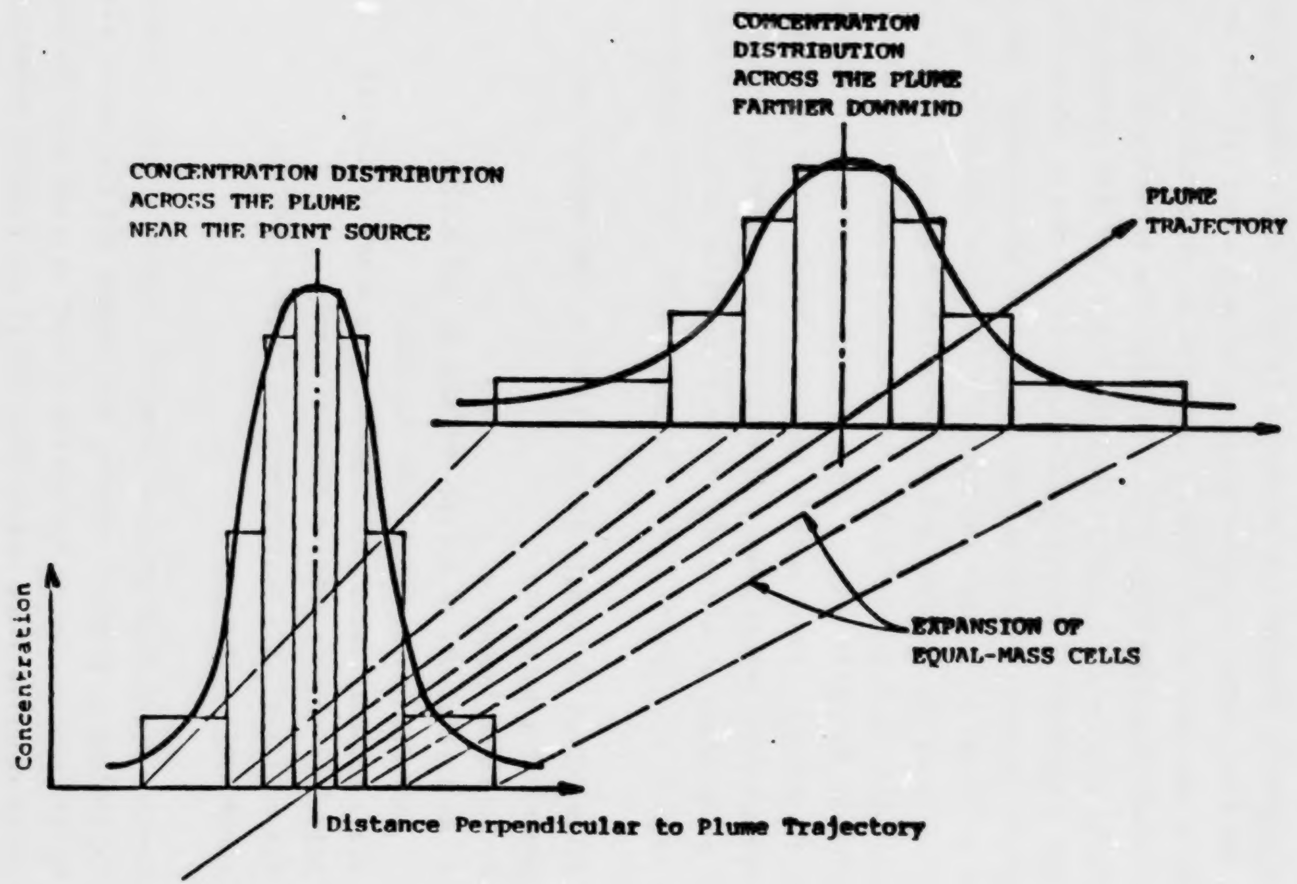
CONCENTRATION DISTRIBUTION ACROSS THE PLUME FARTHER DOWNWIND
CONCENTRATION DISTRIBUTION ACROSS THE PLUME NEAR THE POINT SOURCE
PLUME TRAJECTORY
EXPANSION OF EQUAL-MASS CELLS
Concentration
Distance Perpendicular to Plume Trajectory

Figure 1. Schematic of cell expansion as a function of downwind distance in RPM-II.

models hold considerably greater potential for future refinement than do the simpler approaches, though their computing and data requirements are larger.

3. Trajectory Models

Like reactive plume models, trajectory models are based on the atmospheric diffusion equation (equation 9). These models simulate a hypothetical column or parcel of air, using what is sometimes called a moving-coordinate approach to describe pollutant transport. From a specified starting point, the column moves under the influence of the local meteorological conditions. For example, if the wind speed is 2 miles per hour, then after one hour the column would move 2 miles from its original position in the direction in which the wind is flowing. Emissions are injected into the parcel and undergo vertical mixing. Concurrently, chemical reactions take place in the parcel. Figure 2 represents this trajectory model concept schematically. This approach resembles reactive plume modeling in that a wind trajectory is followed, but it differs in other important respects. These differences are attributable to the several basic assumptions that must be invoked in formulating a trajectory model (Seinfeld, Hecht, and Roth, 1973):

> The horizontal diffusion of pollutants into the air parcel along its sides can be neglected (presuming no concentration variations lateral to the trajectory or within the plume).
> Emissions from sources encountered can be explicitly treated.
> The volume of the parcel is constant and is unaffected by atmospheric wind or turbulence patterns.

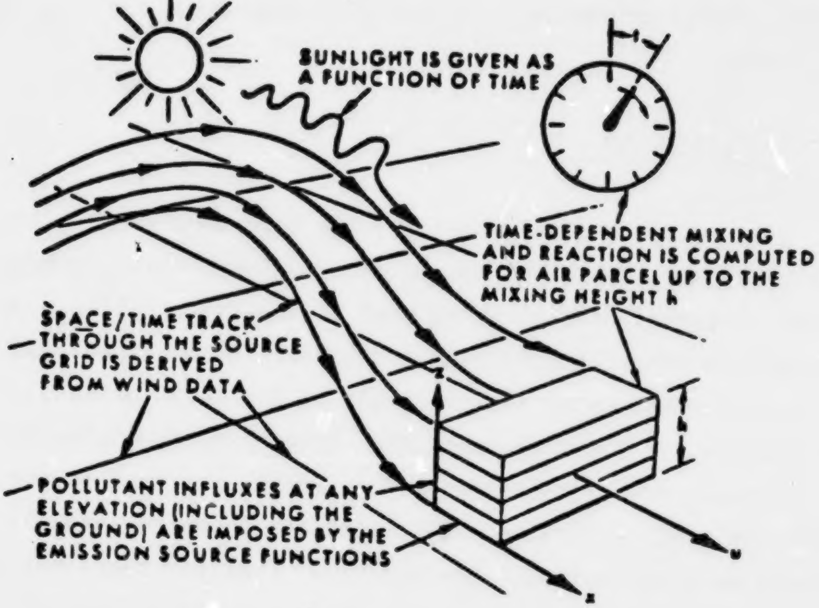
SUNLIGHT IS GIVEN AS A FUNCTION OF TIME
TIME-DEPENDENT MIXING AND REACTION IS COMPUTED FOR AIR PARCEL UP TO THE MIXING HEIGHT h
SPACE/TIME TRACK THROUGH THE SOURCE GRID IS DERIVED FROM WIND DATA
POLLUTANT INFLUXES AT ANY ELEVATION (INCLUDING THE GROUND) ARE IMPOSED BY THE EMISSION SOURCE FUNCTIONS
z
h
x
y

Source: Eschenroeder and Martinez (1971).

Figure 2. Schematic representation of the trajectory model concept.

In general, trajectory models require the same input data as do reactive plume models, except that dispersion data are not required because horizontal dispersion is not considered by the model. Trajectory model performance, like that of reactive plume models, is limited by the user's ability to properly specify temporally and spatially varying winds, especially in complex terrain situations.

One of the most sophisticated trajectory models available is DIFKIN/ARTSIM/ELSTAR, which was developed by Environmental Research and Technology (Eschenroeder, 1975). It has recently been used to model reactive plumes from point and area sources (Taylor, 1977). For application to point sources, the pollutants in a plume emitted from a point source are assumed to mix initially within the large volume of air in the first layer of DIFKIN/ARTSIM/ELSTAR's hypothetical air column. In a short time (i.e., a short distance downwind), the pollutants are mixed completely throughout the entire column. No additional mass of either clean air or pollutants is added to the column during a model run unless the column's trajectory passes directly over another pollutant source on the ground. This is an unrealistic treatment of the dispersion of a point source plume for two reasons. First, the air column in which emissions are mixed is of an arbitrary size; its horizontal dimensions are not related to the dispersion characteristics of the plume being modeled. Second, the plume from a point source expands slowly, becoming more dilute and entraining ambient air continuously as it moves downwind. Entrainment is especially important when photochemical reactions occur in the plume because, as mentioned earlier, the introduction of NO_x or hydrocarbons into the plume may have dramatic effects on NO_2 formation (Liu et al., 1976; Tesche et al., 1976). Furthermore, resolution of crosswind concentration distributions is not possible within the trajectory model's air column.

In short, trajectory models such as DIFKIN/ARTSIM/ELSTAR are not well suited for treatment of point source diffusion. Reactive plume models are much superior and exact roughly the same computational and data requirements as do trajectory models.

4. Grid Models

Grid models are the most sophisticated class of air quality models developed to date. They are based on a stationary two- or three-dimensional array of grid cells within which pollutants are emitted, transported from cell to cell, diffused by turbulence, transformed by chemical reactions, and removed from the grid region by rain, adsorption on the ground, and other means. The complete atmospheric diffusion equation (equation 9) forms the theoretical basis for the grid model concept. As a class, grid models provide a higher level of detail in the treatment of relevant atmospheric processes than any other class of model. Treatment of NO_x chemistry has been included in grid modeling of photochemical systems and also in the modeling of nitrate formation.

Grid models are particulary well suited for the examination of regional NO_2 impacts of point sources. Because concentration predictions are available for numerous locations (both at the ground and aloft) throughout the day and night, these models are applicable to the analysis of regional and subregional impacts due to variations in emissions rates or locations of sources. For example, grid models can be used to develop strategies to control only those emissions directly responsible for the maximum NO_2 concentrations in a region. In general, grid models can be applied to any situation where sufficient data are available to derive the required inputs.

However, resolution of NO_2 impacts in the immediate vicinity of point sources is limited by the grid cell dimensions used in a grid model application. Grid models, as currently designed, are not capable of accurately resolving pollutant concentration distributions at scales smaller than the size of a grid cell. There are practical and theoretical limits to how small the grid cell size can be made. Decreasing the cell size increases the number of cells required to cover a given region; computing cost is also increased, because smaller time steps are required for the numerical solution procedure and because there are more cells. In addition, choice of a grid cell size implies that input data, such as winds, turbulence, and emissions, are reduced to that scale. An important limitation of grid models is the cost of data preparation and simulation. The computing demands of some of the grid models approach the capabilities of even the largest computers. To prepare an adequate data base and exercise a grid model for typical urban areas may cost \$60,000 to \$400,000.

Grid models, then, are well suited for the investigation of regional NO_2 impacts associated with point source emissions, but they are expensive to apply because of their large input data and computing requirements. For near source impacts, grid models are limited by grid resolution, and decreasing cell size is an extremely expensive option for improving grid resolution. Therefore, for near source impacts a sophisticated reactive plume model is a more cost-effective approach.

Various types of grid models have been developed that differ primarily in the number of atmospheric processes accounted for, the level of sophistication in the treatment of these processes, and the numerical procedures used to solve the governing conservation equations. Recently, two three-dimensional grid models, DEPICT/IMPACT and the SAI Airshed Model, have been used to investigate the NO_2 impacts of point sources. A popular two-dimensional grid model, LIRAQ, could also conceivably be used for analyses of regional NO_2 impacts from point sources.

a. DEPICT/IMPACT

DEPICT/IMPACT is specifically designed to predict the air quality impact of both chemically inert and reactive pollutants emitted from major point sources. It uses a second-order flux-corrected finite difference numerical solution scheme. It should be noted that, primarily because of this scheme, unrealistic predictions of slight spreading of plumes upwind of point sources have been observed in DEPICT/IMPACT predictions (Liu, Killus, and Roth, 1977). Based on the Gaussian formula, DEPICT/IMPACT first computes the dispersion of a tracer from a point source. Chemical reactions are accounted for only in the grid cells containing the tracer plume. Ambient pollutant concentrations are assumed to be spatially homogeneous and are derived from measured initial values and a "smog chamber" type of calculation (i.e., one that takes only photochemistry into account, not emissions or meteorology). Spatial variation in ambient concentrations owing to source distributions and meteorological conditions are ignored. This treatment of ambient concentrations may be seriously deficient for NO_x-rich plumes dispersing in hydrocarbon-rich environments. Furthermore, DEPICT/IMPACT currently employs either the Eschenroeder (1972) or the Hecht, Seinfeld, and Dodge (1974) chemical kinetic mechanisms, neither of which is currently a state-of-the-art kinetic mechanism.

b. SAI Airshed Model

The SAI Airshed Model was designed to investigate the impact of both area and point sources within an urban area for both inert and chemically reactive species. It uses the flux-corrected "sharp and smooth transport algorithm" (SHASTA) numerical solution procedure developed by Boris and Book (1973). Point source emissions are injected into the grid cell above the source closest to plume height. The model also accounts for all other point and area sources within the modeling region. The Carbon-Bond photochemical kinetic mechanism (Whitten and Hogo, 1977), a state-of-the-art mechanism, is used in the Airshed Model and is included in the solution for every grid cell. Consideration of all emissions sources, chemistry, and meteorology in each grid cell throughout the modeling region provides a treatment of concentrations outside a point source plume--ambient concentrations--that is superior to what is afforded by DEPICT/IMPACT.

c. LIRAQ

The LIRAQ model is one of the most sophisticated two-dimensional grid models available. Point source emissions are treated in a fashion similar to the SAI Airshed Model except that all emissions must be included in the surface layer; the Airshed Model can inject them into elevated grid cell layers. LIRAQ employs a first-order finite difference scheme to calculate the advective flux between grid cells and a modified Gear (1971) routine to handle chemical reaction terms. The Hecht, Seinfeld, and Dodge (1974) chemical reaction mechanism is installed in LIRAQ; as noted above, this is no longer state-of-the-art. LIRAQ's inability to resolve vertical concentration distributions may affect predictions of ground-level NO_2 concentrations attributable to point sources before complete mixing is achieved downwind. Furthermore, the model cannot track, for later use, plumes that may penetrate the top of the mixed layer if the mixing depth increases, as can three-dimensional models. However, it accounts for most sources, chemistry, and meteorology within the modeling region in computing ambient concentrations in a fashion superior to the three-dimensional DEPICT/IMPACT model.

To summarize, grid models are well suited for predicting the regional impacts of point source NO_x emissions, especially in areas where there are many other pollutant sources (if the model considers all these sources). Practical and theoretical considerations limit the minimum grid cell size that can be used, and the minimum grid cell size limits the spatial resolution achievable with a grid model. For this reason, grid models are not well suited for predicting near point source NO_2 impacts. Also, the large costs and data requirements of these models may preclude their usage in some situations, as they unfortunately are precluded here.

5. Conjoint Models

Conjoint models combine, in one package, a reactive plume model with a grid model, capitalizing on the strengths of these two approaches. The reactive plume model component provides near source resolution of NO_2 impacts, and the grid model component can provide regional impact information and account for the multitude of sources in an urban area.

Two types of arrangements can be conceived for interfacing the two model types. In the first, the reactive plume model is applied to a point source upwind of the urban grid modeling region, providing boundary conditions for a number of grid cells along one side of the grid model (see Figure 3). A larger grid modeling region could be overlaid to provide ambient concentrations for the reactive plume model and the remaining boundary values for the grid model, but its use is optional if a sufficient number of measurements are available. In the second approach, the reactive plume model is nested within the grid model, utilizing grid model predictions of ambient concentrations. Once again, a regional grid model could be used to provide boundary conditions for the urban grid model (see Figure 4).

SAI developed a conjoint model for the investigation of the impacts of reactive plumes on urban areas or downwind of urban areas (Liu, Yocke, and Roth, 1978). Specifically, the intermingling of reactive plumes with urban emissions is the focus of the model, which comprises three component models: SAI's three-dimensional wind model, SAI's RPM-II, and SAI's Airshed Model. The wind model component supplies a three-dimensional wind field for the other two component models. Its use is optional if the wind field can be prescribed by some other means. RPM-II is used to predict pollutant concentrations in a reactive plume within the first few kilometers from the source. The Airshed Model is included to account for all urban area emissions and to account for the interaction of the plume with these emissions. In one application the SAI models were interfaced in the fashion described schematically in Figure 3; in another application they were interfaced as in Figure 4.

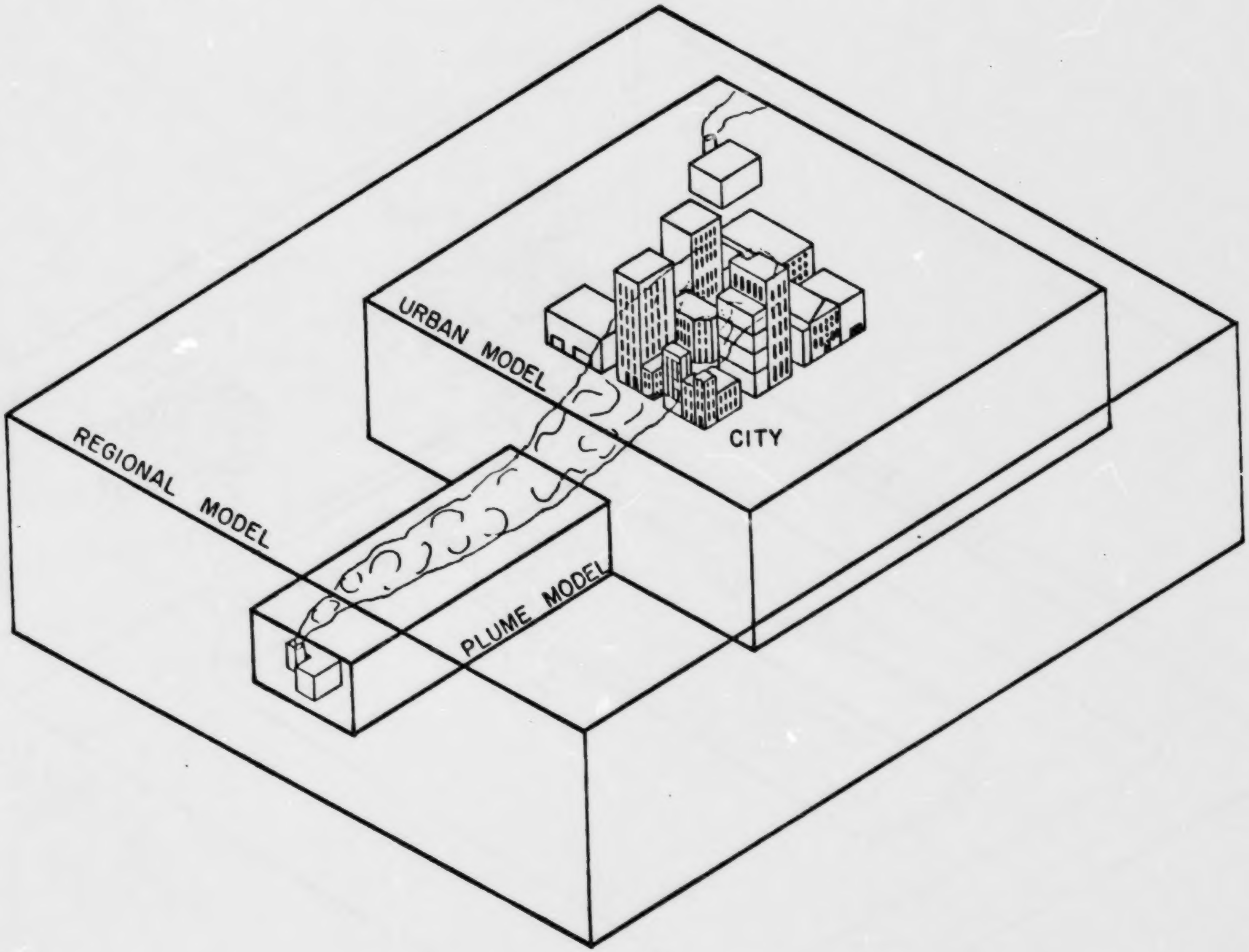
URBAN MODEL
CITY
REGIONAL MODEL
PLUME MODEL

Figure 3. Conjoint model schematic: A reactive plume model supplies a boundary condition for an urban grid model.

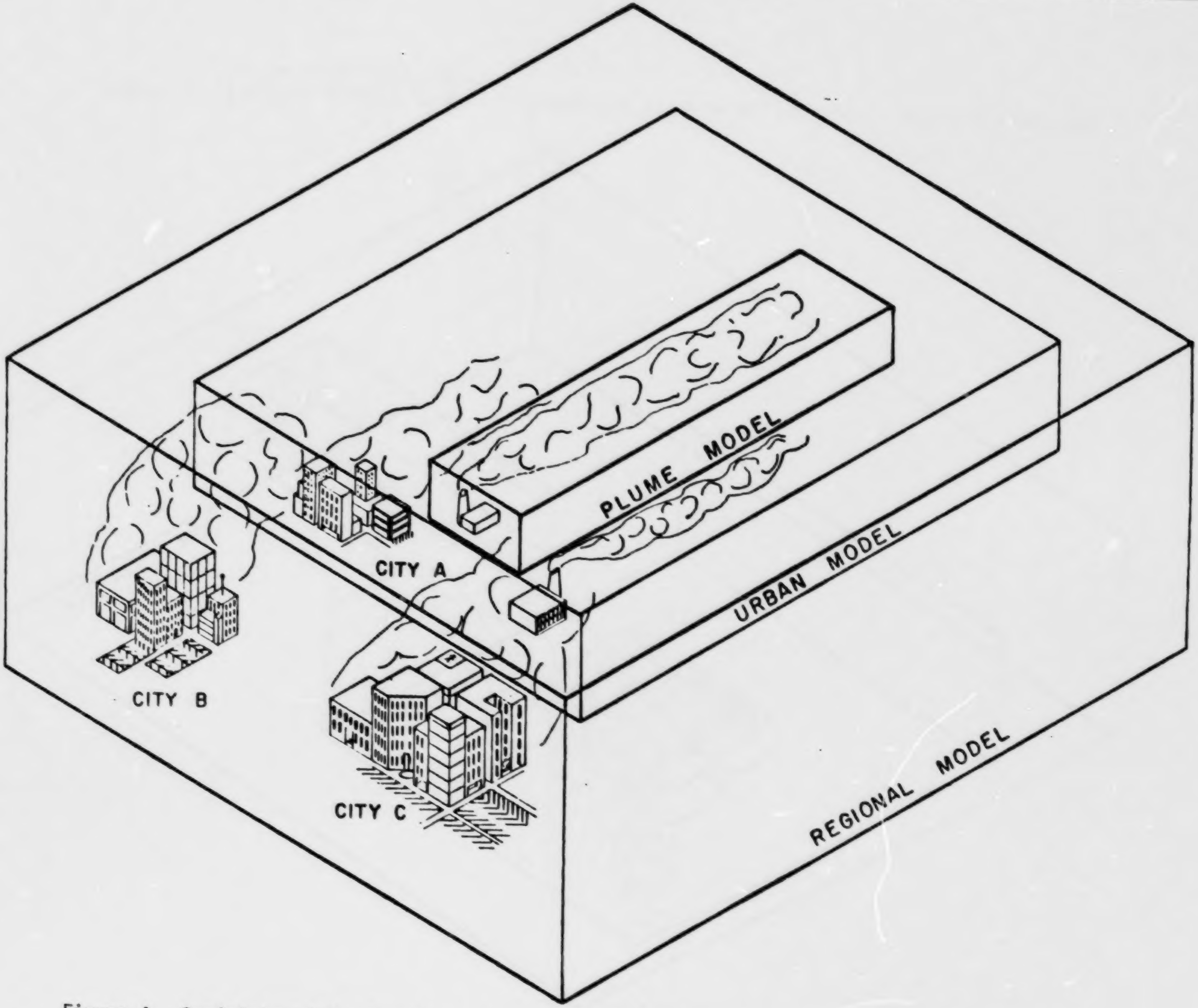
PLUME MODEL
URBAN MODEL
REGIONAL MODEL
CITY A
CITY B
CITY C

Figure 4. Conjoint model schematic: A reactive plume model is nested within an urban grid modeling region.

Although the conjoint modeling approach is unique in its ability to predict NO_2 concentrations in many diverse situations, over a range of spatial and temporal scales, it is by far the most expensive approach available. The input data and computational requirements of the conjoint model are the combined requirements of its component models. Therefore, the use of a conjoint model must be excluded from this study.

III SELECTION OF MODELS FOR THIS STUDY

Based on our discussion of model types and prominent examples within each type presented in the last chapter, we can eliminate those model types and specific models that do not meet the requirements for this study. First, we must eliminate grid and conjoint type models. Although both are sophisticated modeling approaches, the high costs prohibit their use in this study. Second, trajectory type models can be dismissed from further consideration because they do not properly treat horizontal dispersion of point source plumes and entrainment of ambient air into the plume. Furthermore, reactive plume models embody all desirable features of trajectory models (e.g., low computing cost and limited data requirements) but avoid their deficiencies.

Of the reactive plume models, SAI's RPM-II appears to be the most sophisticated nonproprietary model currently operational. Therefore we will apply RPM-II to the MISTT data base in this study. A technical description, more complete than that provided in Chapter II, is given in Appendix A. In Appendices B and C the results of a sensitivity analysis for RPM-I (RPM-II's immediate predecessor) are presented. The results of this analysis indicate the relative sensitivities of RPM-I's ozone predictions to variations in input parameters. Sensitivities of the model's NO_2 predictions to these factors are nearly the same, since the NO_2 predictions are related to O_3 concentrations through the photostationary approximation. The relative sensitivities of RPM-II's predictions to input variations should be similar to those of RPM-I because the major improvements embodied in RPM-II (spatial resolution of concentrations within the plume and an improved chemical kinetics package) should not affect relative model responses to input variations. For example, the sensitivity of the Carbon-Bond chemical kinetic mechanism used in RPM-II to typical ambient concentration variations is similar to that of the Hecht, Seinfeld, and Dodge mechanism used in RPM-I. However, the absolute accuracy and the range of applicability of the Carbon-Bond Mechanism are much greater (Whitten and Hogo, 1977). The results of the sensitivity analyses are valuable because they highlight the relative importance of the accuracies of the RPM-II input data. The sensitivity study indicates that RPM-II is most sensitive to ambient hydrocarbon concentrations, followed by the NO_2 photolysis rate, ambient NO_x concentrations, and ambient ozone concentrations, in order of decreasing sensitivity.

In addition to evaluating RPM-II, this study also evaluates the simple equilibrium techniques. Although it is recognized that these techniques are strictly applicable only to very limited situations and that they do not meet the basic technical requirements specified in the scope of the study, they are nevertheless attractive for use as very inexpensive screening procedures. They can be applied quickly, using only a hand calculator and very limited data, and they may provide estimates of the rough magnitude of NO_2 impacts due to point source emissions. Their evaluation in this study will help in assessing their usefulness as screening procedures.

IV SELECTION OF CASE STUDIES FROM MISTT DATA

The 1976 MISTT study* was carried out over 18 days during June, July, and August, 1976. Meteorology Research Incorporated (MRI) and Washington University (WU) collected aerometric data on 13 days. MRI and WU were in the field together on only 7 days. Table 1 contains a summary of the plume sampling dates for both MRI and WU, and a summary of the data collected on each date.

To assess properly the value and meaning of this data relative to the purposes of this study it is necessary to carefully examine all data as a function of time and place of collection. For data in raw form (as delivered to us on tape) this is a formidable task. Some efforts had been made by Washington University to develop computer plotting programs and to plot the MISTT data. Unfortunately, only small portions of the MISTT data base were plotted and WU's computer programs were written specifically for their in-house computer. Therefore, as a first step in selecting case study days, a significant amount of work in this study was devoted to developing new computer plotting programs and then plotting all 1976 MISTT data. Such a great number of plots were generated that they are included in a separate volume (Volume II) of this report. The numbers in Table 1 and all subsequent discussions of the MISTT data are based on careful examination of the data plots presented in Volume II.

A. SELECTION OF 10 CASE STUDY DAYS

The scope of this study calls for the selection of at least 10 case study days from the MISTT program. Of the 18 days described in Table 1,

---

* The MISTT study involved measurements of the Labadie Power Plant and St. Louis urban plumes. The objective of the MISTT program was to characterize plume sulfur and aerosol transport and transformations, not to support model evaluation activities.

TABLE 1. SUMMARY OF 1976 MISTT DATA BASE

	Number of Discernible Plumes/Total Number of Traverse Paths												
	MRI							Washington					
Date	O_3	NO	NO_2	NO_x	SO_2	CN	B_{scat}	O_3	SO_2	CN	B_{scat}	Pibal Winds Available	Number of Traverse Paths
July													
1	5/16	4/16	3/16	5/16	6/16	7/16	3/16	-	-	-	-	Yes	4
2	5/10	4/10	8/10	8/10	8/10	4/10	4/10	-	-	-	-	Yes	4
5	11/23	4/23	12/23	14/23	21/23	16/23	2/23	2/5	6/5	0/5	1/5	Yes	14
7	0/11	0/11	2/11	2/11	7/11	7/11	0/11	5/13	13/13	0/13	0/13	Yes	11
14	19/39	17/39	23/59	23/39	26/39	21/39	13/39	2/8	6/8	0/8	4/8	Yes	12
15	5/9	1/9	4/9	6/9	8/9	5/9	2/9	3/13	11/13	0/13	5/13	Yes	7
18	11/23	6/25	8/23	10/23	17/23	4/23	7/23	0/11	10/11	0/11	10/11	Yes	18
20	3/17	3/17	6/17	6/17	7/17	4/17	1/17	0/6	6/6	0/6	0/6	Yes	11
23	9/18	9/18	8/18	9/18	15/18	4/18	7/18	4/7	5/7	0/7	0/7	Yes	8
23-24*	0/11	0/11	1/11	1/11	1/11	1/11	1/11	-	-	-	-	Yes	9
26	0/9	4/9	3/9	4/9	4/9	0/9	0/9	-	-	-	-	Yes	4
27	2/3	0/3	1/3	2/3	2/3	0/3	0/3	-	-	-	-	No	1
26	8/24	12/24	17/24	19/24	20/24	14/24	3/24	-	-	-	-	Yes	4
30	6/29	3/29	8/29	14/29	23/29	9/29	8/29	-	-	-	-	Yes	12
June													
27	-	-	-	-	-	-	-	1/4	2/4	0/4	0/4	No	4
July													
9	-	-	-	-	-	-	-	4/15	4/15	0/15	4/15	Yes	3
9-10*	-	-	-	-	-	-	-	4/7	5/7	0/7	2/7	Yes	4
12	-	-	-	-	-	-	-	3/5	5/5	0/5	5/5	Yes	4
13	-	-	-	-	-	-	-	3/4	1/4	0/4	2/4	No	2
August													
3	-	-	-	-	-	-	-	0/6	5/6	5/6	0/6	No	5

---

* Measurements taken on July 9 and 23 extended somewhat past midnight; late night readings are shown separately, as 9-10 and 23-24 July, respectively.

we eliminated those days on which WU was monitoring alone (i.e., MRI was not monitoring) because WU's aircraft did not monitor NO_x concentrations. Since NO_x measurements are essential to the application and evaluation of all reactive plume models, case study days were chosen from the remaining 13 days. We chose the 7 days that both MRI and WU flew sampling missions primarily because of the larger amounts of data collected then. Careful examination of the other 6 MRI sampling days led to selection of 3 more days--2, 28, and 30 July, 1976. These 3 days were selected mainly because of the inadequacies of the 3 days not chosen (1, 26, and 27 July, 1976). There were no pibal data and only one traverse path available on 27 July; on 26 July, only a few traverse paths were flown, all traverses were at the same general location, and ozone data were not collected. And it appears, on the basis of measured concentrations and pibal wind directions, that on 1 July the MRI aircraft was upwind of all large pollutant sources.

To summarize, the case study days selected from the MISTT program are 2, 5, 7, 14, 15, 18, 20, 23-24, 28, and 30 July, 1976. Review of the data presented in Table 1 and Volume II indicates that these 10 days are the best available from the MISTT program for case studies of reactive plume models. A detailed examination of the data collected on these days is presented in the following section.

B. PREPARATION OF MODEL INPUTS

The following data are required to exercise RPM-II.

- Atmospheric stability, dispersion coefficient, or horizontal plume spread as a function of downwind distance and time.
- Point source emissions rates for NO, NO_2, SO_2, sulfates and hydrocarbons.
- Source data:
    - Plume heights.
    - Source parameters: flow rates, stack temperatures.
    - Source locations.

- Ambient concentrations for all species as functions of location and time.
- Sunlight intensity as a function of location and time.
- Inversion heights or vertical plume spreads as functions of location and time.
- Wind field.

These data will also satisfy all requirements of the simple NO_2 estimation procedures.

1. Plume Dispersion (Horizontal and Vertical)

The first step in obtaining estimates of plume dispersion from the MISTT data base is to determine the location of the plume. This is not a simple task because the MISTT concentration measurements often show several "plume-like" profiles along a particular traverse. (This study is concerned with the Labadie Power Plant plume only because it was the focus of monitoring efforts on the 10 days we selected. The scope of work for the study calls for case studies of urban as well as point source plumes, and occasionally the St. Louis urban plume and other urban point source plumes are also visible in the data. However, urban emissions rates are extremely difficult to quantify accurately and an insufficient number of aircraft traverses were available to initialize RPM-II urban plume runs.) Pibal data collected during the program were used in conjunction with information about the location of other pollutant sources to deduce which, if any, is most likely the Labadie plume profile. We have mapped, in Figure 5(a) through 5(z), our estimates of the positions and widths of the Labadie plumes along the various MRI and WU traverse paths on the 10 case study days selected. Also shown in those figures are estimates of the St. Louis urban plume positions and widths. Labadie plume silhouettes drawn with dashed lines indicate that these are guesses of the plume paths that were made on the basis of wind data and very limited concentration data. Widths shown in these figures are the maximum widths observed at any altitude along a given traverse path.

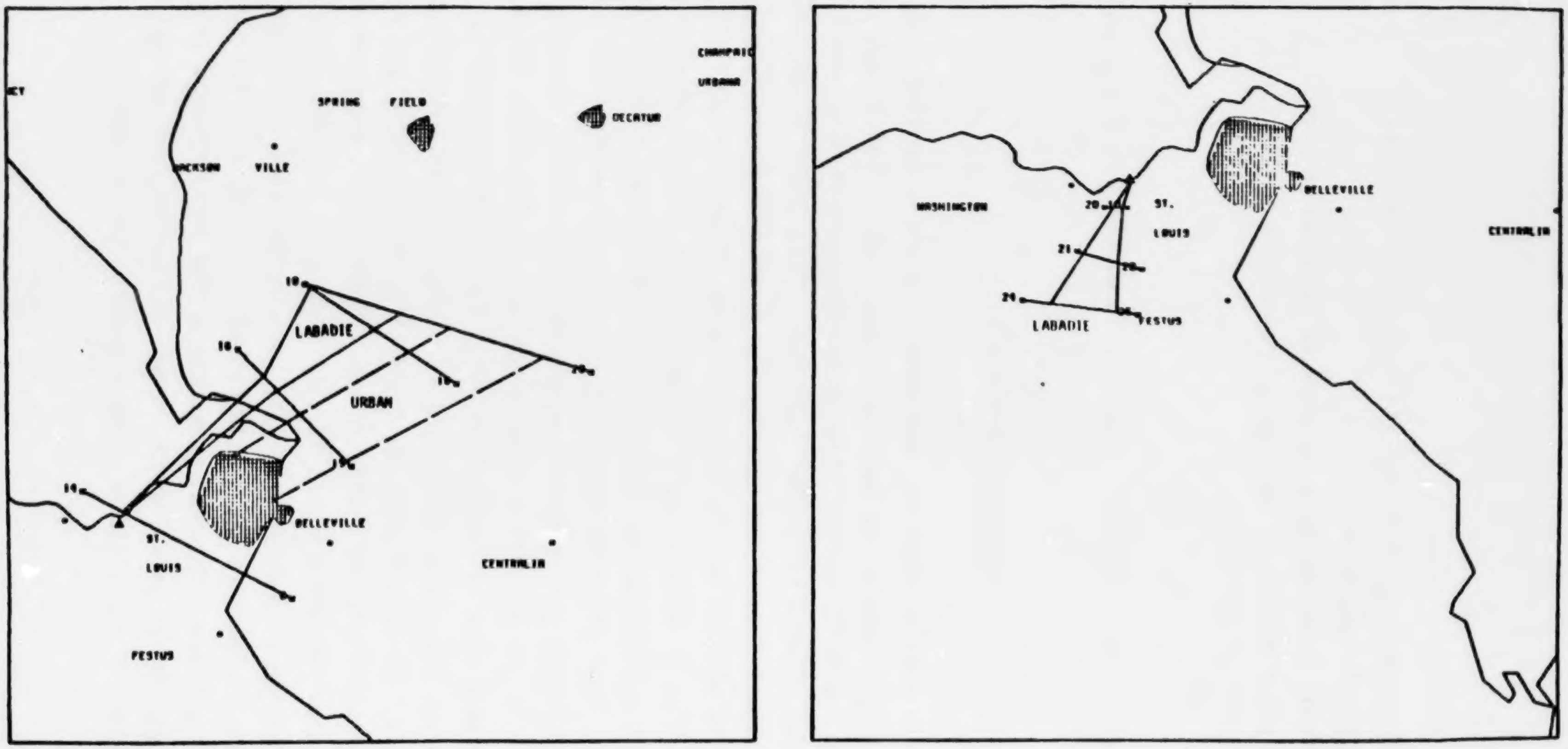
SPRING FIELD
DECATUR
CHAMPAIG
URBANA
JACKSON VILLE
LABADIE
URBAN
BELLEVILLE
ST. LOUIS
CENTRALIA
FESTUS
WASHINGTON
20
21
24
LABADIE

(a) 2 July 1976

(b) 5 July 1976

Figure 5. Positions and widths of Labadie plumes on the 10 case study days.

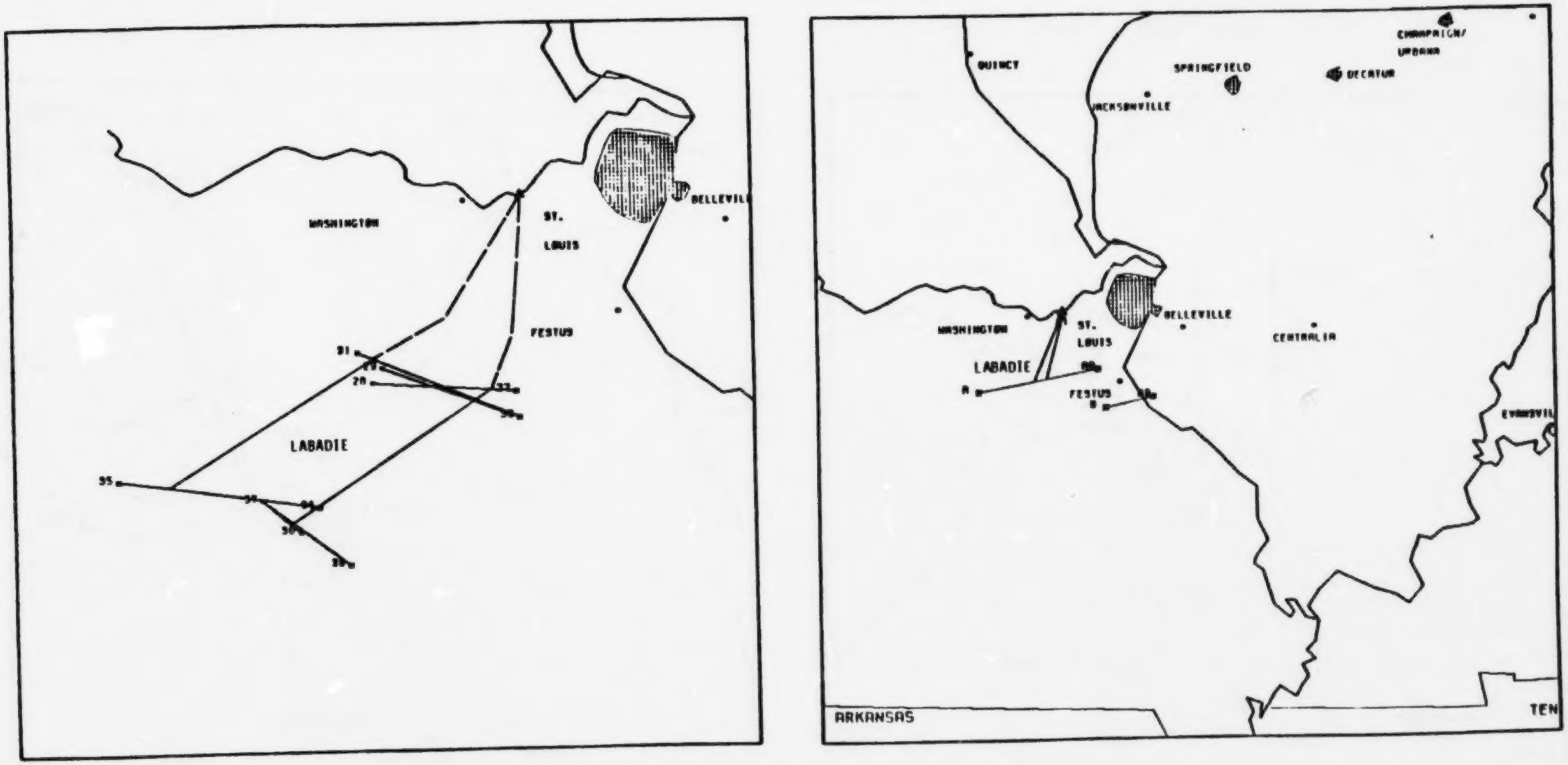
WASHINGTON
ST.
LOUIS
BELLEVIL
FESTUS
LABADIE
91
28
95
QUINCY
SPRINGFIELD
DECATUR
CHAMPAIGN/
URBANA
JACKSONVILLE
WASHINGTON
ST.
LOUIS
BELLEVILLE
CENTRALIA
LABADIE
A
FESTUS
B
EVANSVIL
ARKANSAS
TEN

(c) 5 July 1976

(d) 5 July 1976

Figure 5 (Continued).

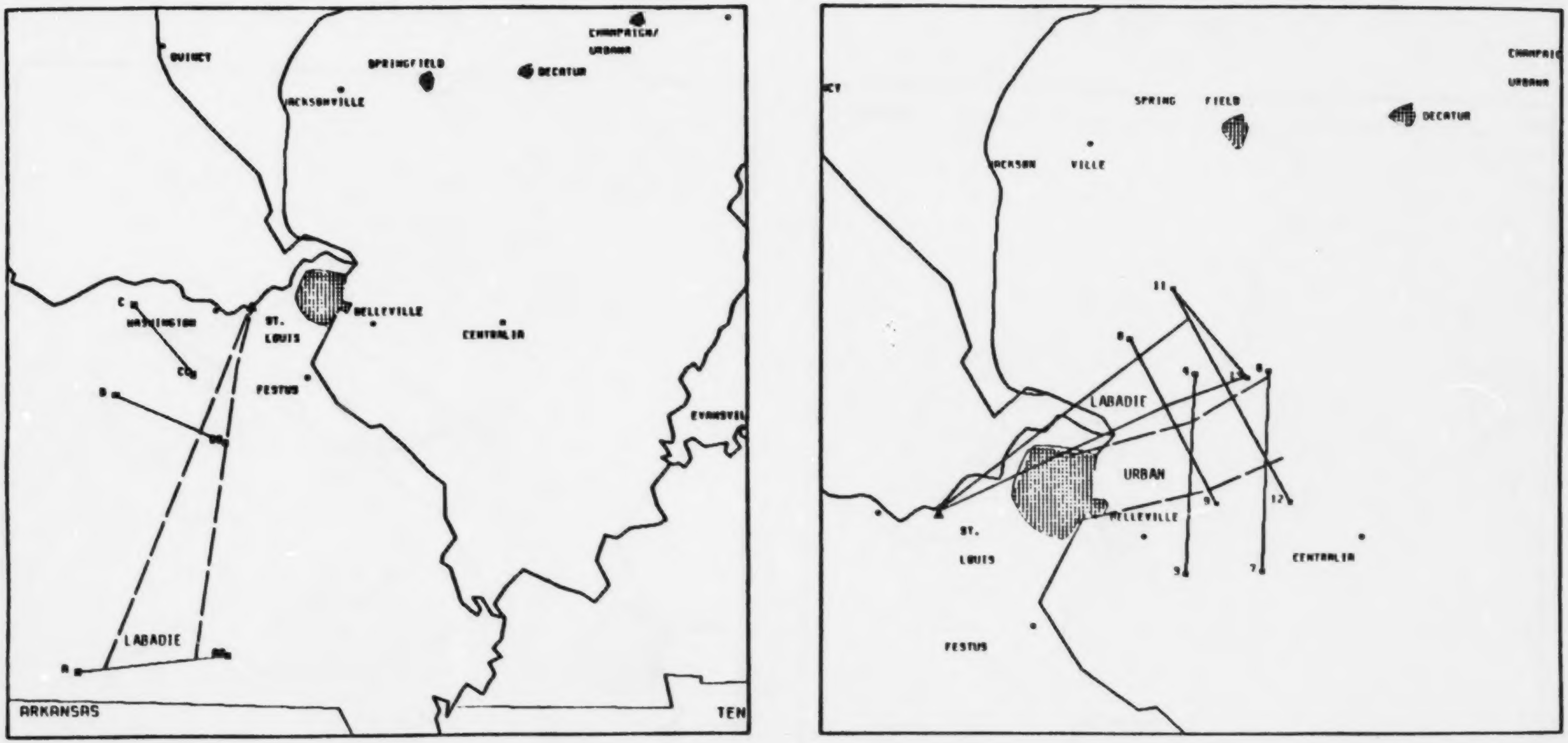
QUINCY
SPRINGFIELD
JACKSONVILLE
CHAMPAIGN/
URBANA
DECATUR
BELLEVILLE
CENTRALIA
ST.
LOUIS
WASHINGTON
FESTUS
EVANSVIL
LABADIE
ARKANSAS
TEN
SPRING FIELD
JACKSON VILLE
URBAN
7
8
9
11
12

(e) 5 July 1976

(f) 7 July 1976

Figure 5 (Continued).

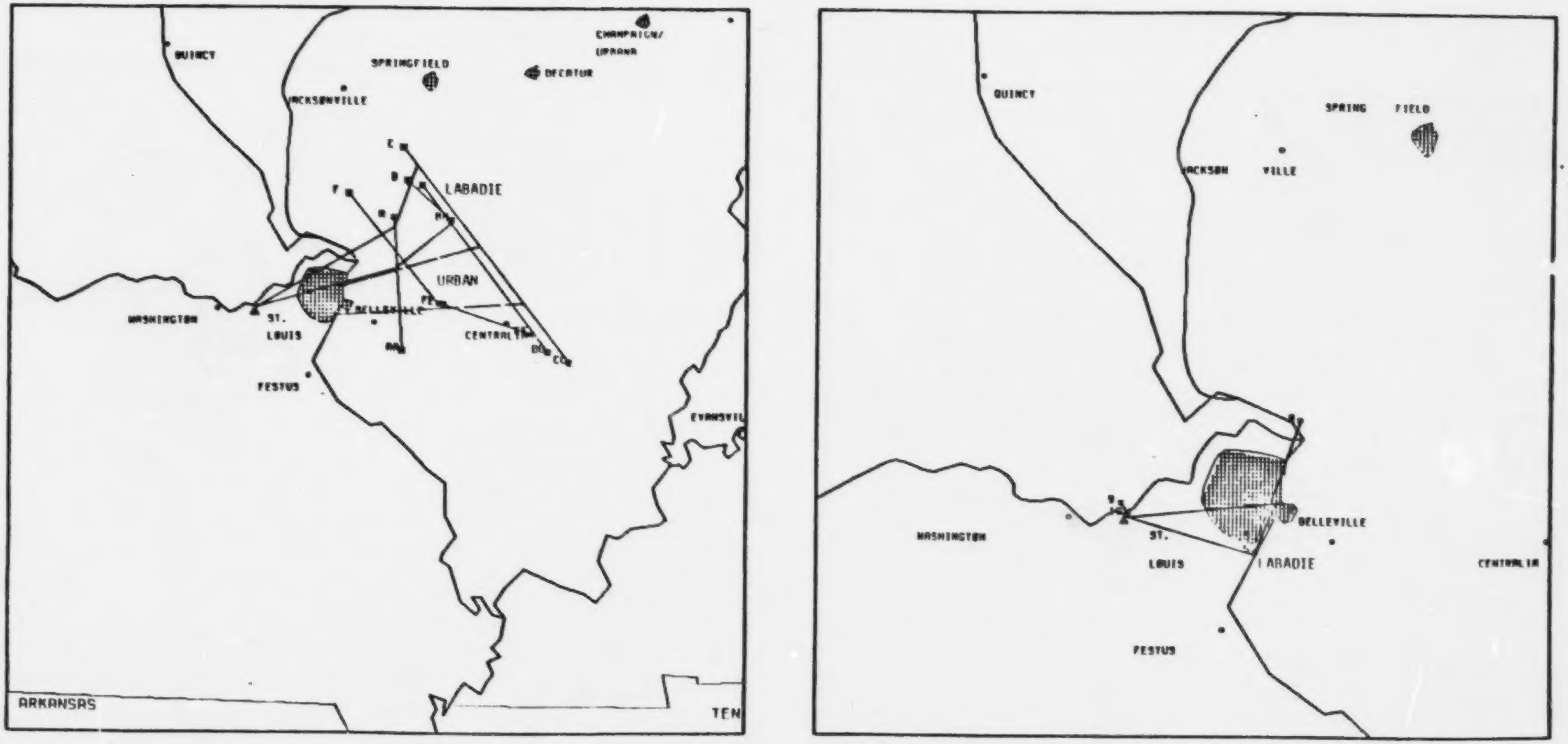
QUINCY
SPRINGFIELD
CHAMPAIGN/
URBANA
DECATUR
JACKSONVILLE
LABADIE
URBAN
BELLEVILLE
WASHINGTON
ST.
LOUIS
CENTRALIA
FESTUS
EVANSVIL
ARKANSAS
TEN
QUINCY
SPRING FIELD
JACKSON VILLE
WASHINGTON
ST.
LOUIS
BELLEVILLE
LABADIE
CENTRALIA
FESTUS

(g) 7 July 1976

(h) 14 July 1976

Figure 5 (Continued).

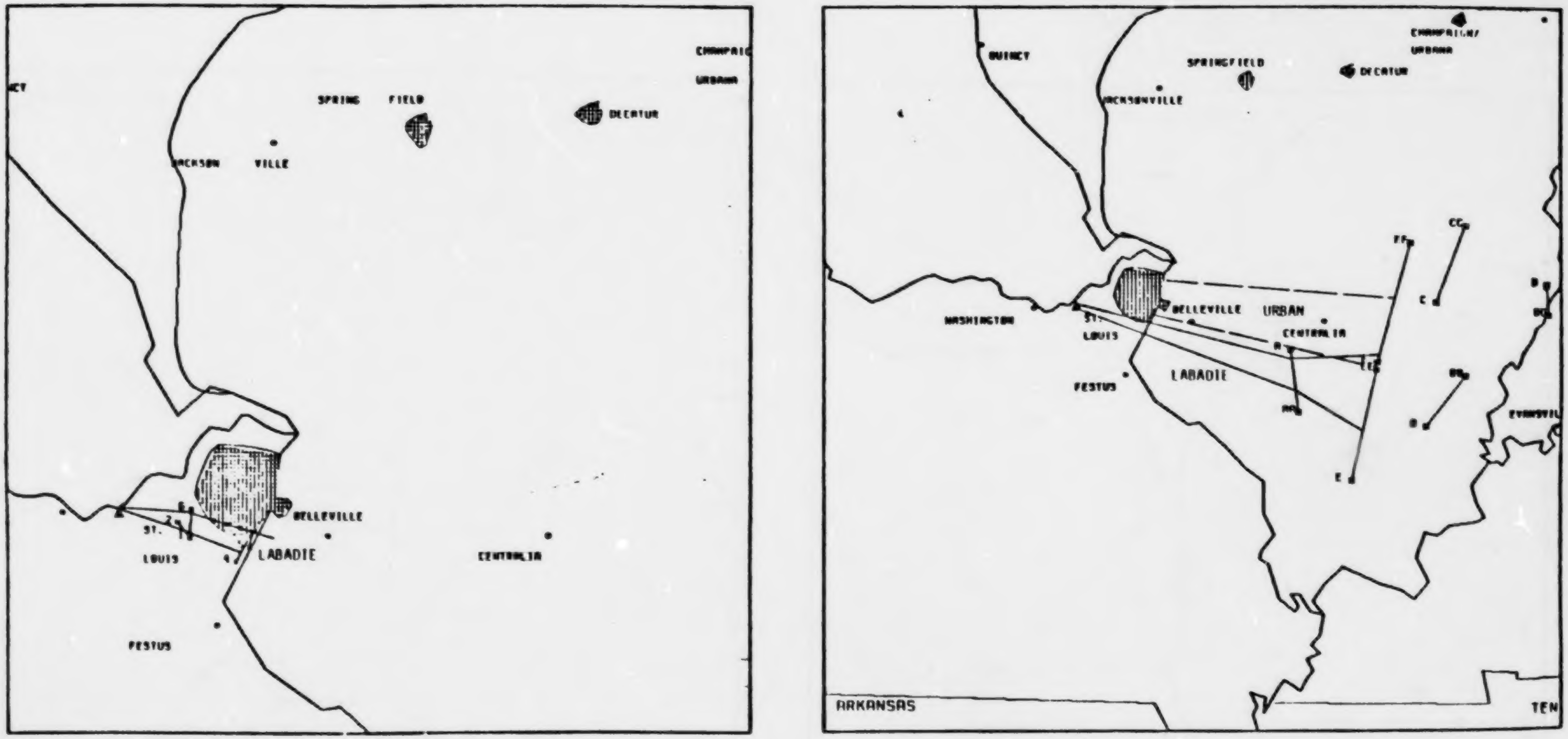
SPRING FIELD
DECATUR
CHAMPAIG
URBANA
JACKSON VILLE
ST. LOUIS
BELLEVILLE
LABADIE
CENTRALIA
FESTUS
QUINCY
SPRINGFIELD
CHAMPAIGN/URBANA
JACKSONVILLE
WASHINGTON
URBAN
EVANSVIL
ARKANSAS
TEN

(i) 14 July 1976

(j) 14 July 1976

Figure 5 (Continued).

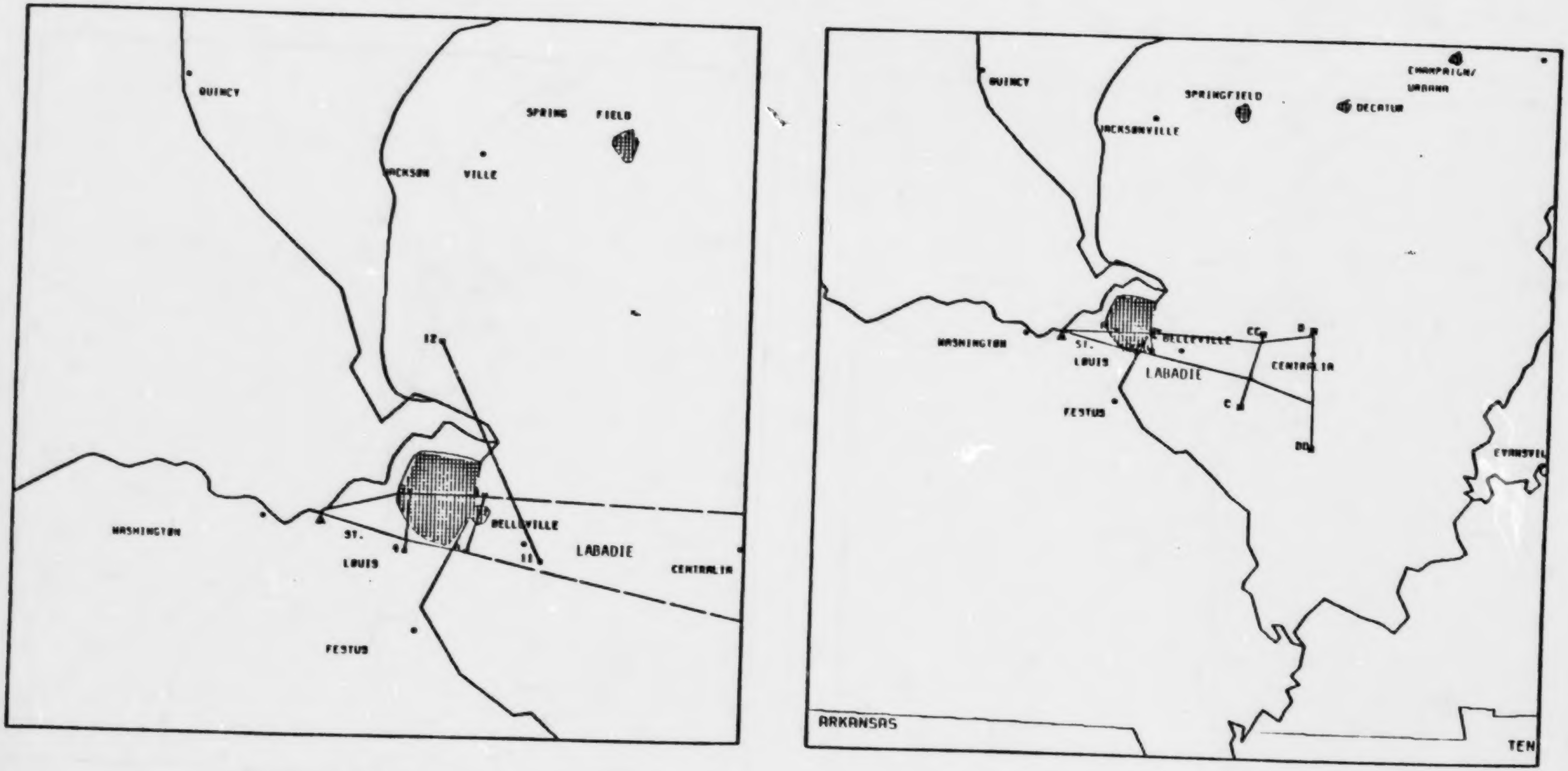
QUINCY
JACKSON
VILLE
SPRING
FIELD
12
WASHINGTON
ST.
LOUIS
4
BELLEVILLE
11
LABADIE
CENTRALIA
FESTUS
QUINCY
JACKSONVILLE
SPRINGFIELD
DECATUR
CHAMPAIGN/
URBANA
WASHINGTON
ST.
LOUIS
BELLEVILLE
LABADIE
CC
B
CENTRALIA
C
DD
FESTUS
EVANSVIL
ARKANSAS
TEN

(k) 15 July 1976

(1) 15 July 1976

Figure 5 (Continued).

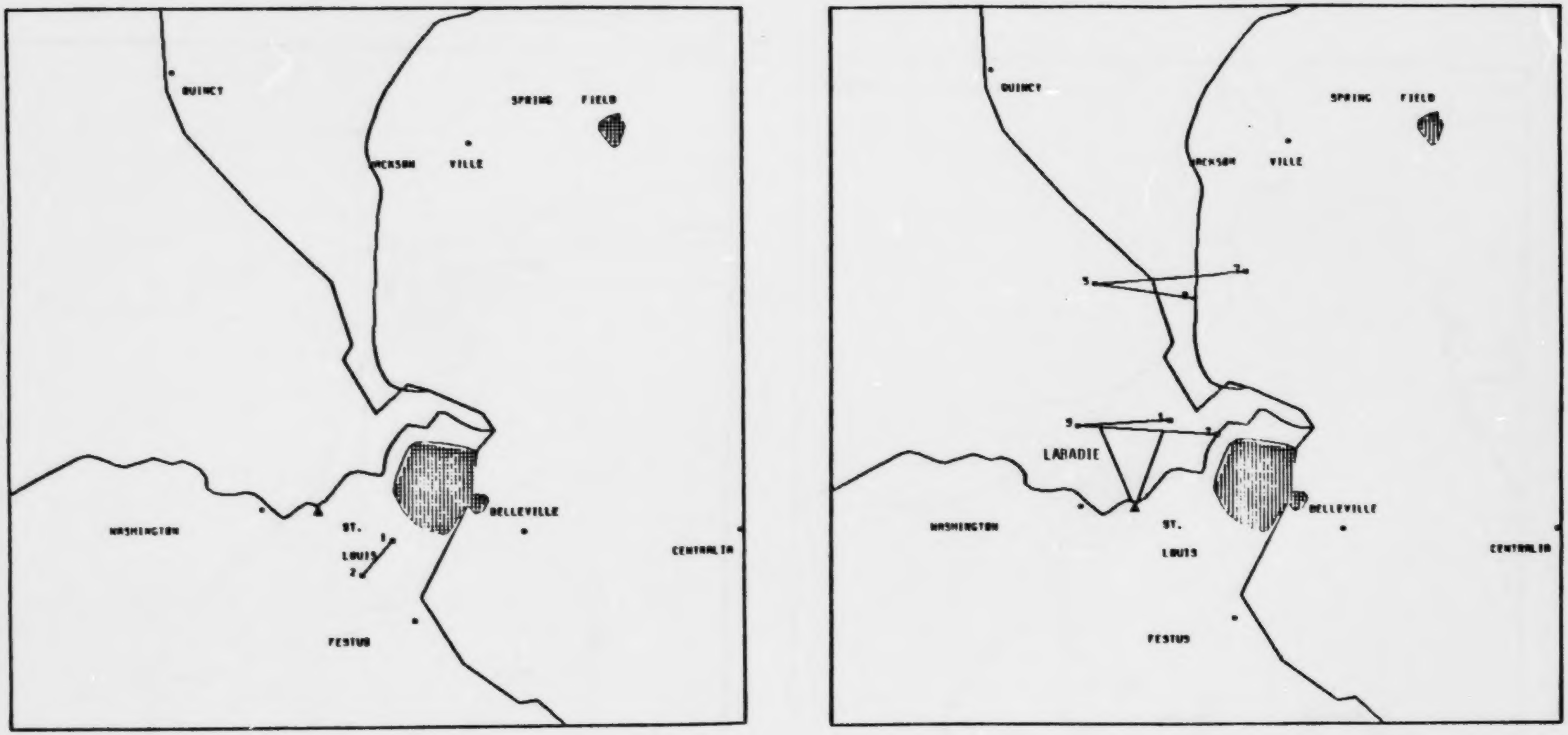
QUINCY
SPRING FIELD
ACKSON VILLE
WASHINGTON
ST. LOUIS
BELLEVILLE
CENTRALIA
FESTUS
1
2
LABADIE
5
2
9
1
3

(m) 18 July 1976

(n) 18 July 1976

Figure 5 (Continued).

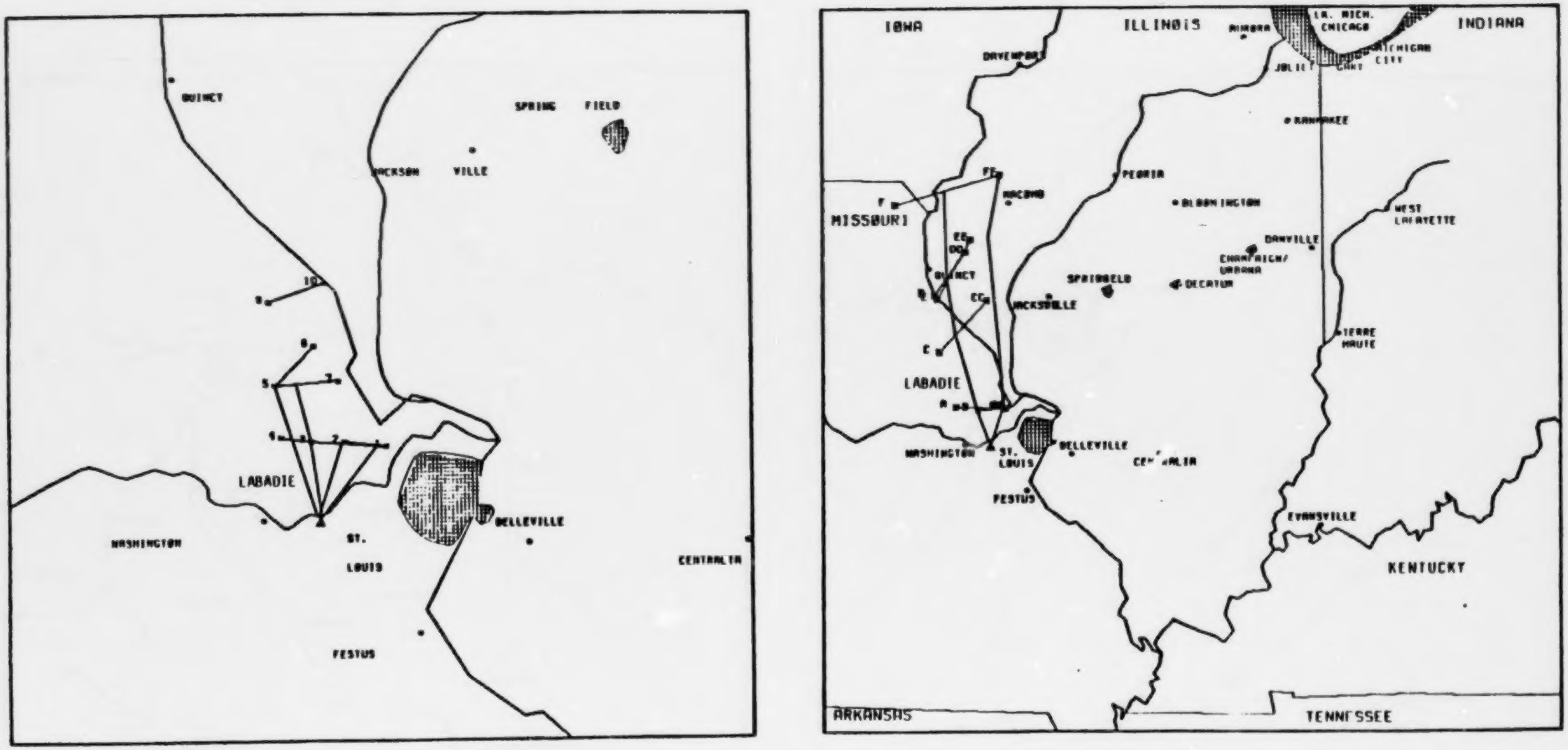
QUINCY
SPRING FIELD
JACKSON VILLE
10
9
8
5
7
4
3
2
1
LABADIE
WASHINGTON
ST. LOUIS
BELLEVILLE
CENTRALIA
FESTUS
IOWA
ILLINOIS
AURORA
LA. MICH.
CHICAGO
INDIANA
MICHIGAN CITY
DAVENPORT
JOLIET
GARY
KANKAKEE
FF
F
MACOMB
MISSOURI
PEORIA
BLOOMINGTON
WEST LAFAYETTE
EE
DD
DANVILLE
CHAMPAIGN/ URBANA
QUINCY
SPRINGFIELD
DECATUR
B
CC
JACKSONVILLE
TERRE HAUTE
C
LABADIE
A
WASHINGTON
ST. LOUIS
BELLEVILLE
CENTRALIA
FESTUS
EVANSVILLE
KENTUCKY
ARKANSAS
TENNESSEE

(o) 18 July 1976

(p) 18 July 1976

Figure 5 (Continued).

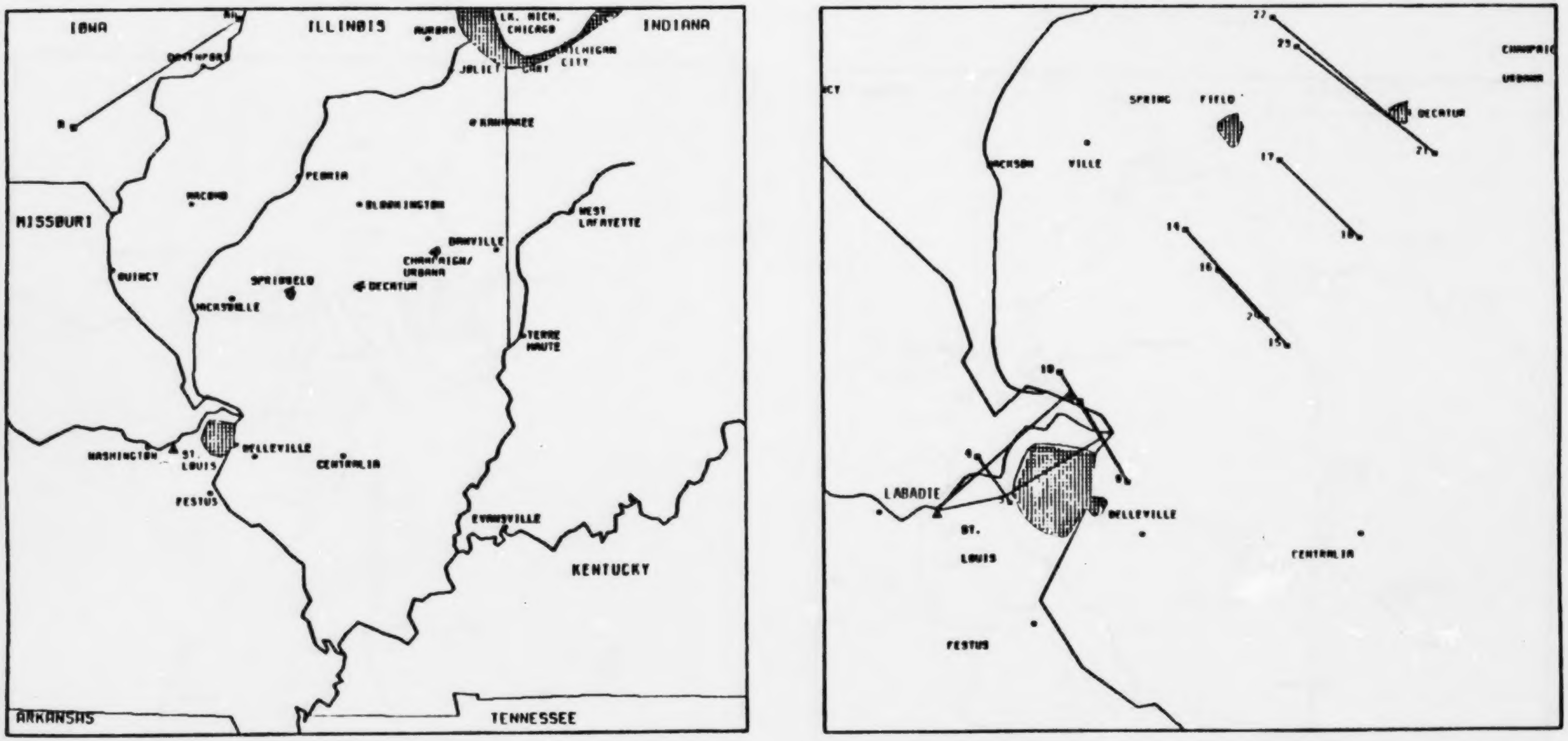
IOWA
ILLINOIS
INDIANA
LK. MICH.
CHICAGO
AURORA
DAVENPORT
MICHIGAN CITY
JOLIET
GARY
KANKAKEE
PEORIA
MACOMB
BLOOMINGTON
MISSOURI
WEST LAFAYETTE
DANVILLE
CHAMPAIGN/ URBANA
QUINCY
SPRINGFIELD
DECATUR
JACKSONVILLE
TERRE HAUTE
WASHINGTON
ST. LOUIS
BELLEVILLE
CENTRALIA
FESTUS
EVANSVILLE
KENTUCKY
ARKANSAS
TENNESSEE
27
25
CHAMPAIGN
URBANA
SPRING FIELD
DECATUR
JACKSON VILLE
21
17
14
18
16
20
15
10
LABADIE
ST. LOUIS
BELLEVILLE
CENTRALIA
FESTUS

(q) 18 July 1976

(r) 20 July 1976

Figure 5 (Continued).

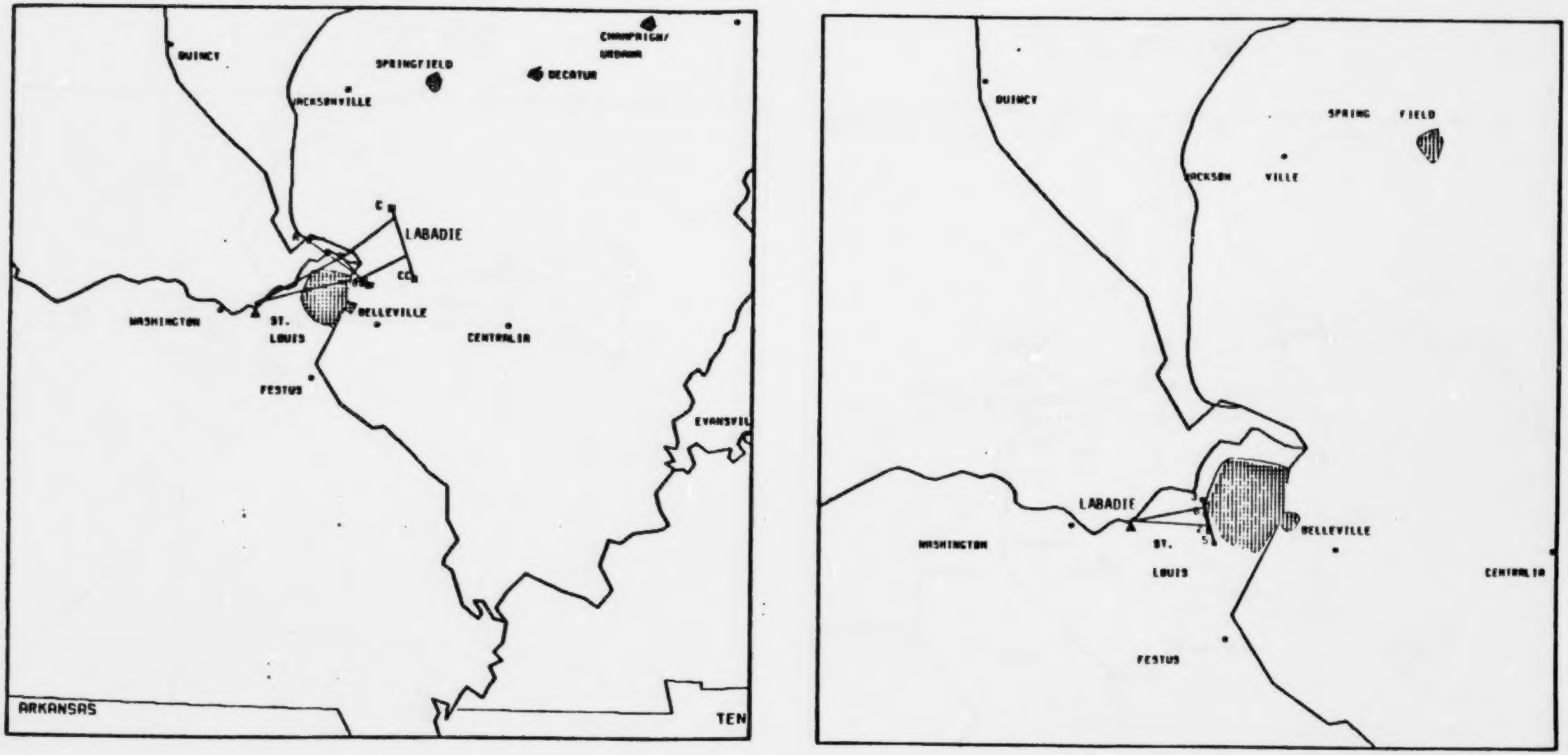
QUINCY
SPRINGFIELD
CHAMPAIGN/
URBANA
DECATUR
JACKSONVILLE
C
LABADIE
CC
WASHINGTON
ST.
LOUIS
BELLEVILLE
CENTRALIA
FESTUS
EVANSVIL
ARKANSAS
TEN
QUINCY
SPRING FIELD
JACKSON VILLE
LABADIE
WASHINGTON
ST.
LOUIS
BELLEVILLE
CENTRALIA
FESTUS

(s) 20 July 1976

(t) 23 July 1976

Figure 5 (Continued).

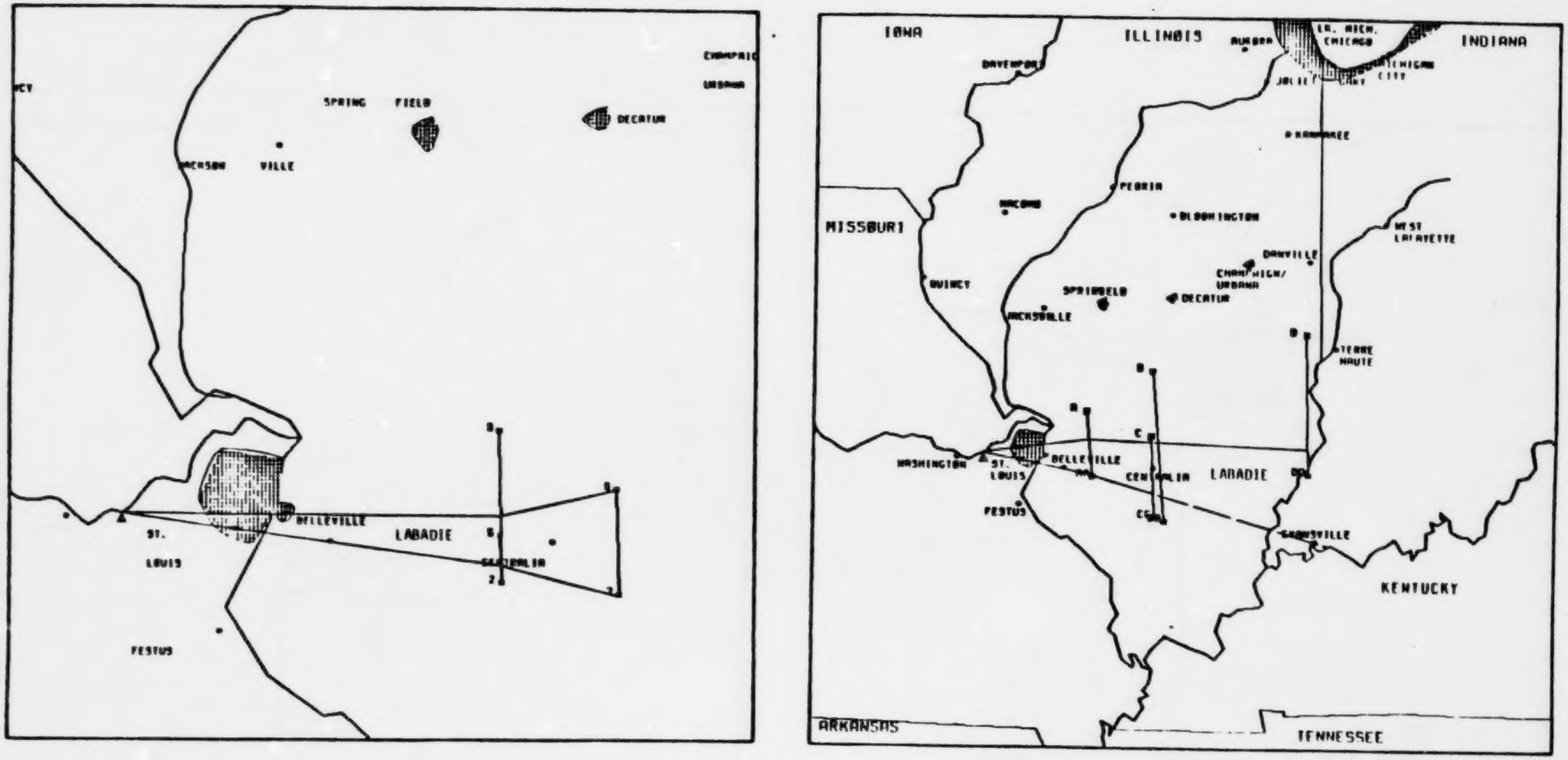
CHAMPAIG
URBANA
SPRING FIELD
DECATUR
JACKSON VILLE
BELLEVILLE
LABADIE
CENTRALIA
ST. LOUIS
FESTUS
IOWA
ILLINOIS
INDIANA
MISSOURI
KENTUCKY
TENNESSEE
ARKANSAS
AURORA
LK. MICH.
CHICAGO
MICHIGAN CITY
JOLIET
GARY
DAVENPORT
KANKAKEE
PEORIA
MACOMB
BLOOMINGTON
WEST LAFAYETTE
DANVILLE
CHAMPAIGN/URBANA
QUINCY
SPRINGFIELD
JACKSONVILLE
TERRE HAUTE
WASHINGTON
EVANSVILLE
A
B
C
D

(u) 23 July 1976

(v) 23 July 1976

Figure 5 (Continued).

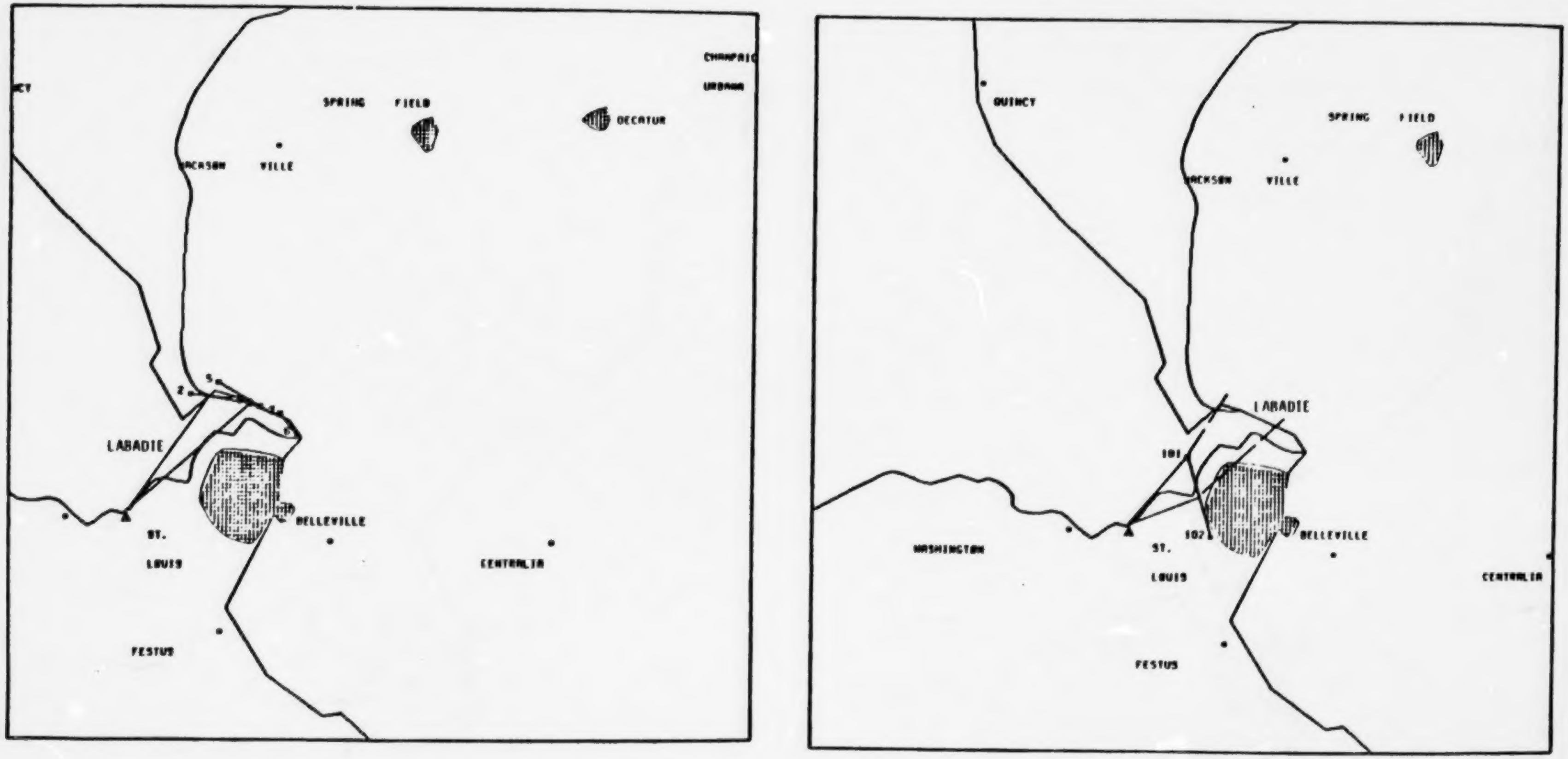
SPRING FIELD
DECATUR
URBANA
VILLE
LABADIE
ST. LOUIS
BELLEVILLE
CENTRALIA
FESTUS
2
5
QUINCY
101
102
WASHINGTON

(w) 28 July 1976

(x) 28 July 1976

Figure 5 (Continued).

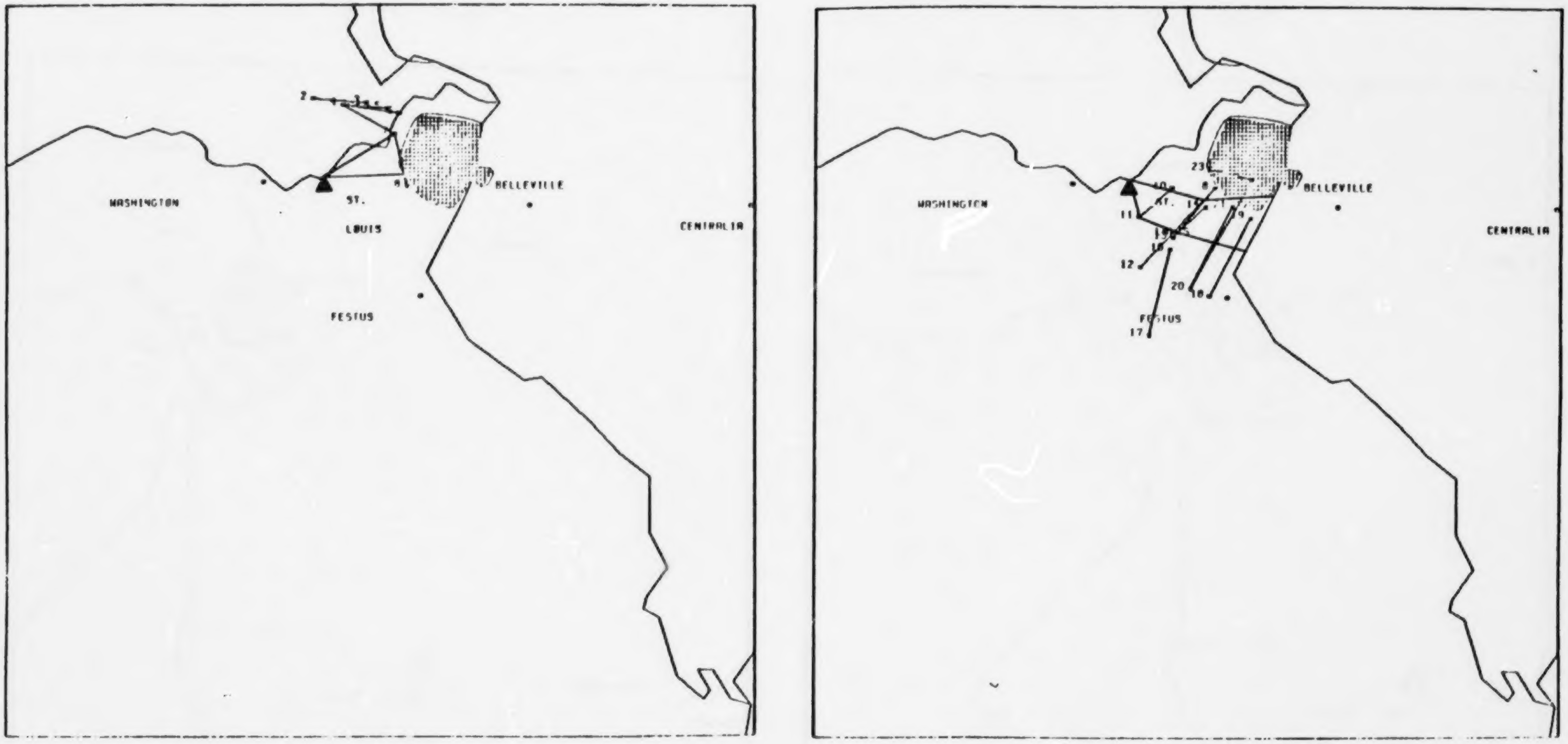
WASHINGTON
ST.
LOUIS
FESTUS
BELLEVILLE
CENTRALIA
2
WASHINGTON
ST.
FESTUS
BELLEVILLE
CENTRALIA
23
8
10
11
12
17
20
9

(y) 30 July 1976

(z) 30 July 1976

Figure 5 (Concluded).

Shown in Figure 6(a) through 6(j) are rough estimates of the spread of the Labadie plume as a function of altitude and distance from the Labadie Power Plant. It should be noted, however, that there is considerable uncertainty associated with these estimates of plume width. They were determined by examining the widths of our alleged Labadie SO_2, NO_x, and O_3 plume profiles measured at a number of altitudes along the aircraft traverse paths shown in the figures. Widths were estimated by assuming the concentrations at the plume boundaries to be about 10 percent above (or below in the case of O_3 depletion) background levels. The uncertainty in our estimates of plume widths is attributable to the potential for error in determining plume position; the error associated with the estimate of a width along a single traverse path; and the distortion of the plume signature owing to instrument response and averaging times. Unfortunately, we have no way to estimate the magnitude of the combined uncertainty, but we can examine the variability of estimated plume widths between passes to provide a lower bound estimate of the uncertainty associated with the plume spread values.

The estimated plume widths plotted in Figure 6 help one visualize the shapes of Labadie plume cross sections at various downwind distances. When spirals (vertical traverses) through the plumes were available at given downwind distances, we also show the estimated depth of the plume in these figures by sketching in a cross-sectional shape. Where no spirals were made, estimates of the depth and shape of the plume are speculative. Indeed, on some days only one traverse was made at some distances, providing no vertical resolution of plume geometry (e.g., 2 July 1976 at 21 km, 5 July 1976 at 42 km, and others). At other times, several traverses were made--along one the concentration data may indicate the presence of a plume, and along another no trace of a plume can be found. This result sometimes occurs even when two traverses are made at nearly the same altitude (e.g., 2 July 1976 at 120 km, 14 July 1976 at 23 and 44 km). Generally, the concentration data measured by MRI and WU aircraft and plotted in these figures do not provide clear pictures of Labadie plume geometries.

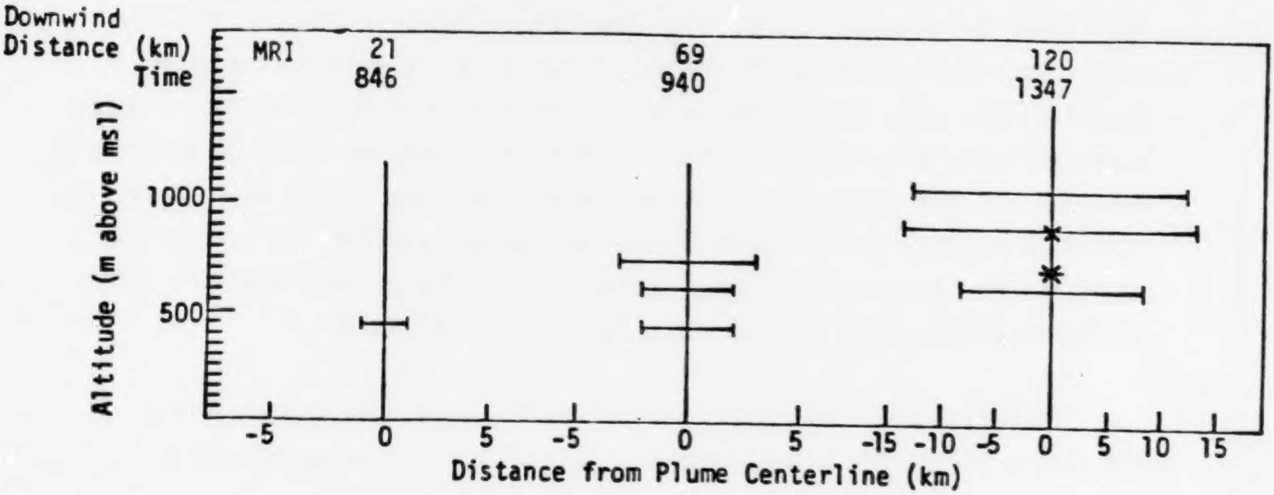

(a) 2 July 1976

Figure 6. Estimates of the spread of the Labadie plume as a function of altitude and distance from the Labadie power plant.

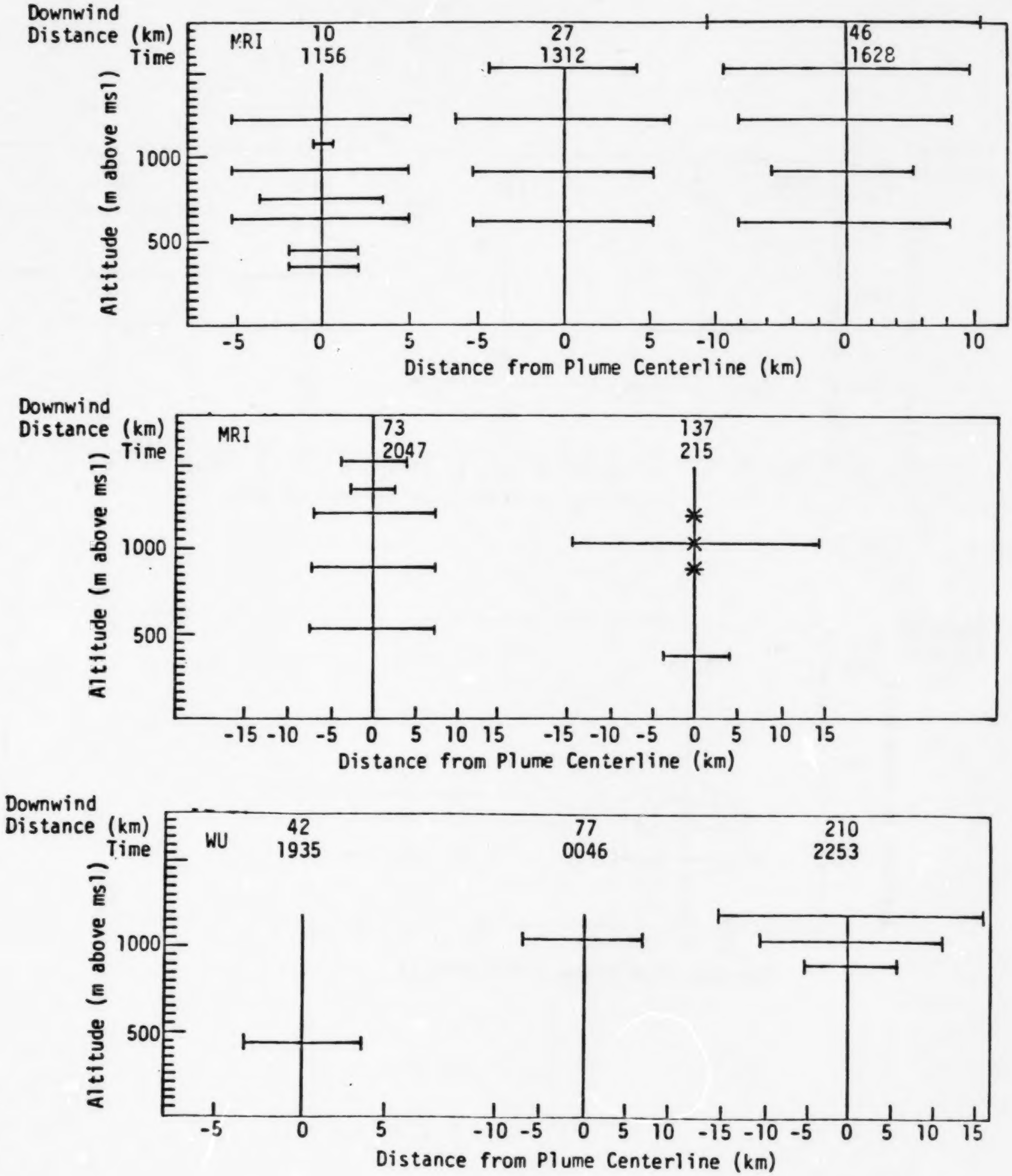

(b) 5 July 1976

Figure 6 (Continued).

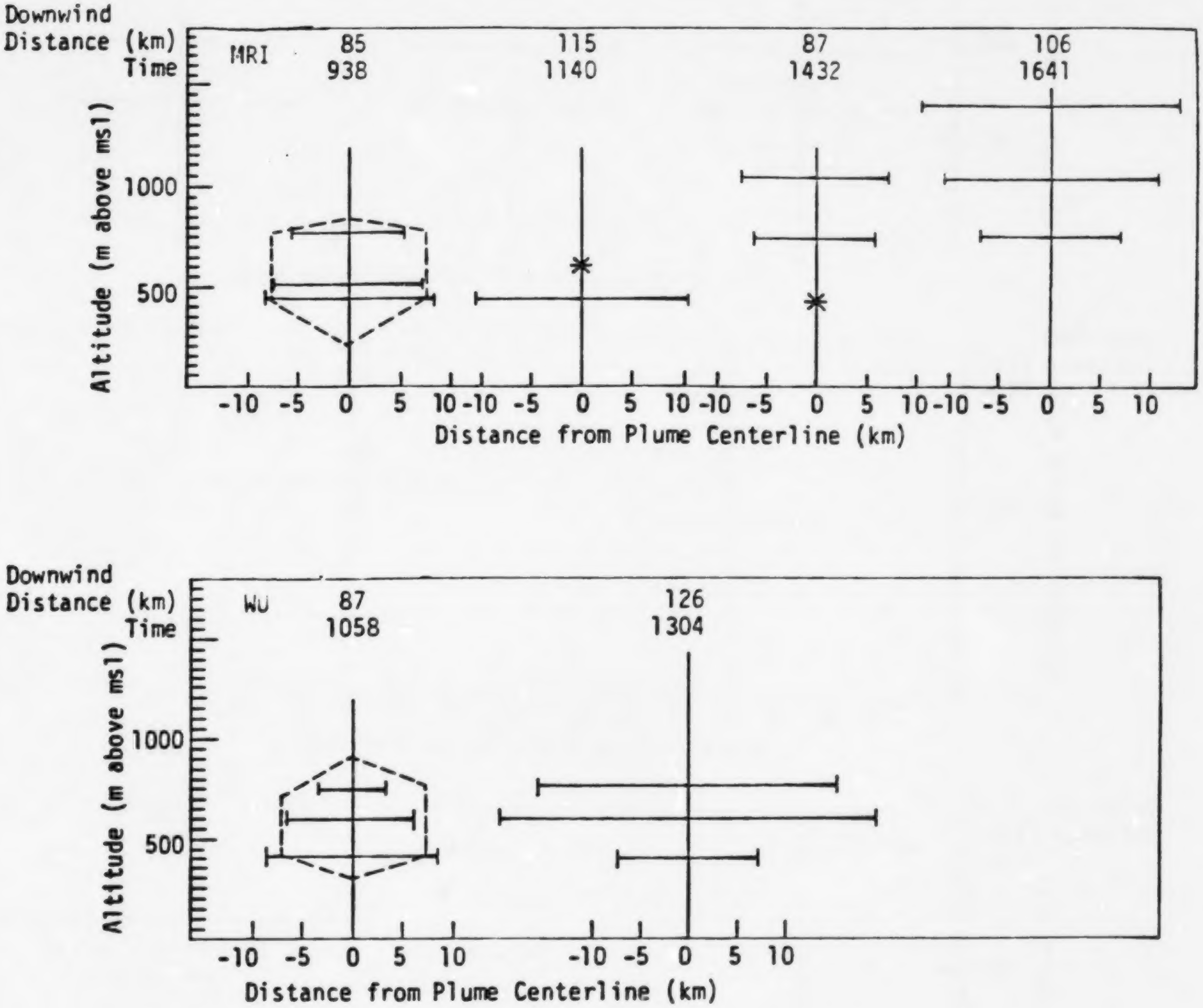

(c) 7 July 1976

Figure 6 (Continued).

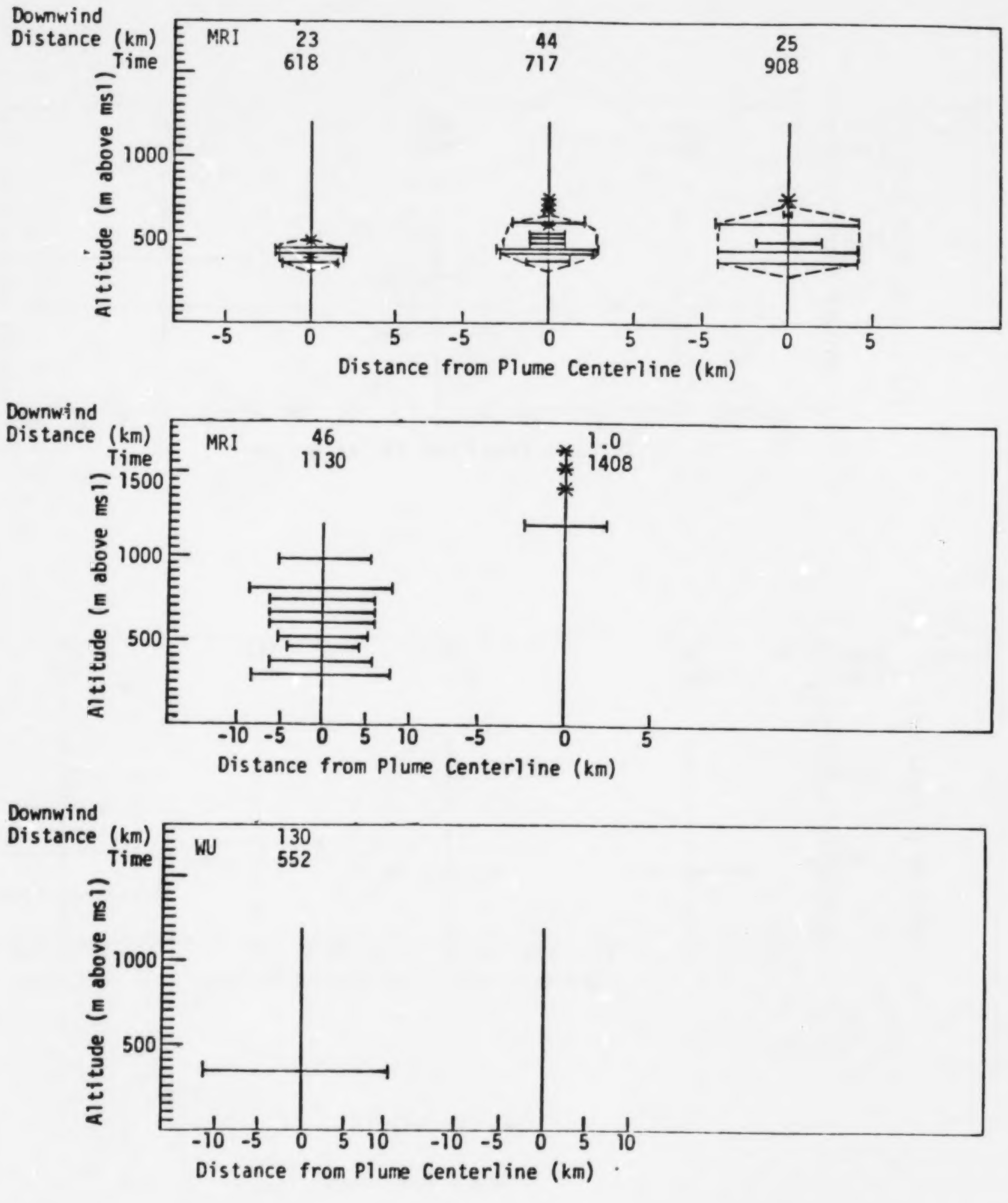

(d) 14 July 1976

Figure 6 (Continued).

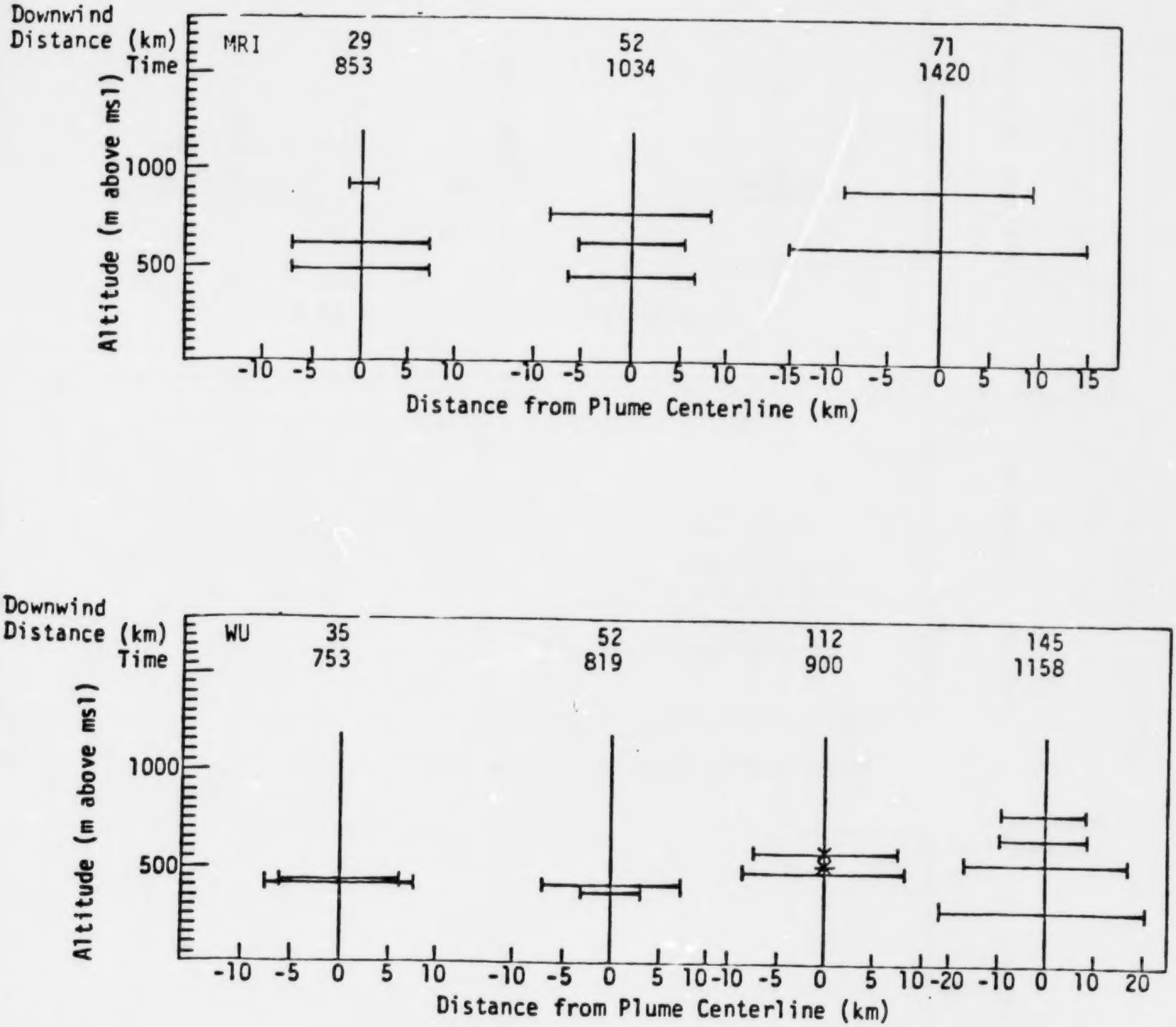

(e) 15 July 1976

Figure 6 (Continued).

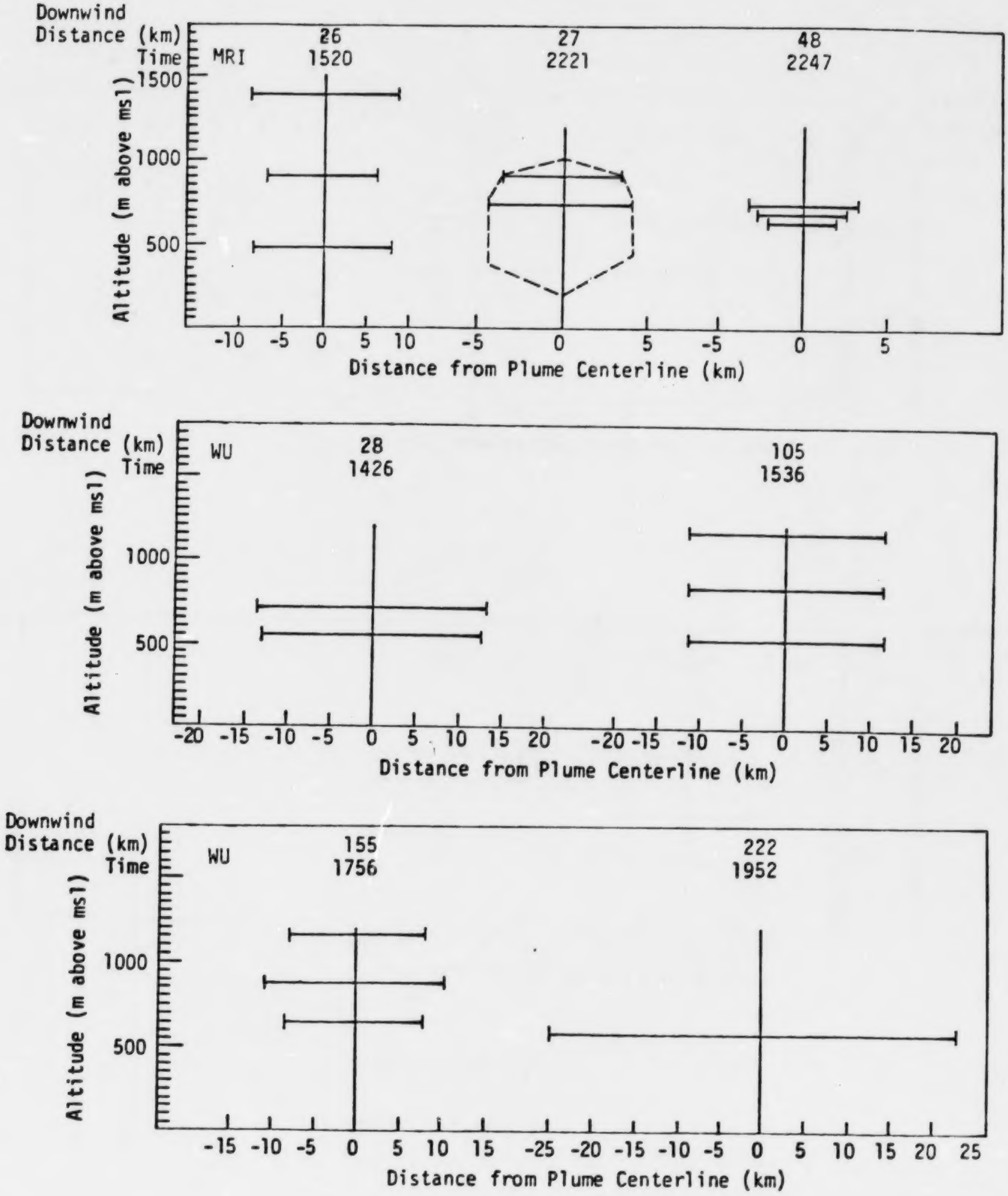

(f) 18 July 1976

Figure 6 (Continued).

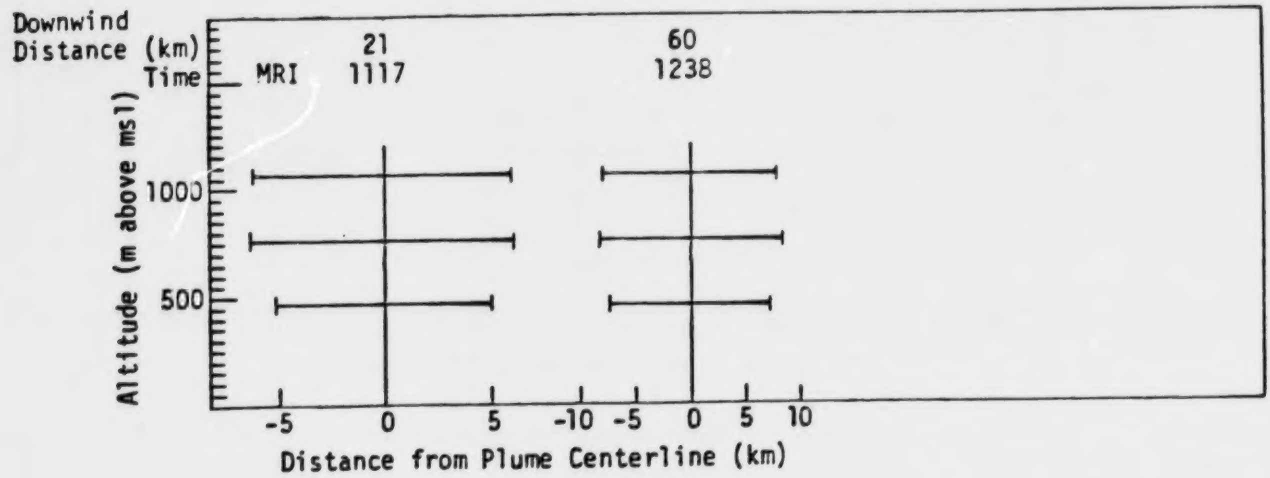

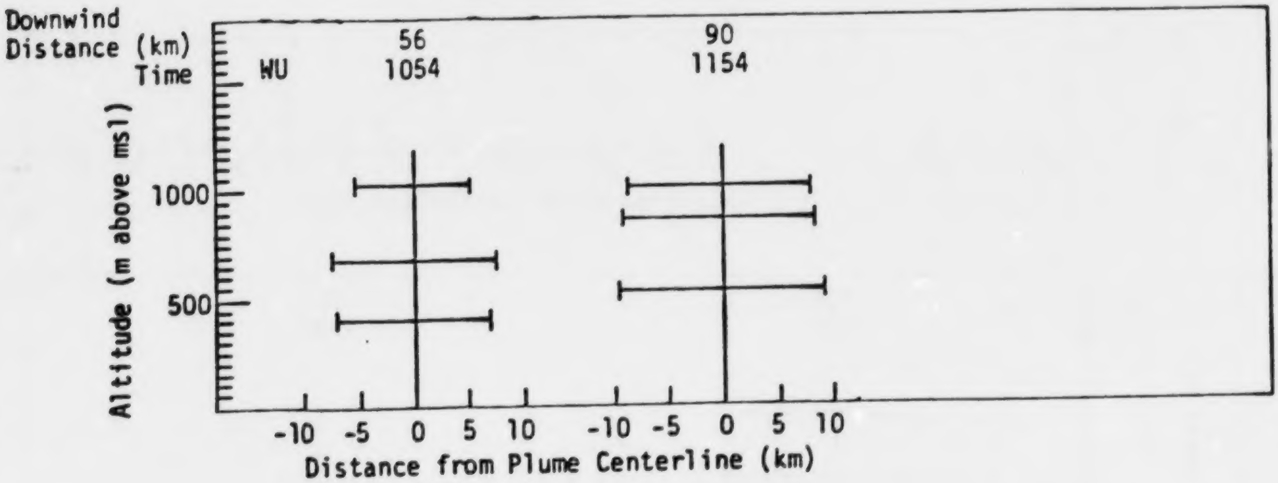

(g) 20 July 1976

Figure 6 (Continued).

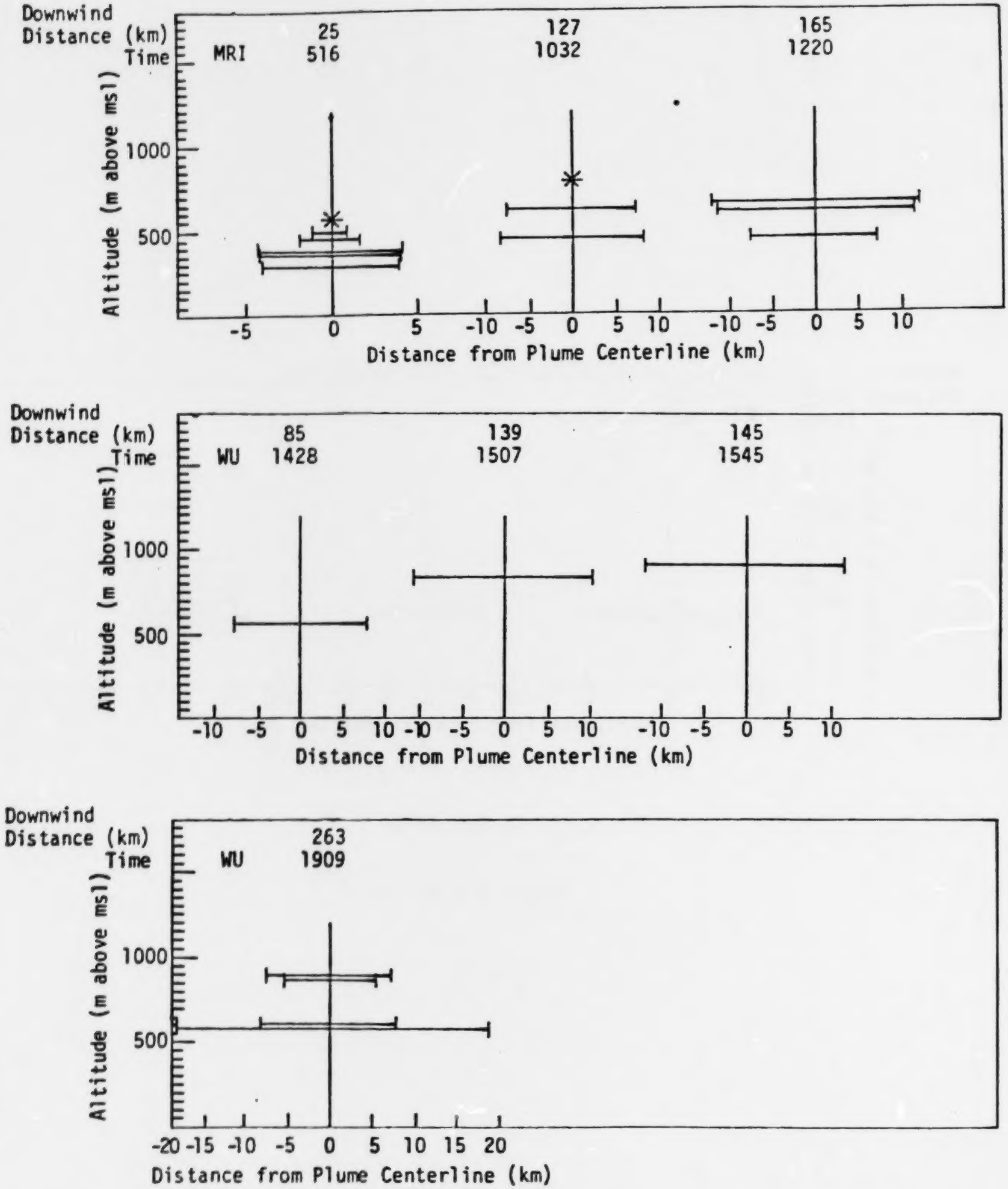

(h) 23 July 1976

Figure 6 (Continued).

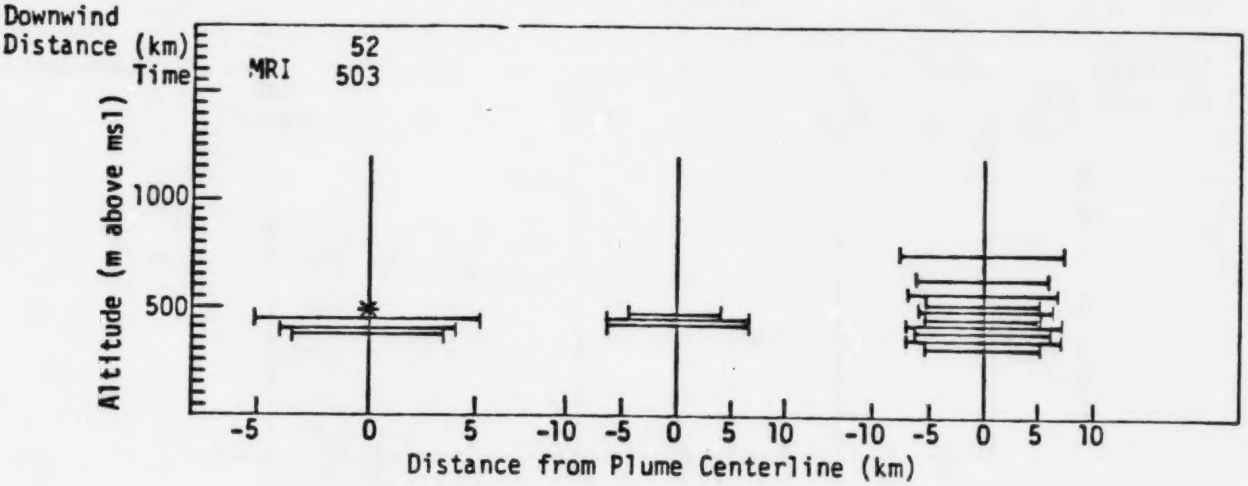

(i) 28 July 1978

Figure 6 (Continued).

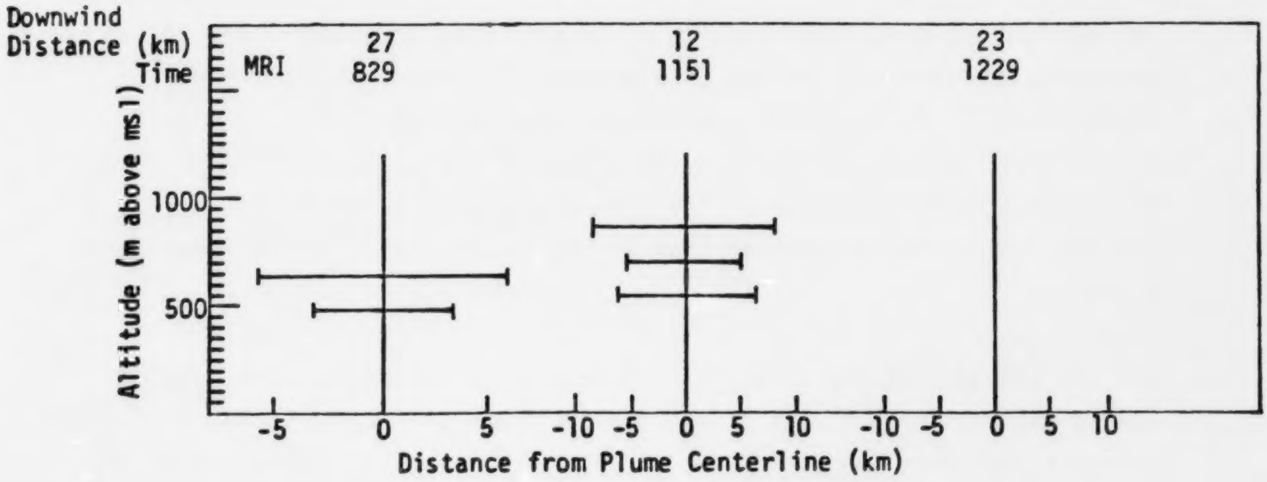

(j) 30 July 1978

✱ Indicates traverse at that altitude shows no plume.

Figure 6 (Concluded).

The plume geometry and location problems described above can be attributed to the nature of aircraft concentration measurements. First, since the aircraft is moving at about 100 knots, measurements of concentrations at any point are virtually instantaneous and distorted because of lags in the measurement system. The sampling ports of the aircraft are very small (on the order of inches), so the instantaneous measurements are also only representative of small volumes of air. These small spatial and temporal scales inherent in aircraft measurement are inconsistent with those associated with the air quality models being used, which are based on temporal and spatial averaging of processes (scales greater than 15 minutes and 100 meters, respectively). For example, the aircraft may pass through a plume puff on one traverse but not the next (this may, in fact, have occurred on some MISTT traverses); the value of the time-averaged plume concentration, on the other hand, may be between that of the instantaneous puff concentration and zero.

In addition to the aircraft measurements of concentrations, limited remote sensing measurements of the Labadie plume were carried out by Stanford Research Institute (SRI) and Environmental Measurements, Incorporated (EMI) during the 1976 MISTT program. SRI used a ground-based LIDAR device to measure plume dimensions, and EMI supplied airborne correlation spectrometer (COSPEC) measurements of plume concentration burdens. Both types of measurements are valuable for plume modeling because they are usually representative of large spatial and temporal scales. Unfortunately, both the SRI and MRI measurement activities were very limited during the 1976 MISTT program; neither group collected much data, nor were they funded to prepare data summaries. Only the limited LIDAR data published by Uthe and Wilson (1977) are available to us for this study. We used them to corroborate the MRI and Washington University data.

Examination of the plume concentration measurements on the relatively data-rich days, 5 and 14 July, provides some indication of the magnitude of the uncertainty in plume dispersion estimates. For both days, we have tabulated (see Table 2) ranges of plume widths and depths derived from the concentration data and associated ranges of stability categories. Typically, these ranges would result in order-of-magnitude ranges of computed maximum ground-level concentrations [see Turner (1969), for example]. Obviously, we cannot rely on these estimates of plume geometry to provide exact specifications of plume dispersion for the plume models. In Chapter V, we suggest a method to improve the dispersion estimates.

2. Emissions Rates and Source Data

The rates of NO, NO_2, and SO_2 emissions from the Labadie stacks will be computed for the pertinent hours on each of the 10 case study days from data supplied by the contract monitor. In addition, the contract officer has provided source data such as stack heights, flow rates, diameters, and temperatures. Preparation of these data for input to the model is a relatively simple task.

3. Ambient Concentrations

Ambient concentrations of O_3, NO, NO_2, SO_2, and hydrocarbons will be determined from aircraft measurements outside the plume. Included will be data from hydrocarbon grab samples analyzed by gas chromatography during the program in the field. Ambient data will be spatially (horizontally and vertically) averaged for each downwind location. Coding of this information in a form suitable for model input is also a relatively simple task.

It should be noted that there appear to be some problems with the hydrocarbon analyses carried out on the grab samples. Higher hydrocarbon (i.e., large carbon number molecules) determinations by gas chromatography appear to be in error (Rasmussen et al., 1976). In any case, the analysis method currently employed does not permit identification of the complete hydrocarbon composition nor accurate portrayal of the reactivities of the hydrocarbon mass. The

TABLE 2. RANGES OF LABADIE PLUME WIDTHS AND DEPTHS ON 5 AND 14 JULY 1976

Date	Time	Downwind Distance (km)	Measurement Group	Plume Width or Range of Widths (km)	Plume Depth or Range of Depths (m)	Corresponding Stability Category or Range of Stability Categories
July						
5	1156	10	MRI	7-10	850-1500	A-D
	1312	27	MRI	10-12	900-2000	B-D
	1628	46	MRI	16-22	1200-1800	A-D
	1935	42	WU	9	?	D
	2047	73	MRI	14-16	1000-1500	C-D
	2253	210	WU	10-34	7300	E-F
	0046	77	WU	15	?	C-D
	0215	137	MRI	30	?	B-C
14	0532	130	WU	22	?	C
	0618	23	MRI	4	100-200	A-F
	0717	44	MRI	2-6	250-400	C-F
	0908	25	MRI	4-8	250-400	C-F
	1130	46	MRI	8-16	700-1300	B-F
	1408	1.0	MRI	4	?	>A

chemical rate processes imbedded in RPM-II are sensitive to the ambient hydrocarbon concentrations and composition. Therefore, uncertainties in model predictions owing to these hydrocarbon analysis problems may be large.

4. Sunlight Intensity

Ultraviolet light (UV) intensities measured at six ground-level RAPS stations will be averaged over short time periods (about 10 minutes) for all simulation periods. The RAPS UV data were supplied by the contract monitor. Input for these averaged values to the model do not present any problems.

5. Wind Fields

Wind speeds and directions are obtained from the pibal study carried out as part of MISTT. At each aircraft traverse location, wind information is obtained for releases closest in time and altitude. If multiple pibals were released, their data are vector-averaged at each time and altitude. Wind data to be input to the model are shown with the concentration plots in Volume II.

V EVALUATION OF RPM-II AND SIMPLE MODEL PERFORMANCE

Ten case study days have been selected from the MISTT data base for use in evaluating the performance of RPM-II and the simple NO_2 model predictions, as described in the previous chapter. An evaluation of the models was conducted using a "restricted data base," which is comparable to the data base available from NWS, state, and local meteorological and air monitoring stations. The restricted data base will resemble the information that would be available to a typical user. A strict evaluation or validation of model performances is not possible because of the data problems previously discussed. Instead, the relative performances of RPM-II and the three simple models can be evaluated; that is, how each model performs under generalized conditions compared to the other models. From these comparisons it can be learned under what types of conditions or situations the simple models might be appropriate and under what conditions a more sophisticated model such as RPM-II is required. Furthermore, inherent limitations and general tendencies in the predictions of each model may be discerned by comparison of simple statistics computed for each model's predictions.

This chapter outlines the procedures followed in specifying input data for the models, given the limitations of the MISTT data base and the requirements for the restricted data base. It presents the input data used for each modeling scenario along with the predictions of RPM-II and of three simple models (CNOM, OLM, and TCM). Finally, the performance of the model is discussed.

A. PROCEDURES FOR THE SPECIFICATION OF INPUT DATA

In Chapter IV the input requirements of RPM-II and the simple models were discussed. The data collected during the MISTT program that could be used to satisfy these requirements were also presented. However, some special problems regarding the estimation of ambient hydrocarbon and plume dispersion rates from the MISTT data were noted. Procedures used to specify ambient hydrocarbon levels and plume dispersion rates for model input are identified in the first part of this section. Furthermore, computations are described that are used to supplement MISTT data in preparing photolysis rates, initial concentrations, and ambient NO and NO_2 concentration inputs to the models.

A description of the procedures followed in constructing a restricted data base are presented in the second part of this section. The discussion centers on specification of wind speeds and dispersion data using meteorological data collected at Lambert Field in St. Louis. Procedures for specifying other parameters in the restricted data set are identical to those used for specifying the "unrestricted" MISTT data set. With the exception of airborne measurements of ambient NO, NO_2, and O_3 concentrations, the typical model user would have access to types of model input data similar to those that were available to us in preparing the MISTT data base for model exercises. As is apparent from the MISTT data (from concentration and temperature soundings), vertical mixing was rather vigorous during the 10 case study days. For that reason, and also to spare the added cost of acquiring and collating ground-level aerometric data (e.g., from the RAMS network), we assume that the airborne measurements of ambient NO, NO_2 and O_3 are representative of what would be measured at ground-level if ground-level interferences were eliminated.

1. Procedures for the Specification of the Unrestricted Data Set

a. Ambient Concentrations

All four models require estimates of ambient concentrations as a function of downwind distance. TCM requires only ambient NO_2; OLM requires ambient NO_2 and O_3; CNOM requires ambient NO, NO_2, and O_3; and RPM-II requires ambient NO, NO_2, O_3, and hydrocarbons (separated into paraffin, olefin, aromatics, and aldehyde species groupings).

Ambient SO_2, NO, NO_2, and O_3 concentrations were computed by averaging all available MRI and W.U.* aircraft measurements made outside what was identified as the Labadie plume at each downwind traverse location. Most often, average NO concentrations determined in this fashion were nearly as large as the average NO_x concentration;† this situation results in unrealistically low ambient NO_2 concentrations if NO_2 values are computed by substracting NO from NO_x values. The discrepancy is probably caused by instrument errors--for example, during MISTT, MRI calibrated their aircraft's NO_x monitor with NO only. Therefore, the following relationship, derived from the photostationary state assumption, was used to compute the ambient NO_2 concentration for model input:

$$[NO_2] = [O_3]\,[NO]\,k_3/k_1 \quad . \qquad (12)$$

The photostationary state assumption is known in many cases to approximate closely the relationship between atmospheric NO, NO_2, and O_3 in the presence of sunlight (Calvert, 1976). However, it has been shown that in some cases observed NO_2 concentrations are lower than the equilibrium values estimated from equation (12) (Hegg et al., 1977), probably because the reaction rates are limited by the rate of reactant mixing. For ambient concentrations, one would not expect the chemistry to be limited by the mixing because concentrations are relatively low and reaction rates are relatively slow; in a plume near the stack, however, where concentrations are high, the mixing rate could significantly affect the reaction rates. Despite these potential problems, equation (12) was also used in computing plume NO_2 concentrations to compare with model output, because most MISTT aircraft plume traversals were made at distances considerably downwind of the stacks (10 to 200 km), and because a more reasonable, convenient method has not been found. In hours of darkness, NO_2 could be determined only by subtracting the averaged NO value from the averaged NO_x value.. On a few occasions--daylight only--the measured NO values were of questionable validity;* in these cases, NO_2 was computed using the form of the photostationary state relationship dependent on NO_x rather than NO:

---

* W.U. aircraft did not measure NO or NO_x.

† Only NO and NO_x concentrations--not NO_2 concentrations--were reported by MRI.

$$[NO_2] = [NO_x] \bigg/ \left[1 + \frac{k_1}{k_3 [O_3]}\right] \quad , \qquad (13)$$

and NO concentrations were also adjusted using:

$$[NO] = [NO_x] \bigg/ \left[\frac{k_3 [O_3]}{k_1} + 1\right] \quad . \qquad (14)$$

Otherwise, no adjustments were made to NO or O_3 plume and ambient concentrations.

The uncertainties associated with concentrations of ambient hydrocarbons on the case study days are of greater concern to us than the uncertainties associated with NO, NO_2, and O_3. As noted earlier, there were problems with hydrocarbon analyses carried out on MISTT grab samples. In addition to the insensitivity of the best, currently available, practical analysis technique (gas chromatography) to many reactive hydrocarbon species, the MISTT samples analyzed using this technique appear to have been contaminated (Rasmussen et al., 1976). Therefore, we were forced to rely on the only alternative source of hydrocarbon data, RAPS hydrocarbon sample analyses, to characterize the hydrocarbons entrained into the Labadie plume. However, because RAPS samples were collected at ground level at times and locations removed from the MISTT plume sampling times and locations, the RAPS analyses could provide only general guidance in specifying input to RPM-II. But RPM-II predictions, as mentioned earlier, are quite sensitive to ambient hydrocarbon values, because the speed of a photochemical reaction system is determined by both the concentration and reactivity of the hydrocarbons present. Because of undesirably large uncertainties in these particularly important input data, the method for specifying the input values and its effects on the conclusions we reach concerning model performance must be clearly stated.

---

* Usually when NO was near zero while NO_x had a large nonzero value.

The large uncertainties in hydrocarbons input data (and in the plume dispersion rates to be discussed next) preclude an evaluation, in the strict sense of the word, of model performance. It is, nevertheless, worthwhile to see whether models can match the observation of plume concentrations within the bounds of instrument accuracy, if the flexibility is allowed to adjust the crucial concentration input parameters within reasonable bounds. Such an exercise certainly does not constitute a verification of model(s) performance, but it is still of some value because it facilitates the following determinations:

> How well the model(s) performs within expected limits of input uncertainties.

> Whether the model(s) is consistent with existing knowledge about O_3 and NO_2 formation in plumes.

> Whether the model(s) is consistent with the observed phenomena.

To compensate for the uncertainties in hydrocarbon measurements, the ambient total reactive hydrocarbon concentrations input to RPM-II were adjusted between 0.1 ppmC and 0.4 ppmC. This range of concentrations appears to be fairly representative of ambient values measured by the RAPS network in St. Louis during the summer of 1976 (Cardwell, 1978). RPM-II plume ozone predictions were used as the key to adjustments of RPM-II input ambient hydrocarbon concentrations; if predicted plume ozone production was high or low compared with plume ozone measurements, total ambient hydrocarbons were decreased or increased, respectively, within the stated range of concentrations. Hydrocarbons were split into the paraffin, olefin, aromatic, aldehyde, and ethylene groupings required by the Carbon-Bond Mechanism used in RPM-II. Splits were derived from the reported results of the gas chromatographic analyses of RAPS grab samples (Cardwell, 1978); the following factors (fractions by weight) were used regardless of the ambient total hydrocarbon concentration selected: 60 percent paraffins, 2 percent olefins, 25 percent aromatics, 5 percent aldehydes, 2 percent ethylene, and 6 percent nonreactive species.

b. Plume Dispersion Rates

The simple models and RPM-II require dispersion rate information as a function of downwind distance. RPM-II requires this information in the form of plume widths and plume depths at various downwind distances. All three simple models rely upon the input of the dispersion parameter α (defined in equation V-5) at various downwind distances. After final adjustments to RPM-II input of plume widths and depths are established following the procedures described below, the dispersion parameters required by the simple models are computed using equation (V-5).

As explained in the previous chapter, the dispersion rates of the Labadie plume could not be determined precisely from the MISTT data. At best, plume dimensions* determined from MISTT aircraft measurements could be used to give a lower bound on the dispersion rates because of sampling time limitations inherent in the measurements and aircraft position uncertainties. Although the time required to complete a single pass through the plume is on the order of minutes, the model predictions are to be used to evaluate one hour impacts. But plume spread increases with increasing averaging periods, so the measured plume spreads can be expected to be smaller than those representative of one-hour average plume behavior required for model input. Because the time spent making multiple aircraft plume traversals at a variety of altitudes along a given path was usually about one hour (30 to 90 minutes), plume concentrations averaged during a series of traversals can be accepted as representative of about one hour averages within a large plume parcel. Therefore, to improve our estimation of plume spread input in the models, the following equation, based on mass conservation, was used for NO_x or SO_2:

---

* Plume dispersion rates refer to the rate at which a plume expands as it is advected downwind. Downwind plume dimensions are a manifestation of the plume dispersion rate; plume dimensions are computed by multiplying the dispersion rate by the downwind distance and dividing by the wind speed.

$$A(S) = [(E_i/U(S) - (C_{ia}\ A_o)]/(C_{ip}(S) - C_{ia}) \quad , \qquad (15)$$

where

$A(S)$ = plume cross-section area at downwind distance S (m^2),
E_i = emissions rate of species i (NO_x or SO_2), (ppm-m^3/sec or gm/sec),
$U(S)$ = wind speed at distance s (m/sec),
C_{ia} = measured ambient concentration of species i (ppm or gm/m^3),
A_0 = exit area of stacks (121.2 m^2),
$C_{ip}(S)$ = measured average plume concentration of species i at distance S (ppm or gm/m^3).

The purpose of this study is to evaluate the reactive species (NO_2, O_3, and NO) predictions of the model(s), so we used the areas computed for NO_x as a first guess; these generally agreed fairly well with areas computed for SO_2 at the same downwind distances. When an NO_x plume was not distinguishable in the aircraft data at a given downwind distance, the area computed for SO_2 was used as a first guess. Areas were computed for each distance at which aircraft traversals of the Labadie plume were made on the 10 case study days. Plume widths and depths used were consistent with these computed areas and with the general plume configurations, which are plotted in Figure 6. However, the RPM-II predictions in the study are not sensitive to how much of the cross-sectional plume area changes are attributable to width or depth changes (as long as both monotonically increase), because the same ambient concentrations are entrained on all sides of the plume.

Neither NO_x nor SO_2 is truly a conservative plume species, because some conversions to nitric acid, nitrates, PAN, sulfates, aerosols, and other species occur. Therefore, the areas computed using equation (15) are probably too large.* Nevertheless, the computed areas were input to RPM-II for a trial run; subsequent runs were made after adjusting plume areas to compensate for the conversion of NO_x predicted by RPM-II.

After final adjustment to the plume cross-sectional areas were made in RPM-II input, the dispersion parameters, α, required for the simple models were computed using

$$\alpha(S) = u^I A^I / [u(S)A(S) - u^I A^I] \quad , \qquad (16)$$

where u^I and A^I are the initial wind speed and plume cross-sectional area, respectively, and all other terms are defined as for equation (15).

c. Initial Concentrations

In this study RPM-II and the simple models simulations were initialized just downwind (≈1 km) of the stacks. RPM-II must be started farther downwind because the extremely high concentrations close to the stack cause instabilities in the numerical solution procedures and, furthermore, they are far beyond the range of concentrations for which the Carbon-Bond Mechanism was developed.

Although the simple models can be initialized at the stack without any difficulties, they were initialized in the same manner as RPM-II for the sake of consistency in comparison of predictions. TCM and OLM require that initial NO_x concentrations be input; CNOM requires initial NO, NO_2, and O_3 concentrations; RPM-II requires initial NO, NO_2, O_3, hydrocarbons (split into paraffin, olefin, aromatic, and aldehyde species groupings). Initial NO and NO_2 concentrations were computed assuming 10 percent and 90 percent of emitted NO_x as NO_2 and NO, respectively. Initial plume concentrations are computed using the following expression derived from the mass continuity relationship:

---

* Areas computed in equation (15) are too large because the plume concentrations of NO_x are reduced by chemical transformations and by dilution (i.e., plume dispersion). Equation (15) does not account for chemical transformations so it calculates greater dilution than required.

$$C_{pi}^I = [E_i/u + C_{ai}A^I - C_{ai}A_o]/A^I \quad , \qquad (17)$$

where

C_{pi}^I = initial plume concentration of species i,
E_i = emissions rate of species i,
u = wind speed,
C_{ai} = ambient concentration of species i,
A_o = stack exit area,
A^I = initial plume cross-sectional area.

In all runs 125,000 m^2 was assumed for A^I, which is a typical value for the cross-sectional area of an elevated plume in neutral to unstable conditions (Pasquill, 1976) and is confirmed through limited LIDAR measurements of the Labadie plume (Uthe and Wilson, 1977).

Emissions rates were derived from a listing of hourly averaged Labadie emissions rates provided by the Project Officer. The emissions release hour was computed by subtracting the time of transit to the first aircraft traverse location, computed from the average pibal winds, from the time of the traversal.

d. Photolysis Rates

Only RPM-II and CNOM require the specification of NO_2 photolysis rate in their input data. Both require photolysis information as a function of time or downwind distance.

Using a simple SAI computer package (Killus et al., 1977), time-varying solar-zenith angles for each of the 10 case study days were computed for the St. Louis area. Figure 7 shows the dependence of the NO_2 photolysis rate (k_1) on zenith angle assuming clear skies. Adjustments were made to the photolysis rates to account for the presence of cloud cover or other

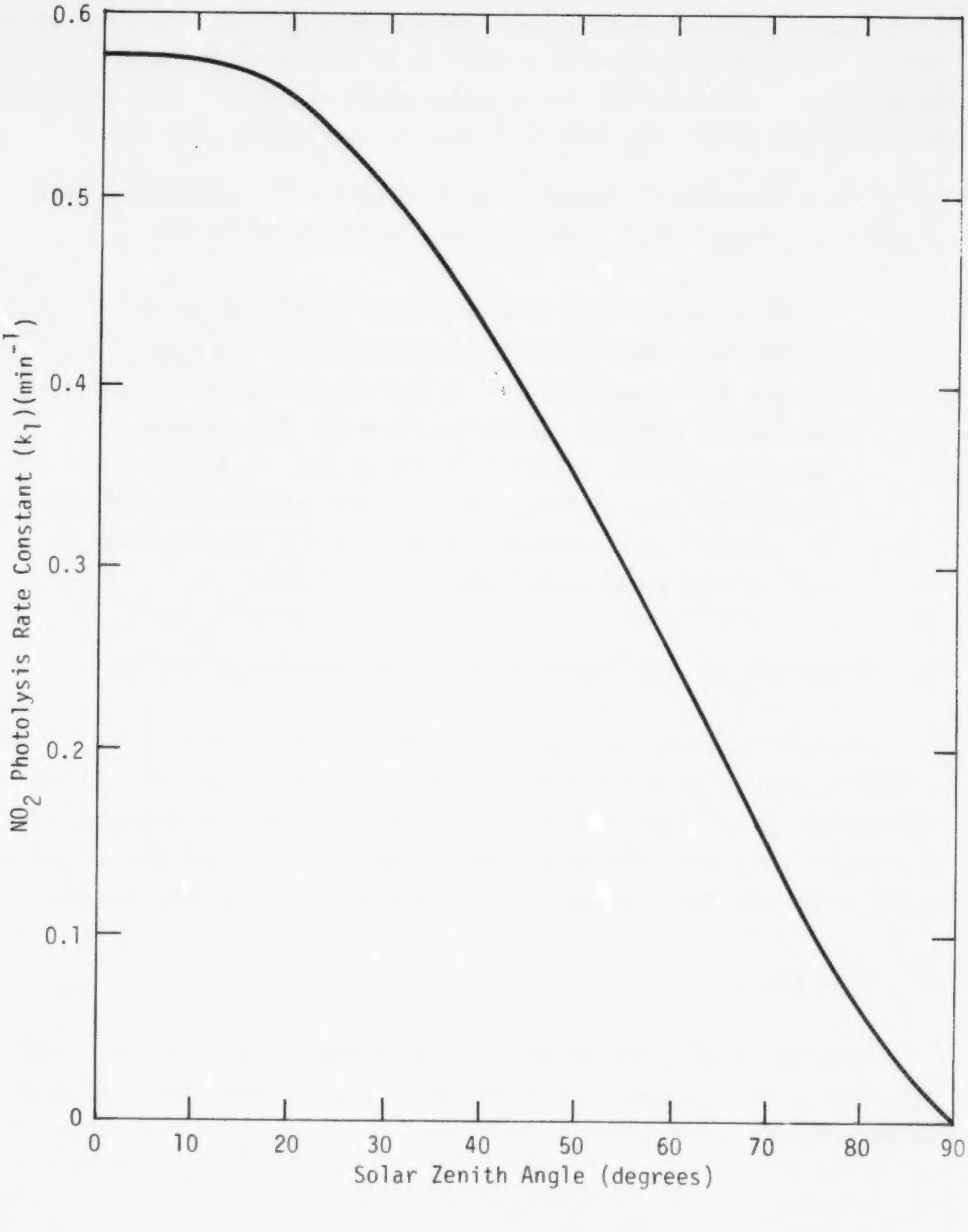

Figure 7. Estimated NO_2 photolysis rate constant as a function of solar zenith angle for unpolluted clear skies case.

radiation attenuation. The averaged measurements of solar ultraviolet (u.v.) intensity measured in several RAPS stations were used to make these adjustments. Adjustments to k_1 were assumed to be simply proportional to the deviation of u.v. intensity from its expected clear sky value. All other photolysis rates are adjusted by RPM-II to vary proportionally with k_1.

This procedure was adopted as an alternative to relating k_1 input directly to measured u.v. intensity for the following reasons:

> The RAPS stations are at ground level, not plume height.
> The RAPS u.v. measurements were rather noisy and subject to some drift problems, making them unreliable for specifying the absolute u.v. intensity; however, they provide useful indications of relative changes in u.v. intensity.
> The typical user of RPM-II or the simple models will probably not have u.v. measurements available to him and most likely will rely on solar zenith angle computations.

2. Procedures for the Specification of the Restricted Data Set

With the exception of wind speeds and dispersion rates (i.e., plume widths and depths as a function of downwind distance), all data in the restricted set are identical to those in the unrestricted data set. The procedures for determining wind speeds at stack height and plume dispersion rates using only NWS-type data sources are described in this section.

a. Wind Speeds

Wind speeds at plume height were determined by using surface-level wind speeds measured at Lambert Field and the following power law wind relationship Turner (1971):

$$u_p = u_o(h/7)^p \quad , \qquad (18)$$

where u_p = wind speed at stack height, u_o = surface level wind speed (7 m above ground), h = stack height (213 m for Labadie stacks), and the exponent p is dependent on stability class.

b. Dispersion Rates

Pasquill-Gifford stability classes were determined at various times during the day using the criteria presented by Turner (1971) and surface wind speed and cloud cover observations made at Lambert Field in St. Louis. Using these stability classes, horizontal plume spread parameters, σ_y, were determined using the plots of σ_y versus downwind distance and stability class presented by Turner (1971). Plume widths input to the model are simply four times σ_y.

Vertical plume depths were determined by using temperature sounding data collected at Lambert Field* and the TVA plots of σ_z versus downwind distance for the appropriate stability classes given by Carpenter et al. (1971). These were used instead of Pasquill-Gifford curves because TVA dispersion curves were developed using plume data collected for large power plants. Since the TVA temperature gradients were measured at plume height, the data show no unstable conditions, although there is an extremely high probability that unstable conditions existed near the ground (as in most of the cases discussed here) because a large portion of the data were collected during the midday hours and during the summer season (Weber, 1976). TVA curves were not used for σ_y estimates because of the very short sampling times involved in measurements of the horizontal plume dispersion of TVA plumes (Weber, 1976). Although typical of the type of information available to a model user, the dispersion estimates determined in this fashion may be underestimates of true one-hour-average dispersion rates. Plume depths were computed by adding 2 σ_z to the plume height if the plume height was less than 2 σ_z; otherwise, plume depth was assumed to be simply 4 σ_z. Even though no elevated temperature inversions were observed, we placed an upper limit of 3000 m on plume depths, because we felt that larger computed plume depths would be unreasonable for the St. Louis area.

---

* Collected as part of the RAPS program but are available at other sites as routine measurements.

B. MODEL INPUT WITH THE UNRESTRICTED DATA SET

The model input values of k_1, wind speed, plume depth, plume width, initial concentrations, ambient concentrations, and α are given as a function of time and downwind distance in Table 3. For some of the case study days, more than one modeling scenario is indicated. This occurred because not all of the aircraft plume traversals were made through the same Lagrangian plume parcel.* RPM-II is a Lagrangian model, and it can only simulate one parcel per run; separate runs are required to simulate additional plume segments. The data shown in Table 3 were used as input to RPM-II and the three simple models, CNOM, TCM, and OLM.

C. MODEL INPUT WITH THE RESTRICTED DATA SET

Model input values for all parameters in the restricted data set are identical to those in the unrestricted set, except for the wind speeds, plume widths, and plume depths. Shown in Table 4 are the meteorological parameters measured at Lambert Field and the input parameters derived from those measurements.

---

* A "Lagrangian" plume parcel is one that moves downwind with the mean wind.

TABLE 3. MODEL INPUT DATA FOR UNRESTRICTED DATA SET

(a) Case Study Date: 2 July 1976 (Scenario 1)

Local Time	Elapsed Time (min)	Downwind Distance (km)	k_1 (ppm/min)	Wind Speed (m/sec)	Plume Depth (m)	Plume Width (m)	Ambient (and Initial)* Concentrations (ppb)										
							SO_2	NO	NO_2	O_3	CO	PAR	OLE	ARO	CARB	ETH	α
							4170.0	2010.0	226.0	5.9	1630.0	181.0	6.8	75.2	15.8	6.0	
0800	0	0.1	0.185	9.0	250.0	500.0	0.0	14.0	82.0	45.3	1620.0	180.0	6.0	75.0	15.0	6.0	
0809	9	5.0	0.193	9.0	500.0	8000.0	0.6	14.0	82.0	61.0	1620.0	180.0	6.0	75.0	15.0	6.0	7.12×10^{-5}
1040	160	69.0	0.314	5.3	600.0	10,000.0	3.6	13.7	54.2	49.3	1620.0	180.0	6.0	75.0	15.0	6.0	7.98×10^{-5}
1246	286	120.0	0.196	8.0	1100.0	21,073.0	2.2	11.4	57.9	51.0	1620.0	180.0	6.0	75.0	15.0	6.0	1.35×10^{-5}

(b) Case Study Date: 5 July 1976 (Scenario 1)

Local Time	Elapsed Time (min)	Downwind Distance (km)	k_1 (ppm/min)	Wind Speed (m/sec)	Plume Depth (m)	Plume Width (m)	Ambient (and Initial)* Concentrations (ppb)										
							SO_2	NO	NO_2	O_3	CO	PAR	OLE	ARO	CARB	ETH	α
							4870.0	2320.0	180.0	1.59	1710.0	60.9	2.9	25.3	5.9	2.0	
1100	0	0.1	0.490	7.9	250.0	500.0	14.3	5.1	11.7	47.5	1620.0	60.0	2.0	25.0	5.0	2.0	
1121	21	10.0	0.517	7.9	1200.0	10,225.0	14.3	5.1	11.7	52.8	1620.0	60.0	2.0	25.0	5.0	2.0	2.98×10^{-5}
1155	55	27.0	0.558	8.5	1450.0	21,669.0	5.0	4.2	9.0	51.0	1620.0	60.0	2.0	25.0	5.0	2.0	1.05×10^{-5}
1241	101	46.0	0.335	5.3	1600.0	22,000.0	4.0	2.2	11.8	59.3	1620.0	60.0	2.0	25.0	5.0	2.0	1.39×10^{-5}

(c) Case Study Date: 5 July 1976 (Scenario 2)

Local Time	Elapsed Time (min)	Downwind Distance (km)	k_1 (ppm/min)	Wind Speed (m/sec)	Plume Depth (m)	Plume Width (m)	Ambient (and Initial)* Concentrations (ppb)										
							SO_2	NO	NO_2	O_3	CO	PAR	OLE	ARO	CARB	ETH	α
							7560.0	3630.0	323.0	2.1	1620.0	151.0	6.4	62.9	13.9	5.0	
1400	0	0.1	0.550	5.3	250.0	500.0	4.0	16.4	14.6	20.5	1620.0	138.0	4.6	57.5	11.5	5.0	
1624	144	46.0	0.379	5.3	1500.0	6106.0	4.0	16.4	14.6	59.3	1620.0	138.0	4.6	57.5	11.5	5.0	4.71×10^{-5}
1810	250	73.0	0.225	4.4	1500.0	50,493.0	4.8	15.4	14.6	80.2	1620.0	138.0	4.6	57.5	11.5	5.0	7.83×10^{-6}

TABLE 3 (Continued)

(d) Case Study Date: 7 July 1976 (Scenario 1)

Local Time	Elapsed Time (min)	Downwind Distance (km)	k_1 (ppm/min)	Wind Speed (m/sec)	Plume Depth (m)	Plume Width (m)	Ambient (and Initial)* Concentrations (ppb)										
							SO_2	NO	NO_2	O_3	CO	PAR	OLE	ARO	CARB	ETH	σ
							4410.0	2110.0	178.0	0.3	1700.0	151.0	5.8	62.7	13.3	5.0	
0700	0	0.1	0.085	9.0	250.0	500.0	1.3	4.2	24.8	21.0	1620.0	150.0	5.0	62.5	12.5	5.0	
0937	157	85.0	0.226	9.0	750.0	30,880.0	1.3	4.2	24.8	50.0	1620.0	150.0	5.0	62.5	12.5	5.0	1.42×10^{-5}

(e) Case Study Date: 7 July 1976 (Scenario 2)

Local Time	Elapsed Time (min)	Downwind Distance (km)	k_1 (ppm/min)	Wind Speed (m/sec)	Plume Depth (m)	Plume Width (m)	Ambient (and Initial)* Concentrations (ppb)										
							SO_2	NO	NO_2	O_3	CO	PAR	OLE	ARO	CARB	ETH	σ
							3060.0	1470.0	118.0	1.9	1680.0	60.5	2.6	25.2	5.6	2.0	
1200	0	0.1	0.562	13.0	250.0	500.0	1.7	6.1	11.6	45.0	1620.0	60.0	2.0	25.0	5.0	2.0	
1346	106	83.0	0.291	13.0	1200.0	23,000.0	1.6	6.1	11.6	39.7	1620.0	60.0	2.0	25.0	5.0	2.0	4.33×10^{-6}
1419	139	108.0	0.218	12.0	1350.0	26,193.0	2.7	2.6	9.9	35.5	1620.0	60.0	2.0	25.0	5.0	2.0	3.27×10^{-6}

(f) Case Study Date: 14 July 1976 (Scenario 1)

Local Time	Elapsed Time (min)	Downwind Distance (km)	k_1 (ppm/min)	Wind Speed (m/sec)	Plume Depth (m)	Plume Width (m)	Ambient (and Initial)* Concentrations (ppb)										
							SO_2	NO	NO_2	O_3	CO	PAR	OLE	ARO	CARB	ETH	σ
							4450.0	2210.0	170.0	0.9	1840.0	211.0	7.9	87.7	18.4	7.0	
0600	0	0.1	0.285	8.6	250.0	500.0	19.6	1.7	10.3	71.8	1750.0	210.0	7.0	87.5	17.5	7.0	
0644	44	23.0	0.366	8.6	500.0	4060.0	19.6	1.7	10.3	71.6	1750.0	210.0	7.0	87.5	17.5	7.0	1.55×10^{-4}
0727	87	44.0	0.429	7.6	600.0	6498.0	16.8	2.1	12.7	64.1	1750.0	210.0	7.0	87.5	17.5	7.0	9.53×10^{-5}

TABLE 3 (Continued)

(g) Case Study Date: 14 July 1976 (Scenario 2)

Local Time	Elapsed Time (min)	Downwind Distance (km)	k_1 (ppm/min)	Wind Speed (m/sec)	Plume Depth (m)	Plume Width (m)	Ambient (and Initial)* Concentrations (ppb)										
							SO_2	NO	NO_2	O_3	CO	PAR	OLE	ARO	CARB	ETH	α
							8250.0	3920.0	285.0	0.9	1900.0	133.0	6.0	55.5	12.6	4.4	
0900	0	0.1	0.285	5.0	250.0	500.0	49.6	3.4	11.2	39.3	1750.0	132.0	4.4	55.0	11.0	4.4	
1133	153	46.0	0.516	5.0	800.0	38,750.0	49.6	3.4	11.2	75.3	1750.0	132.0	4.4	55.0	11.0	4.4	1.88×10^{-5}

(h) Case Study Date: 15 July 1976 (Scenario 1)

Local Time	Elapsed Time (min)	Downwind Distance (km)	k_1 (ppm/min)	Wind Speed (m/sec)	Plume Depth (m)	Plume Width (m)	Ambient (and Initial)* Concentrations (ppb)										
							SO_2	NO	NO_2	O_3	CO	PAR	OLE	ARO	CARB	ETH	α
							4750.0	2270.0	173.0	0.8	1370.0	133.0	5.3	53.2	11.9	4.4	
0800	0	0.1	0.235	8.7	250.0	500.0	2.7	2.2	8.8	38.2	1280.0	132.0	4.4	55.0	11.0	4.4	1
0855	55	29.0	0.295	8.7	1000.0	20,860.0	2.7	2.2	8.8	48.0	1280.0	132.0	4.4	55.0	11.0	4.4	1.68×10^{-5}
0944	104	52.0	0.312	6.8	1000.0	29,540.0	2.8	2.2	10.8	64.3	1280.0	132.0	4.4	55.0	11.0	4.4	1.41×10^{-5}

(i) Case Study Date: 18 July 1976 (Scenario 1)

Local Time	Elapsed Time (min)	Downwind Distance (km)	k_1 (ppm/min)	Wind Speed (m/sec)	Plume Depth (m)	Plume Width (m)	Ambient (and Initial)* Concentrations (ppb)										
							SO_2	NO	NO_2	O_3	CO	PAR	OLE	ARO	CARB	ETH	α
							6660.0	3010.0	228.0	1.7	1740.0	91.1	4.2	37.9	8.7	3.0	
1400	0	0.1	0.550	5.7	250.0	500.0	20.3	3.8	10.5	63.1	1620.0	90.0	3.0	37.5	7.5	3.0	1
1516	75	26.0	0.484	5.7	1800.0	28945.0	20.3	3.8	10.5	52.3	1620.0	90.0	3.0	37.5	7.5	3.0	1.64×10^{-5}

TABLE 3 (Continued)

(j) Case Study Date: 20 July 1976 (Scenario 1)

Local Time	Elapsed Time (min)	Downwind Distance (km)	k_1 (ppm/min)	Wind Speed (m/sec)	Plume Depth (m)	Plume Width (m)	Ambient (and Initial)* Concentrations (ppb)										
							SO_2	NO	NO_2	O_3	CO	PAR	OLE	ARO	CARB	ETH	α
							6870.0	3290.0	248.0	1.3	1060.0	61.3	3.3	25.4	6.3	2.0	
1000	0	0.1	0.403	6.0	250.0	500.0	5.0	3.9	10.4	45.1	926.0	60.0	2.0	25.0	5.0	2.0	
1058	58	21.0	0.485	6.0	1000.0	27,620.0	5.0	3.9	10.4	57.7	926.0	60.0	2.0	25.0	5.0	2.0	1.84×10^{-5}
1300	180	60.0	0.562	4.7	1050.0	28,571.0	5.3	4.2	13.5	75.0	926.0	60.0	2.0	25.0	5.0	2.0	1.68×10^{-5}

(k) Case Study Date: 23 July 1976 (Scenario 1)

Local Time	Elapsed Time (min)	Downwind Distance (km)	k_1 (ppm/min)	Wind Speed (m/sec)	Plume Depth (m)	Plume Width (m)	Ambient (and Initial)* Concentrations (ppb)										
							SO_2	NO	NO_2	O_3	CO	PAR	OLE	ARO	CARB	ETH	α
							5320.0	2550.0	184.0	0.0	577.0	61.0	3.0	25.3	6.0	2.0	
0500	0	0.1	0.0	6.9	250.0	500.0	11.6	10.0	0.8	0.0	525.0	60.0	2.0	25.0	5.0	2.0	
0600	60	25.0	0.065	6.9	500.0	15,362.0	11.6	10.0	0.8	5.1	525.0	60.0	2.0	25.0	5.0	2.0	4.81×10^{-5}
0958	298	127.0	0.469	7.3	750.0	53,333.0	9.7	11.0	51.1	91.3	525.0	60.0	2.0	25.0	5.0	2.0	7.48×10^{-6}
1153	413	165.0	0.558	3.7	750.0	258700.0	14.0	10.7	39.1	84.3	525.0	60.0	2.0	25.0	5.0	2.0	3.53×10^{-6}

(l) Case Study Date: 28 July 1976 (Scenario 1)

Local Time	Elapsed Time (min)	Downwind Distance (km)	k_1 (ppm/min)	Wind Speed (m/sec)	Plume Depth (m)	Plume Width (m)	Ambient (and Initial)* Concentrations (ppb)										
							SO_2	NO	NO_2	O_3	CO	PAR	OLE	ARO	CARB	ETH	α
							2010.0	961.0	72.5	0.0	1200.0	120.0	4.4	50.0	10.4	4.0	
0400	0	0.1	0.0	14.0	250.0	500.0	5.2	4.3	3.2	0.0	1160.0	120.0	4.0	50.0	10.4	4.0	
0502	62	52.0	0.0	14.0	450.0	7573.0	5.2	4.3	3.2	0.9	1150.0	120.0	4.0	50.0	10.0	4.0	4.15×10^{-5}

TABLE 3 (Concluded)

(m) Case Study Date: 28 July 1976 (Scenario 2)

Local Time	Elapsed Time (min)	Downwind Distance (km)	k_1 (ppm/min)	Wind Speed (m/sec)	Plume Depth (m)	Plume Width (m)	Ambient (and Initial)* Concentrations (ppb)										
							SO_2	NO	NO_2	O_3	CO	PAR	OLE	ARO	CARB	ETH	α
							7160.0	3430.0	271.0	0.9	1160.0	133.0	5.8	55.4	12.3	4.4	
0900	0	0.1	0.285	5.9	250.0	500.0	3.9	4.5	23.4	62.0	1020.0	132.0	4.4	55.0	11.0	4.4	
1016	76	27.0	0.392	5.9	750.0	40,000.0	3.9	4.5	23.4	84.1	1020.0	132.0	4.4	55.0	11.0	4.4	1.88×10^{-5}

(n) Case Study Date: 30 July 1976 (Scenario 1)

Local Time	Elapsed Time (min)	Downwind Distance (km)	k_1 (ppm/min)	Wind Speed (m/sec)	Plume Depth (m)	Plume Width (m)	Ambient (and Initial)* Concentrations (ppb)										
							SO_2	NO	NO_2	O_3	CO	PAR	OLE	ARO	CARB	ETH	α
							6050.0	2890.0	218.0	0.0	1300.0	181.0	7.2	75.3	16.2	6.0	
0400	0	0.1	0.0	5.0	250.0	500.0	11.8	1.2	7.5	0.0	1190.0	180.0	6.0	75.0	15.0	6.0	
0531	91	27.0	0.0	5.0	600.0	41,667.0	11.8	1.2	7.5	69.8	1190.0	180.0	6.0	75.0	15.0	6.0	1.98×10^{-5}

(o) Case Study Date: 30 July 1976 (Scenario 2)

Local Time	Elapsed Time (min)	Downwind Distance (km)	k_1 (ppm/min)	Wind Speed (m/sec)	Plume Depth (m)	Plume Width (m)	Ambient (and Initial)* Concentrations (ppb)										
							SO_2	NO	NO_2	O_3	CO	PAR	OLE	ARO	CARB	ETH	α
							10400.0	4960.0	380.0	1.3	1270.0	122.0	6.0	50.6	11.9	4.0	
1100	0	0.1	0.411	4.0	250.0	500.0	13.0	4.5	20.8	79.5	1070.0	120.0	4.0	50.0	10.0	4.0	
1150	50	12	0.463	4.0	950.0	73,684.0	13.0	4.5	20.8	79.5	1070.0	120.0	4.0	50.0	10.0	4.0	1.1×10^{-5}
1242	102	23	0.495	3.0	1150.0	79,391.0	12.2	1.5	6.0	84.5	1070.0	120.0	4.0	50.0	10.0	4.0	1.05×10^{-5}

(p) Case Study Date: 30 July 1976 (Scenario 3)

Local Time	Elapsed Time (min)	Downwind Distance (km)	k_1 (ppm/min)	Wind Speed (m/sec)	Plume Depth (m)	Plume Width (m)	Ambient (and Initial)* Concentrations (ppb)										
							SO_2	NO	NO_2	O_3	CO	PAR	OLE	ARO	CARB	ETH	α
							17800.0	8520.0	624.0	1.2	1590	243.0	11.4	101.0	23.4	8.0	
1000	0	0.1	0.385	2.3	250.0	500.0	5.0	1.5	7.5	78.0	1250	240.0	8.0	100.0	20.0	8.0	
1410	250	35.0	0.461	2.3	900.0	19,778.0	5.0	1.5	7.5	84.7	1250	240.0	8.0	100.0	20.0	8.0	6.87×10^{-5}

* The first row of values under this heading are the initial model inputs.

TABLE 4. MODEL INPUT DATA FOR RESTRICTED DATA SET

Date	Time	Downwind Distance (km)	Measured Surface Wind Speed (m/s)	Estimated Wind Speed At Stack Height (m/s)	Measured Cloud Cover (%)	Estimated Stability Category (P-G)	Estimated σ_y (m)	Estimated Plume Width (m)	Measured Lapse Rate (°C/1000 m)	Estimated σ_z (m)	Estimated Plume Depth (m)	α
2 July 1976	0809	5	6	10.0	30	A-B	1,000	4,000	-9	240	960	6.7×10^{-5}
	1040	69	6	10.0	100	B-C	5,000	20,000	-9	2000	3000	4.3×10^{-6}
	1246	120	7	11.6	100	C	7,000	28,000	-9	2200	3000	2.7×10^{-6}
5 July 1976	1121	10	5	8.3	0	A-B	1,600	6,400	-9	400	1600	3.1×10^{-5}
	1155	27	5	8.3	0	A-B	4,000	16,000	-9	1000	3000	6.6×10^{-6}
	1241	46	5	8.3	0	A-B	5,000	20,000	-9	1500	3000	4.4×10^{-6}
	1624	46	11	8.3	20	C-D	2,000	8,000	-10	1500	3000	6.3×10^{-6}
	1810	73	7	11.6	20	C-D	5,000	20,000	-10	1700	3000	3.9×10^{-6}
7 July 1976	0937	85	5	8.3	0	C-D	5,000	20,000	-8	2000	3000	5.5×10^{-6}
	1346	83	8	13.3	70	B-C	6,000	24,000	-8	2000	3000	2.9×10^{-6}
	1419	108	8	13.3	30	B-C	9,000	36,000	-8	2100	3000	1.9×10^{-6}
14 July 1976	0644	23	5	8.3	0	C-D	1,500	6,000	-9	1000	2500	2.1×10^{-5}
	0727	44	5	8.3	0	C-D	2,500	10,000	-9	1500	3000	1.0×10^{-5}
	1133	46	5	8.3	0	B-C	4,000	16,000	-13	1500	3000	7.1×10^{-6}
15 July 1976	0855	29	11	18.3	30	C-D	2,000	8,000	-10	1000	2600	7.4×10^{-6}
	0944	52	8	13.3	30	C-D	4,000	16,000	-10	1600	3000	4.4×10^{-6}
18 July 1976	1516	26	6	10.0	0	B-C	2,500	10,000	-10	1000	2800	8.7×10^{-6}
20 July 1976	1058	21	7	11.7	30	B-C	2,000	8,000	-14	1000	2800	1.1×10^{-5}
	1300	60	4	6.7	30	B-C	5,000	20,000	-14	1700	3000	7.1×10^{-6}
23 July 1976	0600	25	5	8.3	0	D-E	1,500	6,000	+7	1000	2400	2.1×10^{-5}
	0958	127	3	5.0	0	B-C	10,000	40,000	-9	2500	3000	4.2×10^{-6}
	1153	165	3	5.0	0	A-B	20,000	80,000	-11	3000	3000	2.1×10^{-6}
28 July 1976	0502	52	6	10.0	0	C-D	3,000	12,000	+16	1500	3000	5.4×10^{-6}
	1016	27	6	10.0	10	B-C	2,500	10,000	-13	1000	2600	1.1×10^{-5}
30 July 1976	0531	27	3	5.0	0	D-E	1,500	6,000	+16	1000	2700	2.6×10^{-5}
	1150	12	4	6.7	90	C-D	900	3,600	-15	450	1500	7.9×10^{-5}
	1242	23	5	8.3	90	C-D	1,500	6,000	-15	1000	2700	2.1×10^{-5}
	1410	35	5	8.3	90	C-D	2,500	10,000	-15	1200	3000	1.1×10^{-5}

D. RESULTS

RPM-II, TCM, OLM, and CNOM predictions of plume NO_2 concentrations; measured average plume SO_2, NO, NO_2, and O_3 concentrations; and RPM-II-predicted NO, O_3, and SO_2 concentrations are shown in Table 5 for the unrestricted cases and in Table 6 for the restricted cases.

For the sake of comparison with model predictions, all plume concentrations shown in these tables are averages of all concentrations of a particular species measured during multiple aircraft passes through the plume at a given downwind traverse distance. Such averaging tends to make the concentrations more representative of one-hour averages, as pointed out earlier.

RPM-II predictions are assumed to be representative of the averaging period of the input data. However, this assumption is not strictly correct because RPM-II's internal computations of chemical transformations are done on varying time scales with a maximum 10-minute averaging time; no significant effect is expected, but it merits some future considerations. For the purposes of this study, we assume the RPM-II predictions are representative of one-hour averages, because we have fit our dispersion data to average concentrations representative of about one-hour averaging periods (generally the aircraft spent about an hour making multiple traverses through the plume at given downwind distances).

E. DISCUSSION OF RESULTS

1. Case Studies with Unrestricted Data Sets

A comparison of measured concentrations with the predictions of RPM-II, TCM, OLM, and CNOM reveals that all performed well. (Table 7 presents computed statistical parameters for the models' predictions of NO_2). This is not surprising because adjustments were made to RPM-II input to improve

TABLE 5. MEASURED CONCENTRATIONS AND CONCENTRATIONS PREDICTED BY RPM-II, TCM, OLM, AND CNOM FOR UNRESTRICTED CASES

(a) Case Study Date 2 July 1976 (sole scenario)

Downwind Distance (km)	RPM-II Concentration Predictions (ppb)				Measured Plume Average Concentrations (ppb)				Simple Method NO_2 Predictions (ppb)		
	SO_2	NO	NO_2	O_3	SO_2	NO	NO_2	O_3	TCM	OLM	CNOM
5.0	145.0	56.7	159.0	25.7	189.0	36.0	159.6*	46.0	193.0	136.0	151.0
69.0	160.0	67.2	160.0	35.2	132.7	54.7	149.2*	34.0	182.0	115.0	130.0
120.0	30.3	13.9	80.7	47.4	8.0	11.0	79.6*	72.7	79.2	79.2	75.6

(b) Case Study Date 5 July 1976 (Scenario 1)

Downwind Distance (km)	RPM-II Concentration Predictions (ppb)				Measured Plume Average Concentrations (ppb)				Simple Method NO_2 Predictions (ppb)		
	SO_2	NO	NO_2	O_3	SO_2	NO	NO_2	O_3	TCM	OLM	CNOM
10.0	41.7	10.3	20.3	43.3	145.8	14.8	26.9	41.5	37.3	37.3	27.1
27.0	22.5	6.2	14.4	52.3	44.0	6.6	13.4	48.5	18.3	18.3	14.9
46.0	26.7	3.0	15.8	69.1	30.8	3.4	13.6	55.5	20.0	20.0	17.6

TABLE 5 (Continued)

(c) Case Study Date 5 July 1976 (Scenario 2)

Downwind Distance (km)	RPM-II Concentration Predictions (ppb)				Measured Plume Average Concentrations (ppb)				Simple Method NO_2 Predictions (ppb)		
	SO_2	NO	NO_2	O_3	SO_2	NO	NO_2	O_3	TCM	OLM	CNOM
46.0	77.0	24.2	43.3	32.1	30.8	18.4	64.6	55.5	68.9	68.9	52.2
73.0	20.4	4.1	31.0	61.3	101.8	18.8	17.8	57.2	23.7	23.7	33.8

(d) Case Study Date 7 July 1976 (Scenario 1)

Downwind Distance (km)	RPM-II Concentration Predictions (ppb)				Measured Plume Average Concentrations (ppb)				Simple Method NO_2 Predictions (ppb)		
	SO_2	NO	NO_2	O_3	SO_2	NO	NO_2	O_3	TCM	OLM	CNOM
85.0	25.2	6.4	32.7	45.5	42.3	6.3	34.7[†]	46.4[§]	37.1	37.1	33.6

(e) Case Study Date 7 July 1976 (Scenario 2)

Downwind Distance (km)	RPM-II Concentration Predictions (ppb)				Measured Plume Average Concentrations (ppb)				Simple Method NO_2 Predictions (ppb)		
	SO_2	NO	NO_2	O_3	SO_2	NO	NO_2	O_3	TCM	OLM	CNOM
83.0	9.2	4.4	16.2	42.9	18.3	6.5	13.8[†]	44.0	18.1	18.1	17.7
108.0	7.7	3.0	15.6	44.9	15.0	3.1	14.4[†]	43.0	16.2	16.2	14.5

TABLE 5 (Continued)

(f) Case Study Date 14 July 1976 (Scenario 1)

Downwind Distance (km)	RPM-II Concentration Predictions (ppb)				Measured Plume Average Concentrations (ppb)				Simple Method NO_2 Predictions (ppb)		
	SO_2	NO	NO_2	O_3	SO_2	NO	NO_2	O_3	TCM	OLM	CNOM
23.0	298.5	87.9	72.8	18.3	395.3	26.5	128.8	50.0	165.0	96.8	75.3
44.0	190.0	41.0	60.9	33.9	426.1	16.6	81.0†	51.9	101.7	85.3	57.8

(g) Case Study Date 14 July 1976 (Scenario 2)

Downwind Distance (km)	RPM-II Concentration Predictions (ppb)				Measured Plume Average Concentrations (ppb)				Simple Method NO_2 Predictions (ppb)		
	SO_2	NO	NO_2	O_3	SO_2	NO	NO_2	O_3	TCM	OLM	CNOM
46.0	85.5	6.3	22.7	74.6	111.6	6.8	22.6†	76.0	28.1	28.1	23.5

(h) Case Study Date 15 July 1976 (sole scenario)

Downwind Distance (km)	RPM-II Concentration Predictions (ppb)				Measured Plume Average Concentrations (ppb)				Simple Method NO_2 Predictions (ppb)		
	SO_2	NO	NO_2	O_3	SO_2	NO	NO_2	O_3	TCM	OLM	CNOM
29.0	30.7	5.6	19.0	40.3	82.3	6.1	19.2	38.7	23.4	23.4	19.4
52.0	28.0	3.0	16.9	63.5	52.5	4.0	17.5†	59.3	23.9	23.9	21.1

TABLE 5 (Continued)

(i) Case Study Date 18 July 1976 (sole scenario)

Downwind Distance (km)	RPM-II Concentration Predictions (ppb)				Measured Plume Average Concentrations (ppb)				Simple Method NO_2 Predictions (ppb)		
	SO_2	NO	NO_2	O_3	SO_2	NO	NO_2	O_3	TCM	OLM	CNOM
26.0	38.3	5.5	16.6	57.5	34.7	4.3	12.4[†]	55.3	18.2	18.2	15.5

(j) Case Study Date 20 July 1976 (sole scenario)

Downwind Distance (km)	RPM-II Concentration Predictions (ppb)				Measured Plume Average Concentrations (ppb)				Simple Method NO_2 Predictions (ppb)		
	SO_2	NO	NO_2	O_3	SO_2	NO	NO_2	O_3	TCM	OLM	CNOM
21.0	38.0	9.7	21.1	44.6	80.7	8.9	21.2	51.3	26.3	26.3	21.2
60.0	40.2	6.3	19.0	76.4	46.0	8.0	24.3[†]	71.0	28.2	28.2	23.8

TABLE 5 (Continued)

(k) Case Study Date 23 July 1976 (sole scenario)

Downwind Distance (km)	RPM-II Concentration Predictions (ppb)				Measured Plume Average Concentrations (ppb)				Simple Method NO_2 Predictions (ppb)		
	SO_2	NO	NO_2	O_3	SO_2	NO	NO_2	O_3	TCM	OLM	CNOM
25.0	106.0	52.1	6.9	47.0	271.5	51.2	3.1	42.8	45.8	10.3	8.3
127.0	25.2	10.6	31.9	57.9	32.0	11.0	43.4*	77.5	59.0	59.0	56.9
165.0	17.1	9.8	37.7	88.3	24.0	9.7	38.2*	91.0	42.3	42.3	41.3

(1) Case Study Date 28 July 1976 (Scenario 1)

Downwind Distance (km)	RPM-II Concentration Predictions (ppb)				Measured Plume Average Concentrations (ppb)				Simple Method NO_2 Predictions (ppb)		
	SO_2	NO	NO_2	O_3	SO_2	NO	NO_2	O_3	TCM	OLM	CNOM
52.0	107.0	52.1	7.3	0.0	272.3	22.6	25.4	0.0	42.3	7.9	6.7

(m) Case Study Date 28 July 1976 (Scenario 2)

Downwind Distance (km)	RPM-II Concentration Predictions (ppb)				Measured Plume Average Concentrations (ppb)				Simple Method NO_2 Predictions (ppb)		
	SO_2	NO	NO_2	O_3	SO_2	NO	NO_2	O_3	TCM	OLM	CNOM
27.0	38.9	8.9	36.1	66.6	100.9	7.9	36.5*	74.8	38.7	38.7	35.3

TABLE 5 (Concluded)

(n) Case Study Date 30 July 1976 (Scenario 1)

Downwind Distance (km)	RPM-II Concentration Predictions (ppb)				Measured Plume Average Concentrations (ppb)				Simple Method NO_2 Predictions (ppb)		
	SO_2	NO	NO_2	O_3	SO_2	NO	NO_2	O_3	TCM	OLM	CNOM
27.0	52.4	2.0	27.5	17.6	104.8	8.6	16.5	62.5	27.7	27.7	28.9

(o) Case Study Date 30 July 1976 (Scenario 2)

Downwind Distance (km)	RPM-II Concentration Predictions (ppb)				Measured Plume Average Concentrations (ppb)				Simple Method NO_2 Predictions (ppb)		
	SO_2	NO	NO_2	O_3	SO_2	NO	NO_2	O_3	TCM	OLM	CNOM
12.0	32.9	6.8	27.8	76.9	137.7	6.0	25.2*	72.3	30.3	30.3	27.5
23.0	31.3	4.2	23.2	105.0	89.2	4.8	21.1	93.2	23.2	25.2	19.2

(p) Case Study Date 30 July 1976 (Scenario 3)

Downwind Distance (km)	RPM-II Concentration Predictions (ppb)				Measured Plume Average Concentrations (ppb)				Simple Method NO_2 Predictions (ppb)		
	SO_2	NO	NO_2	O_3	SO_2	NO	NO_2	O_3	TCM	OLM	CNOM
35.0	137.0	10.8	52.2	104.0	32.3	8.9	66.5*	112.7	72.1	72.1	51.3

---

* Computed using measured NO, O_3, and Photostationary relationship.

† Computed using measured NO_x, O_3, and Photostationary relationship.

§ Washington data only.

TABLE 6. MEASURED CONCENTRATIONS AND CONCENTRATIONS PREDICTED BY RPM-II, TCM, OLM, AND CNOM (RESTRICTED CASES)

(a) Case Study Date: 2 July 1976 (Sole Scenario)

Downwind Distance (km)	RPM-II Concentration Predictions (ppb)				Measured Plume Average Concentrations (ppb)				Simple Method NO_2 Predictions (ppb)		
	SO_2	NO	NO_2	O_3	SO_2	NO	NO_2	O_3	TCM	OLM	CNOM
5.0	127.0	50.0	151.0	28.0	189.0	36.0	159.6[*]	46.0	191.0	136.0	153.0
69.0	11.5	15.6	80.2	57.9	132.7	54.7	149.2[*]	34.0	61.4	61.4	58.8
120.0	8.0	11.7	70.1	69.9	8.0	11.0	79.6[*]	72.7	62.3	62.3	62.9

(b) Case Study Date: 5 July 1976 (Scenario 1)

Downwind Distance (km)	RPM-II Concentration Predictions (ppb)				Measured Plume Average Concentrations (ppb)				Simple Method NO_2 Predictions (ppb)		
	SO_2	NO	NO_2	O_3	SO_2	NO	NO_2	O_3	TCM	OLM	CNOM
10.0	14.3	18.0	28.1	36.2	145.8	14.8	26.9	41.5	41.3	41.3	29.2
27.0	11.2	6.9	15.4	50.5	44.0	6.6	13.4	48.5	16.3	16.3	13.7
46.0	9.1	3.5	14.3	61.5	30.8	3.4	13.6	55.5	16.7	16.7	15.2

(c) Case Study Date: 5 July 1976 (Scenario 2)

Downwind Distance (km)	RPM-II Concentration Predictions (ppb)				Measured Plume Average Concentrations (ppb)				Simple Method NO_2 Predictions (ppb)		
	SO_2	NO	NO_2	O_3	SO_2	NO	NO_2	O_3	TCM	OLM	CNOM
46.0	12.1	40.5	49.6	23.3	30.8	18.4	64.6	55.5	220.0	93.8	79.0
73.0	21.2	4.7	31.3	64.6	101.8	18.8	17.8	57.2	20.5	20.5	31.2

(d) Case Study Date: 7 July 1976 (Scenario 1)

Downwind Distance (km)	RPM-II Concentration Predictions (ppb)				Measured Plume Average Concentrations (ppb)				Simple Method NO_2 Predictions (ppb)		
	SO_2	NO	NO_2	O_3	SO_2	NO	NO_2	O_3	TCM	OLM	CNOM
85.0	27.4	7.3	33.1	42.9	42.3	6.3	34.7[†]	46.4[§]	37.1	37.1	37.1

TABLE 6 (Continued)

(e) Case Study Date: 7 July 1976 (Scenario 2)

Downwind Distance (km)	RPM-II Concentration Predictions (ppb)				Measured Plume Average Concentrations (ppb)				Simple Method NO_2 Predictions (ppb)		
	SO_2	NO	NO_2	O_3	SO_2	NO	NO_2	O_3	TCM	OLM	CNOM
83.0	7.1	4.4	15.2	43.8	18.3	6.5	13.8[†]	44.0	14.2	14.2	15.2
108.0	5.4	3.1	14.6	45.2	15.0	3.1	14.4[†]	43.0	11.7	11.7	11.2

(f) Case Study Date: 14 July 1976 (Scenario 1)

Downwind Distance (km)	RPM-II Concentration Predictions (ppb)				Measured Plume Average Concentrations (ppb)				Simple Method NO_2 Predictions (ppb)		
	SO_2	NO	NO_2	O_3	SO_2	NO	NO_2	O_3	TCM	OLM	CNOM
23.0	53.4	5.1	23.7	67.2	395.3	26.5	128.8	50.0	28.1	28.1	23.6
44.0	39.0	2.3	15.9	93.0	426.1	16.6	81.0[†]	51.9	22.2	22.2	18.6

(g) Case Study Date: 14 July 1976 (Scenario 2)

Downwind Distance (km)	RPM-II Concentration Predictions (ppb)				Measured Plume Average Concentrations (ppb)				Simple Method NO_2 Predictions (ppb)		
	SO_2	NO	NO_2	O_3	SO_2	NO	NO_2	O_3	TCM	OLM	CNOM
46.0	70.9	4.4	16.0	61.1	111.6	6.8	22.6[†]	76.0	22.1	22.1	19.3

(h) Case Study Date: 15 July 1976 (Sole Scenario)

Downwind Distance (km)	RPM-II Concentration Predictions (ppb)				Measured Plume Average Concentrations (ppb)				Simple Method NO_2 Predictions (ppb)		
	SO_2	NO	NO_2	O_3	SO_2	NO	NO_2	O_3	TCM	OLM	CNOM
55.0	26.2	5.7	17.1	35.8	82.3	6.1	19.2	38.7	23.4	23.4	19.4
104.0	18.9	3.6	14.6	45.9	52.5	4.0	17.5[†]	59.3	19.1	19.1	17.4

TABLE 6 (Continued)

(i) Case Study Date: 18 July 1976 (Sole Scenario)

Downwind Distance (km)	RPM-II Concentration Predictions (ppb)				Measured Plume Average Concentrations (ppb)				Simple Method NO_2 Predictions (ppb)		
	SO_2	NO	NO_2	O_3	SO_2	NO	NO_2	O_3	TCM	OLM	CNOM
26.0	54.5	9.0	21.5	51.4	34.7	4.3	$12.4^{\dagger}$	55.3	25.0	25.0	25.0

(j) Case Study Date: 20 July 1976 (Sole Scenario)

Downwind Distance (km)	RPM-II Concentration Predictions (ppb)				Measured Plume Average Concentrations (ppb)				Simple Method NO_2 Predictions (ppb)		
	SO_2	NO	NO_2	O_3	SO_2	NO	NO_2	O_3	TCM	OLM	CNOM
21.0	43.7	11.4	22.7	38.6	80.7	8.9	21.2	51.3	30.2	30.2	23.5
60.0	30.4	7.0	18.1	55.9	46.0	8.0	$24.3^{\dagger}$	71.0	26.7	26.7	22.8

(k) Case Study Date: 23 July 1976 (Sole Scenario)

Downwind Distance (km)	RPM-II Concentration Predictions (ppb)				Measured Plume Average Concentrations (ppb)				Simple Method NO_2 Predictions (ppb)		
	SO_2	NO	NO_2	O_3	SO_2	NO	NO_2	O_3	TCM	OLM	CNOM
25.0	63.2	32.3	4.9	0.5	271.5	51.2	3.1	42.8	24.7	8.23	6.7
127.0	20.2	5.2	18.5	66.9	32.0	11.0	43.4^{*}	77.5	55.8	55.8	54.6
165.0	18.6	3.5	16.2	102.0	24.0	9.7	38.2^{*}	91.0	41.4	41.4	40.7

(l) Case Study Date: 28 July 1976 (Scenario 1)

Downwind Distance (km)	RPM-II Concentration Predictions (ppb)				Measured Plume Average Concentrations (ppb)				Simple Method NO_2 Predictions (ppb)		
	SO_2	NO	NO_2	O_3	SO_2	NO	NO_2	O_3	TCM	OLM	CNOM
52.0	18.5	10.2	4.0	0.07	272.3	22.6	25.4	0.0	67.8	44.4	43.3

TABLE 6 (Concluded)

(m) Case Study Date: 28 July 1976 (Scenario 2)

Downwind Distance (km)	RPM-II Concentration Predictions (ppb)				Measured Plume Average Concentrations (ppb)				Simple Method NO_2 Predictions (ppb)		
	SO_2	NO	NO_2	O_3	SO_2	NO	NO_2	O_3	TCM	OLM	CNOM
27.0	47.5	10.6	39.4	56.0	100.9	7.9	36.5*	74.8	41.2	41.2	37.1

(n) Case Study Date: 30 July 1976 (Scenario 1)

Downwind Distance (km)	RPM-II Concentration Predictions (ppb)				Measured Plume Average Concentrations (ppb)				Simple Method NO_2 Predictions (ppb)		
	SO_2	NO	NO_2	O_3	SO_2	NO	NO_2	O_3	TCM	OLM	CNOM
27.0	74.4	5.9	34.2	14.4	104.8	8.6	16.5	62.5	31.4	31.4	32.5

(o) Case Study Date: 30 July 1976 (Scenario 2)

Downwind Distance (km)	RPM-II Concentration Predictions (ppb)				Measured Plume Average Concentrations (ppb)				Simple Method NO_2 Predictions (ppb)		
	SO_2	NO	NO_2	O_3	SO_2	NO	NO_2	O_3	TCM	OLM	CNOM
12.0	246.0	65.6	78.6	29.3	137.7	6.0	25.2*	72.3	32.5	32.5	29.1
23.0	91.7	17.5	47.7	56.3	89.2	4.8	21.1	93.2	32.7	32.7	26.0

(p) Case Study Date: 30 July 1976 (Scenario 3)

Downwind Distance (km)	RPM-II Concentration Predictions (ppb)				Measured Plume Average Concentrations (ppb)				Simple Method NO_2 Predictions (ppb)		
	SO_2	NO	NO_2	O_3	SO_2	NO	NO_2	O_3	TCM	OLM	CNOM
35.0	80.7	9.9	36.0	65.7	32.3	8.9	66.5*	112.7	46.5	46.5	36.1

---

* Computed using measured NO, O_3, and photostationarity relationship.

† Computed using measured NO_x, O_3, and photostationarity relationship.

§ Washington data only.

TABLE 7. COMPUTED STATISTICAL PARAMETER FOR RPM-II, TCM, OLM, AND CNOM NO_2 PREDICTIONS FOR UNRESTRICTED CASES

Statistics	Models			
	RPM-II	TCM	OLM	CNOM
Mean Difference (ppb)	-3.64	-10.85	-0.785	-3.19
Standard Deviation (ppb)	13.38	11.62	12.15	13.6
Correlation Coefficient	0.95	0.96	0.97	0.95

its NO_2 prediction performance (as described earlier), and these adjusted input values were used also for the simpler models.* Inspection of Figures 8, 9, 10, and 11, which depict scatter diagrams (predicted NO_2 concentrations versus observed NO_2 concentrations) for RPM-II, TCM, OLM, and CNOM based on all 28 observations of average plume NO_2 concentrations on the 10 case study days, reveals that all four models are capable of matching the observations reasonably closely across a wide range of NO_2 concentrations.

a. RPM-II

The best fit line for RPM-II, shown in the scatter diagram in Figure 8, has a slope of 0.887 and an intercept of 1.6 ppb. Compared with an ideal slope of 1.0, RPM-II clearly performed within the expected accuracy of the monitoring instruments ($\approx \pm$ 15 percent of the true value). Indeed, the mean difference between RPM-II predictions and the 28 measured plume NO_2 concentrations was only -3.64 ppb; the standard deviation was 13.38 ppb, and the correlation coefficient was 0.95. These statistics are encouraging, but they do not constitute validation of RPM-II performance because of the input data uncertainties. Rather, these statistics warrant the following conclusions:

- The model is capable of acceptable performance when ambient hydrocarbon and plume dispersion input values are adjusted.
- No apparent defect that affects performance is revealed in the model's formulation, though the formulation does contain several simplifying assumptions.

Validation of the model's NO_2 predictions must await development and/or deployment of monitoring techniques capable of adequately defining these important input parameters.

---

* It should be pointed out that only coarse adjustments were made to RPM-II input; fine tuning of input parameters to minimize the difference between RPM-II NO_2 predictions and measured values was not undertaken because it would have served no substantive purpose.

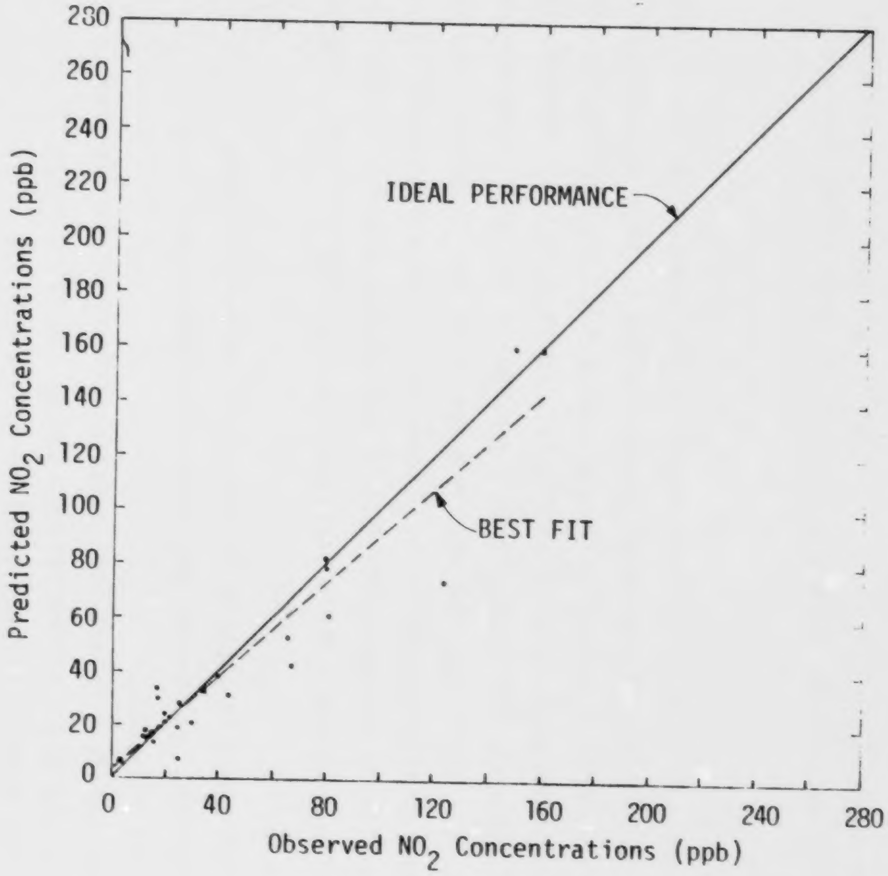

(a) NO_2 Concentrations

Figure 8. Scattergram comparison of concentration values predicted by RPM-II with measured values for "unrestricted" cases.

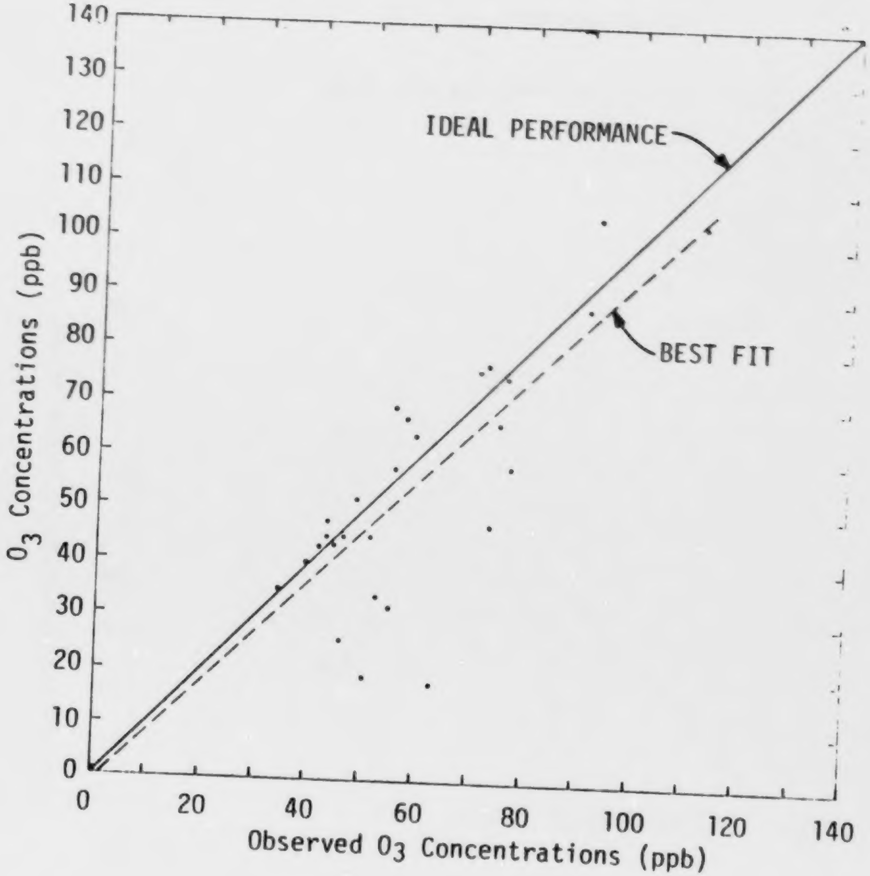

(b) O_3 Concentrations

Figure 8 (Continued).

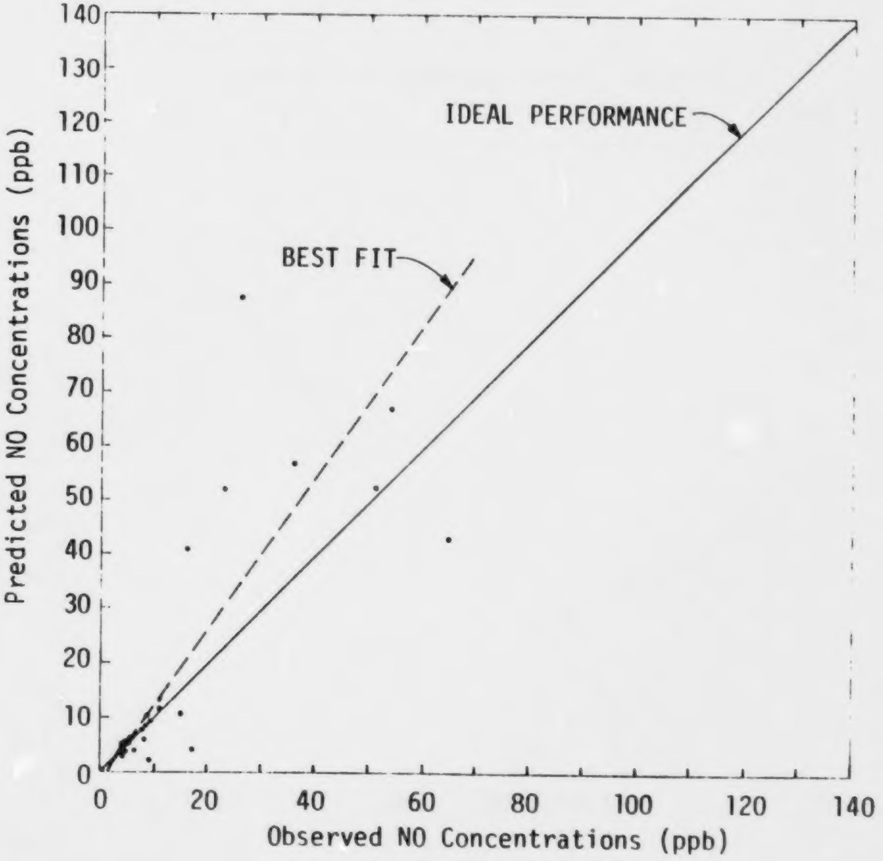

(c) NO Concentrations

Figure 8 (Concluded).

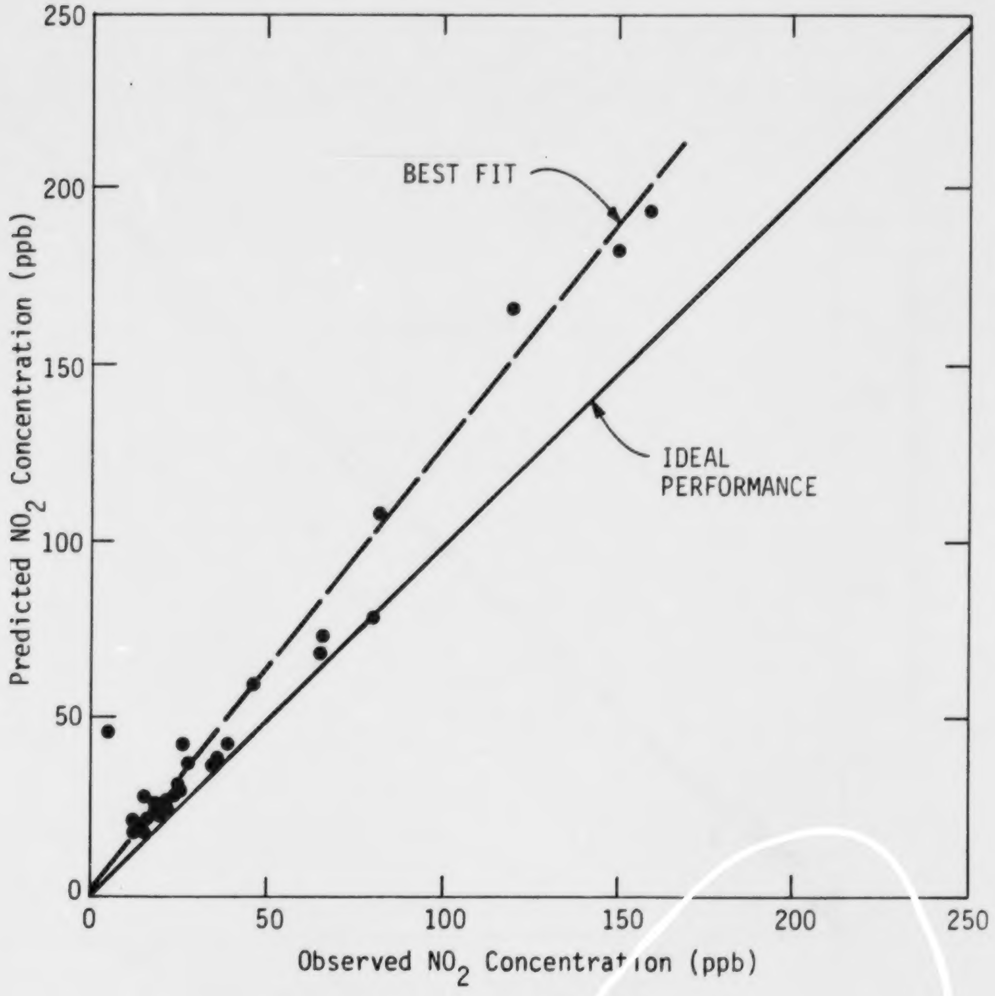

Figure 9. Scattergram comparison of NO_2 concentration values predicted by TCM with measured values for "unrestricted" cases.

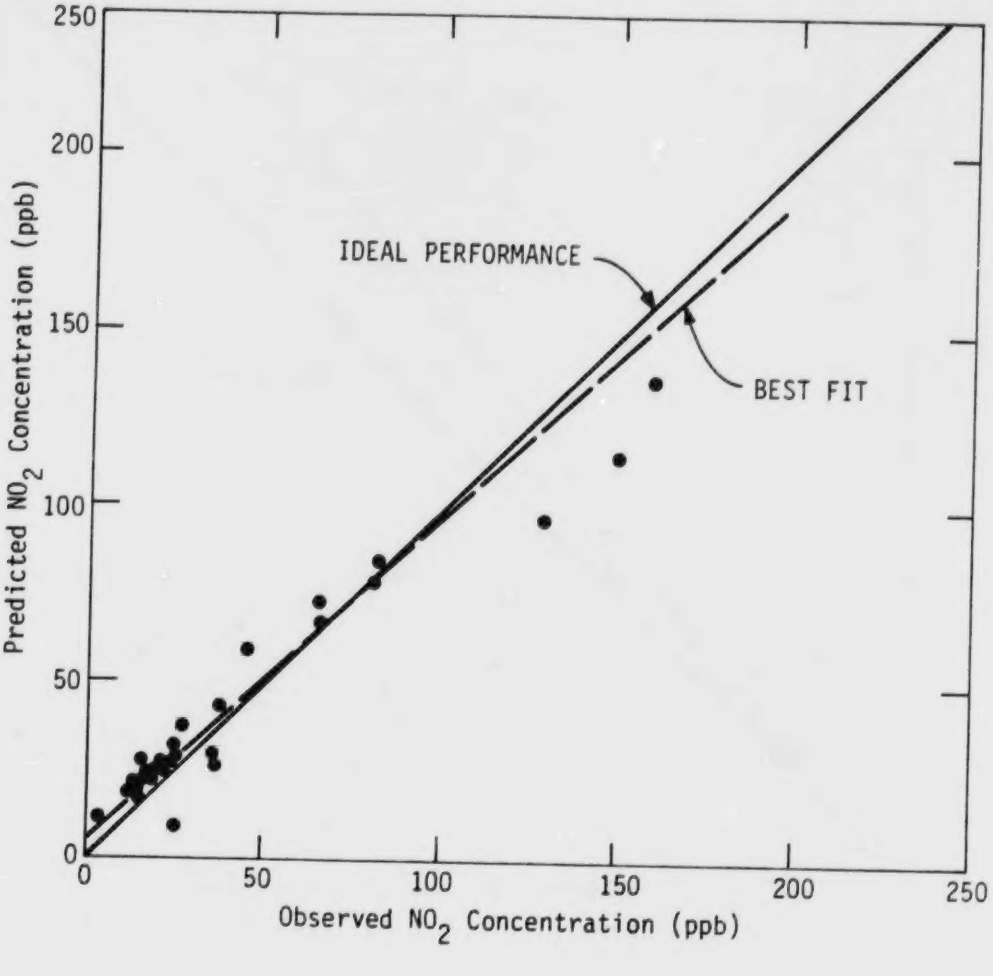

Figure 10. Scattergram comparison of NO_2 concentration values predicted by OLM with measured values for "unrestricted" cases.

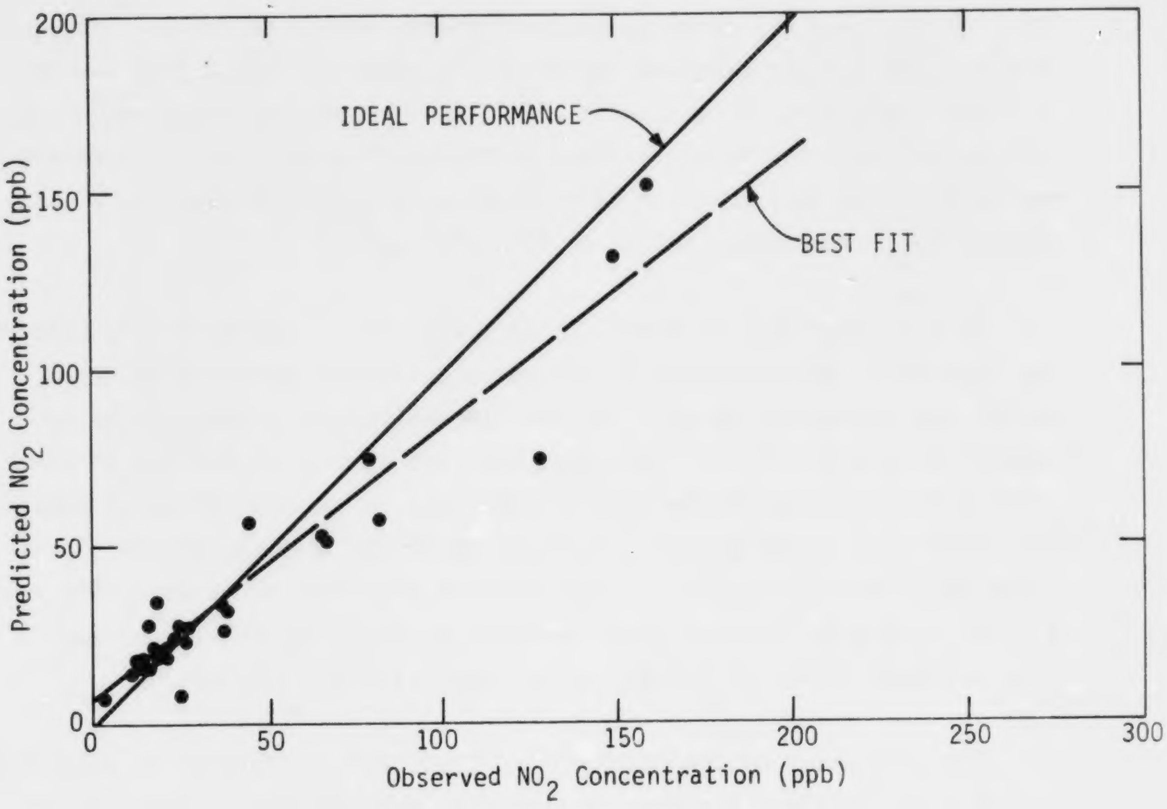

Figure 11. Scattergram comparison of NO_2 concentration values predicted by CNOM with measured values for "unrestricted" cases.

Comparisons of RPM-II O_3 and NO predictions with observations are also encouraging. The means of the differences between RPM-II ozone and NO predictions and observations of these species were -6.91 ppb and 4.66 ppb, respectively; and the correlation coefficients were 0.68 and 0.7, respectively. The scatter diagrams for NO and O_3 shown in Figure 8(b) and (c) are also indicative of reasonable RPM-II performance for these reactive pollutants, but clearly not as good as NO_2 performance. This difference may reflect the fact that the main focus of our input adjustments was to improve NO_2 performance, not O_3 or NO performance.

As a further test of RPM-II performance, it is interesting to compare, qualitatively, the character of secondary pollutant formation observed within the Labadie plume with the RPM-II predictions. Observations on several of the 1976 MISTT study days indicate an initial buildup of ozone above ambient levels at the edge of the plume, gradually spreading toward the centerline of the plume as it moves downwind; this can be seen in the plume profiles observed at various downwind distances on 30 July 1976 and plotted in Figure 12. The plume profiles predicted by RPM-II for the same distance, shown in Figure 13, are qualitatively similar.

The similarity of the observed and predicted profiles on 30 July 1976 can be quantitatively examined by comparing peak-to-mean ratios. At the 12 km traverse distance the observed ratio of peak-to-mean NO_2 concentrations is 1.8:1, and the ratio is 1.2:1 at 23 km. The ratios predicted by RPM-II were approximately 1.26:1 and 1.29:1, respectively. For SO_2 the observed ratios were 2.1:1 and 2.0:1; the predicted ratios were approximately 1.36:1 and 1.39:1 at 12 and 23 km, respectively. Extensive quantitative comparisons of the observed and predicted cross sectional plume distributions are not strictly appropriate, however, because of the disparity between the temporal and spatial scales between the two that was mentioned in an earlier discussion. Nevertheless, the qualitative similarity of the profiles, especially qualitatively correct buildup of ozone at the plume edges, is

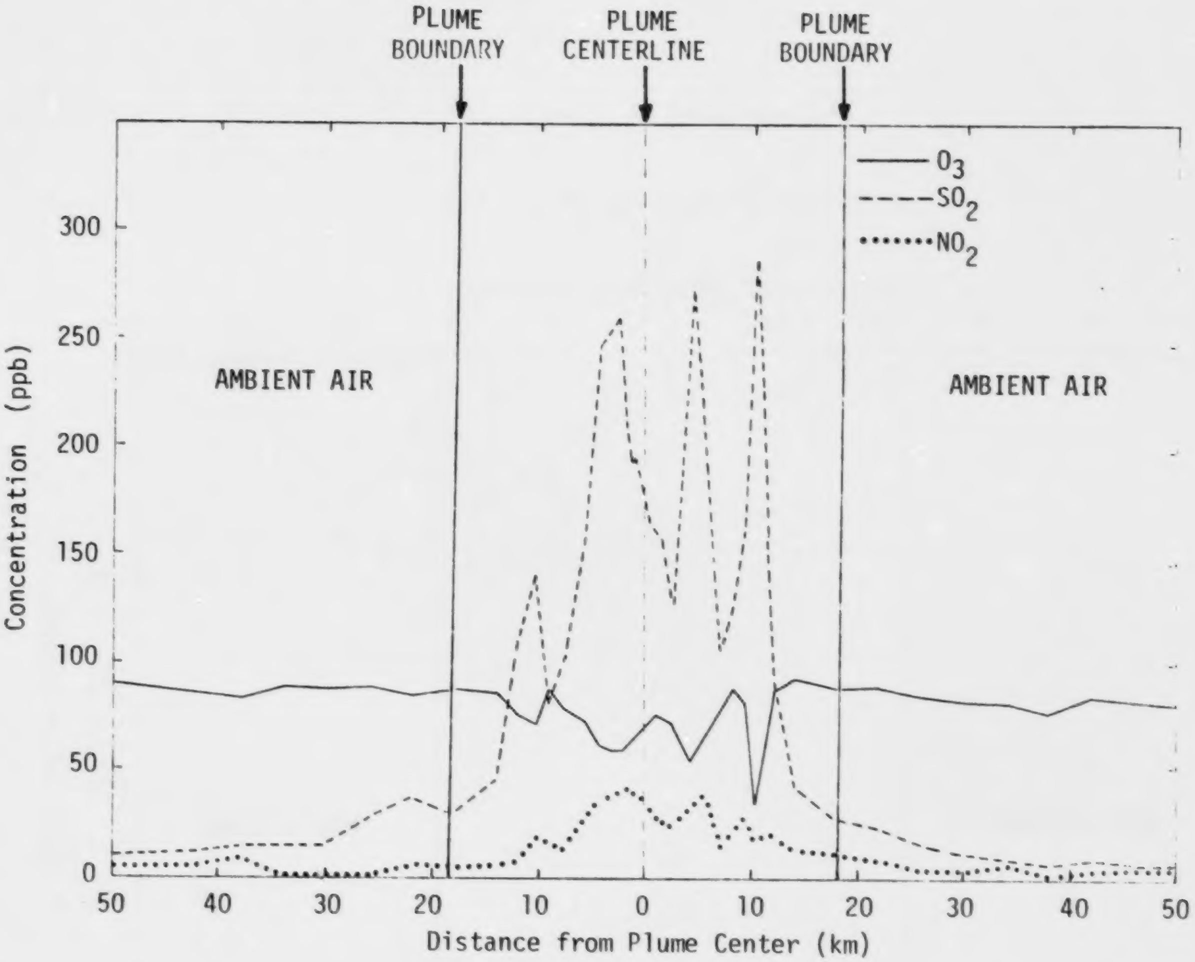

(a) 12 km Downwind of Labadie

Figure 12. Observed plume profiles for 30 July 1976.

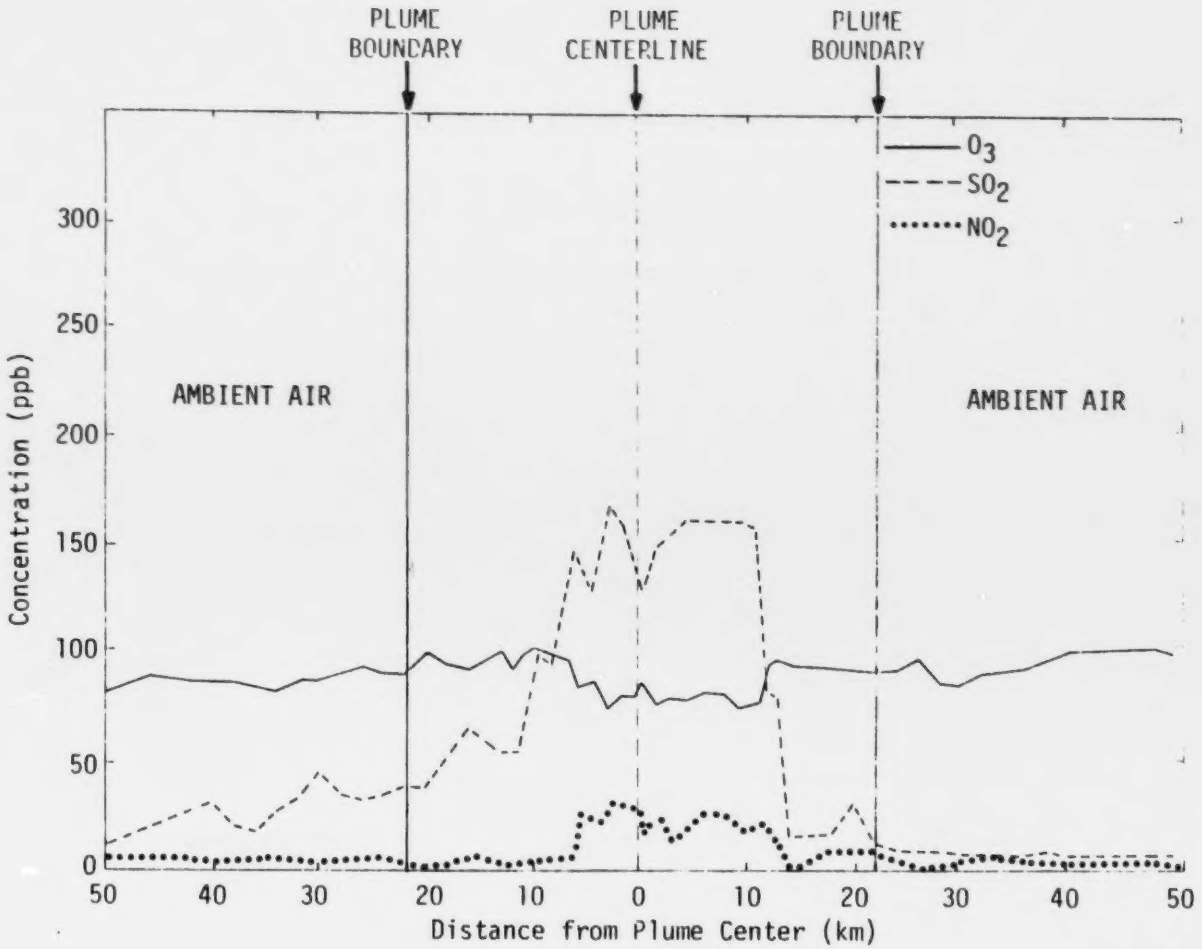

(b) 23 km Downwind of Labadie)

Figure 12 (Concluded).

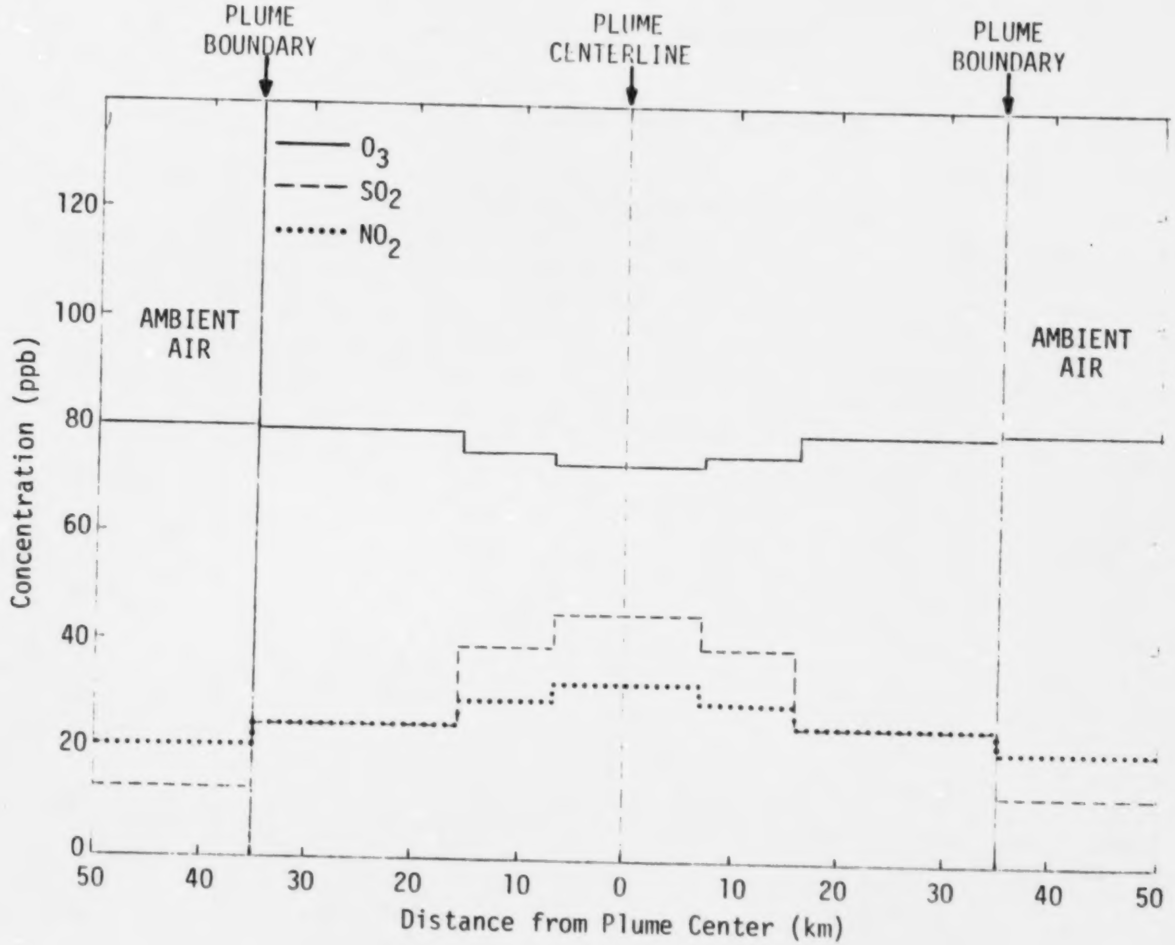

(a) 12 km Downwind of Labadie

Figure 13. Concentration profiles predicted by RPM-II for 30 July 1976, using "unrestricted data set."

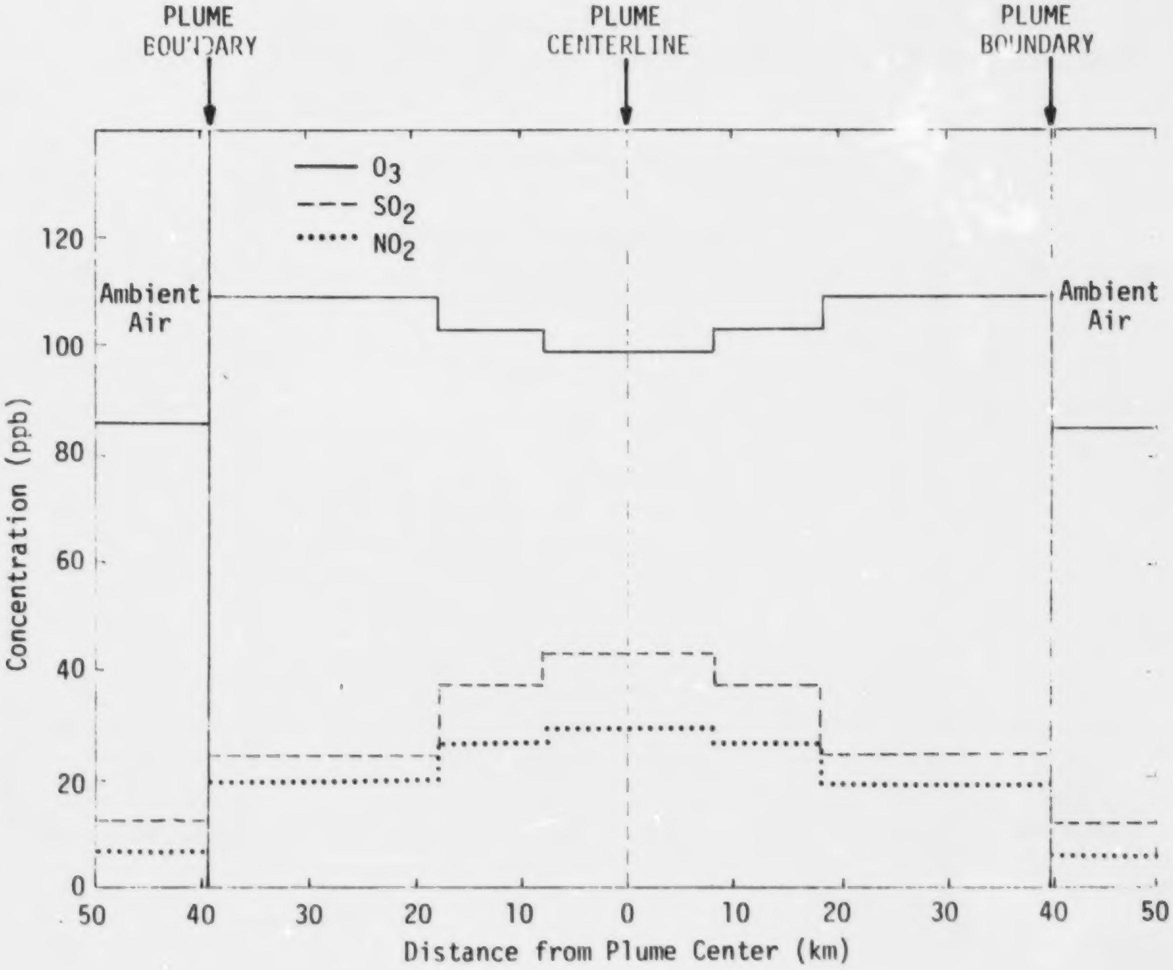

(b) 23 km Downwind of Labadie

Figure 13 (Concluded).

further evidence of the validity of RPM-II's formulation. These results are also qualitatively similar to the plume ozone observations of Miller et al. (1978) and Keiffer et al. (1977). The sensitivity of RPM-II response to ambient hydrocarbons and plume dispersion rates is evidenced by the plots of predicted plume profiles using lower ambient hydrocarbon and plume dispersion rates at these same traverse distances, as shown in Figures 14 and 15. It is interesting to note that the buildup of plume secondary pollutants above ambient levels can be completely eliminated from the 30 July 1976 predictions when total reactive ambient hydrocarbons are reduced to 0.1 ppm (Figure 14), which fact highlights the importance of accurate measurements of ambient hydrocarbons for specifying model inputs. Elimination of ozone buildup within the plume also occurs when plume dispersion rates are reduced, so that plume dimensions are roughly what the aircraft measurements indicate (see Figure 6).

b. The Total Conversion Method (TCM)

As would be expected, the Total Conversion Method (TCM) tended toward overprediction of NO_2 concentrations. The best fit line shown in Figure 9 has a slope of 1.29, clearly an indication of overprediction. When the positions of individual data points in Figure 9 are compared to the ideal performance line (slope = 1.0, intercept = 0.0), it is apparent that TCM overpredicted on all points, except one, over the entire range of observed concentrations and at all downwind distances. Generally, the larger concentrations were more severely overpredicted because they are associated with near-source plume cross-sections, at which point the assumption of total conversion of plume NO to NO_2 is most conservative. Further downwind, where concentrations were lower, the total conversion assumption appears to be more realistic. The mean difference between predicted and measured NO_2 concentrations was 10.85 ppb; the standard deviation of the differences was 11.62 ppb. The correlation coefficient computed between TCM and measurements was 0.96--slightly better than that computed for RPM-II (0.948) even though the absolute mean error for TCM was somewhat larger.

On the basis of its performance, then, TCM appears to be a conservative screening procedure, and the true plume NO_2 concentration should be less than that predicted by TCM if all factors (such as dispersion) are accounted for properly.

c. The Oxidant Limiting Method (OLM)

The Oxidant Limiting Method (OLM) performed slightly better than TCM and CNOM in these case studies and slightly better overall than did RPM-II. The mean difference between OLM NO_2 predictions and measured NO_2 was 0.785 ppb, and the standard deviation of differences was 12.15 ppb. The correlation coefficient computed for OLM was 0.97, slightly better than that for RPM-II, TCM, and CNOM. The best fit line shown in Figure 10 has a slope of 0.9 and an intercept of 5 ppb.

These results indicate that the oxidant-limiting assumption, upon which OLM is based, was valid for these case studies. Furthermore, the 10 percent value used to compensate for thermal oxidation of NO to NO_2 in the stack appears to have been appropriate in these cases. It is not worthwhile to optimize OLM predictions by adjusting the thermal oxidation value because OLM performance was already quite good. The fact that OLM's performance was comparable to that of RPM-II in almost every case suggests that hydrocarbon oxidation did not play an important role in NO_2 formation rates during the MISTT program. Hydrocarbon oxidation may have had a slight effect upon the plume NO_2 concentrations at the 69 km and 120 km downwind distances on 2 July. In these two cases both OLM and CNOM predicted NO_2 values only sightly lower than those observed and those predicted by RPM-II. A slight excess of ozone in the plume above ambient ozone levels was observed at the longer downwind distances on 2 July, which is a further indication of enhancement of photochemical activity by hydrocarbon oxidation. In two other cases when OLM predicted lower NO_2 than did RPM-II (2 July at 5 km and 5 July at 73 km) the underpredictions were most likely due to OLM's inability to account for entrainment of ambient NO because the CNOM predictions were very close to RPM-II's and CNOM cannot account for hydrocarbon oxidation but can account for NO entrainment and subsequent conversion to NO_2.

In general, OLM is intended for screening purposes. The user will most often be interested in peak concentrations of NO_2, which can be expected to occur relatively close to the stack, at which point hydrocarbon oxidation is unimportant because longer times are required for reaction. Therefore, OLM appears to be an adequate screening procedure based upon the foregoing facts and its performance relative to RPM-II's performance in these case studies.

d. The Conservation of NO_x and Oxidant Method (CNOM)

The computed statistics shown in Table 7 indicate that the performance of the Conservation of NO_x and Oxidant Method (CNOM) was similar to that of RPM II. The mean differences were -3.19 ppb and -3.64 ppb; the standard deviations of differences were 12.15 ppb and 13.38 ppb; and the correlation coefficients were 0.95 and 0.95 for both CNOM and RPM-II. A case-by-case comparison of RPM-II and CNOM predictions reveals that in almost all instances the two are within a few ppb of one another. Thus, as stated earlier in the discussion of OLM's performance, it would appear that hydrocarbon oxidation does not play an important role in the NO_2 formation in the power plant plumes studied here, because RPM-II's capacity to account for hydrocarbon oxidation is the main distinction between RPM-II and CNOM. In the 2 July cases, RPM-II did predict NO_2 values higher and closer to observed values than those predicted by CNOM, most notably at the larger downwind distances (69 km in particular). These differences may in fact be attributable to CNOM's inability to treat hydrocarbon oxidation, which is suggested by the observed enhanced plume ozone. However, the maximum discrepancy is only about 18 percent.

In the 23 July scenarios, CNOM predicted NO_2 concentrations higher than those predicted by RPM-II. These may be explained by the conversion of NO_x to nitrates, HNO_3, and other nitrogen-containing compounds during the large transport times required to reach 125 and 165 km. The Carbon-Bond chemical mechanism used in RPM-II includes reaction steps to account for this conversion (albeit with some uncertainties) whereas CNOM cannot account for it. Hence, CNOM predicts NO_2 (and NO_x) concentrations larger than those predicted by RPM-II. Because NO_x conversion to nitrates, etc., and conversion of NO to NO_2 are both stimulated by oxidation of hydrocarbons, some competitive effects may occur. Hydrocarbon oxidation causes an increase in the rate of NO to NO_2 conversion but also accelerates conversion of NO_x to nitrates and other nitrogen compounds that can potentially reduce NO_2 levels.

On the basis of its performance in these case studies, CNOM is an adequate screening model. Close to the source where ground-level concentration peaks normally occur, and where the influence of hydrocarbon oxidation on NO_2 levels, if any, would be insignificant because longer reaction times are required, CNOM's predictions were very close to those of RPM-II. This seems to indicate that sophisticated models like RPM-II are not necessary for evaluation of maximum NO_2 air quality impacts of allowable emissions in situations in which the effects of reactive hydrocarbons are significant further downwind. In such cases, a simple screening model may be sufficient. TCM is definitely the most conservative predictor of the three screening approaches examined, and OLM usually predicts higher values than those predicted by CNOM. Thus it appears that increasing sophistication yields less overly conservative results.

In general, all three simple models appear to be adequate screening models, at least under the variety of conditions tested here. None appears to have any inherent limitations (beyond those discussed earlier) that should exclude their usage in determinations of short-term air quality impacts or allowable NO_x emissions rates.

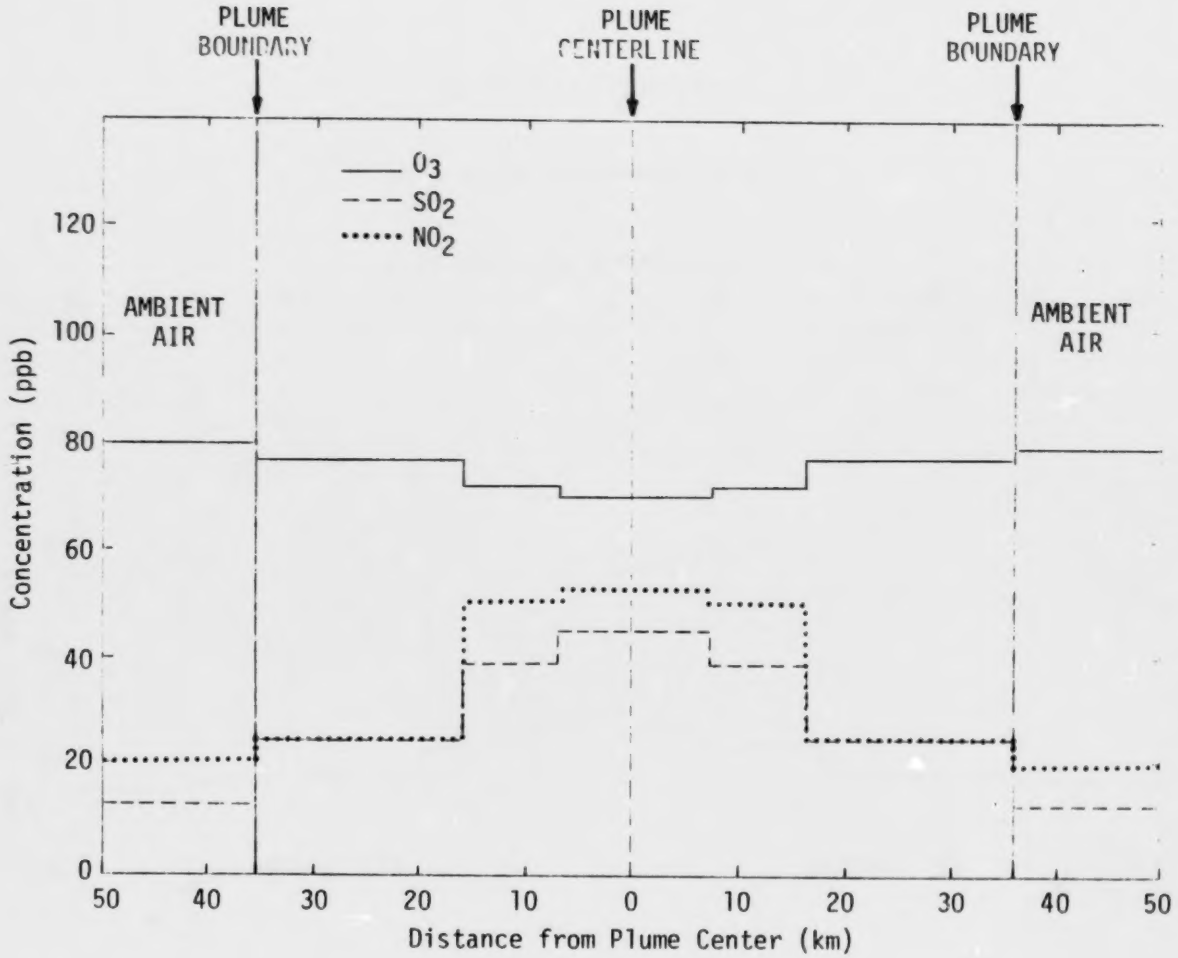

(a) 12 km Downwind of Labadie

Figure 14. Concentration profiles predicted by RPM-II with reduced hydrocarbons for 30 July 1976.

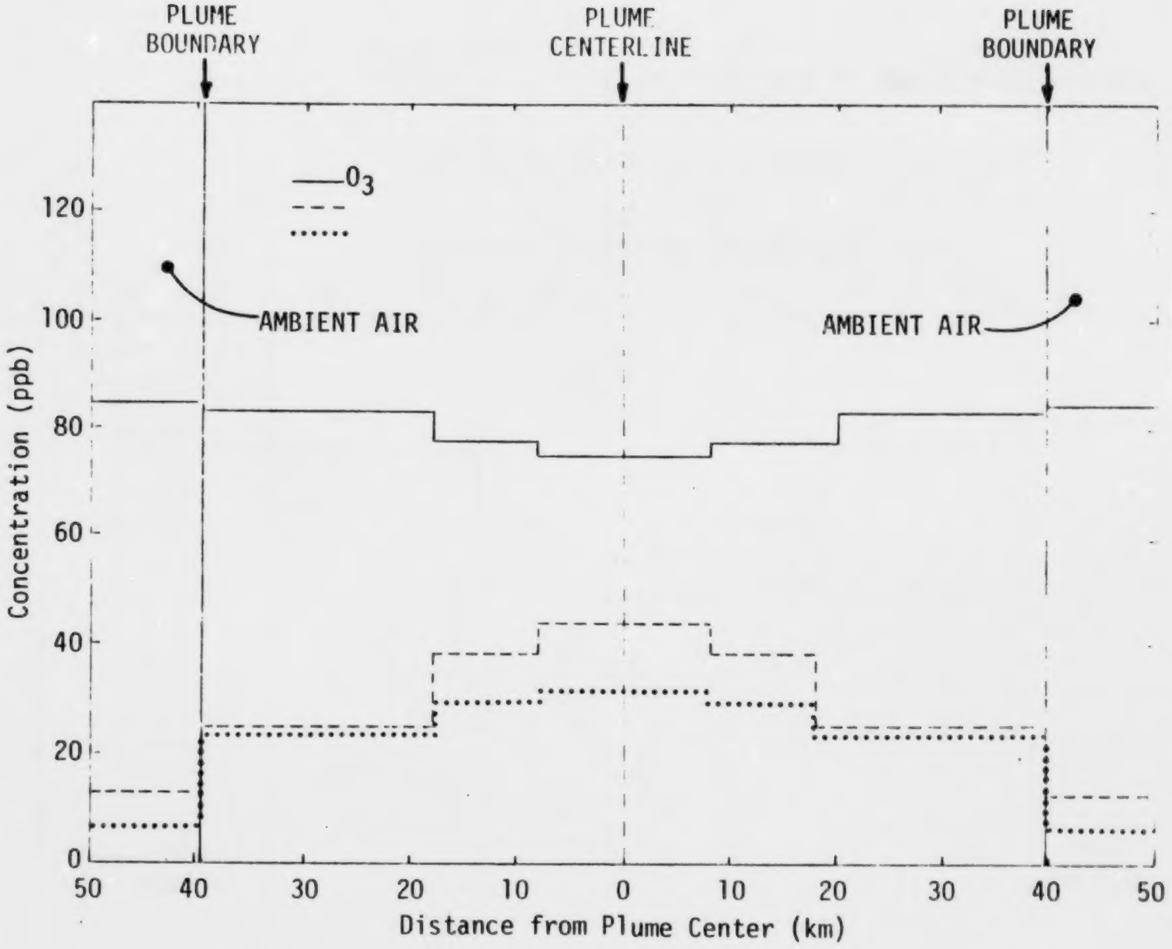

(b) 23 km Downwind of Labadie

Figure 14 (Concluded).

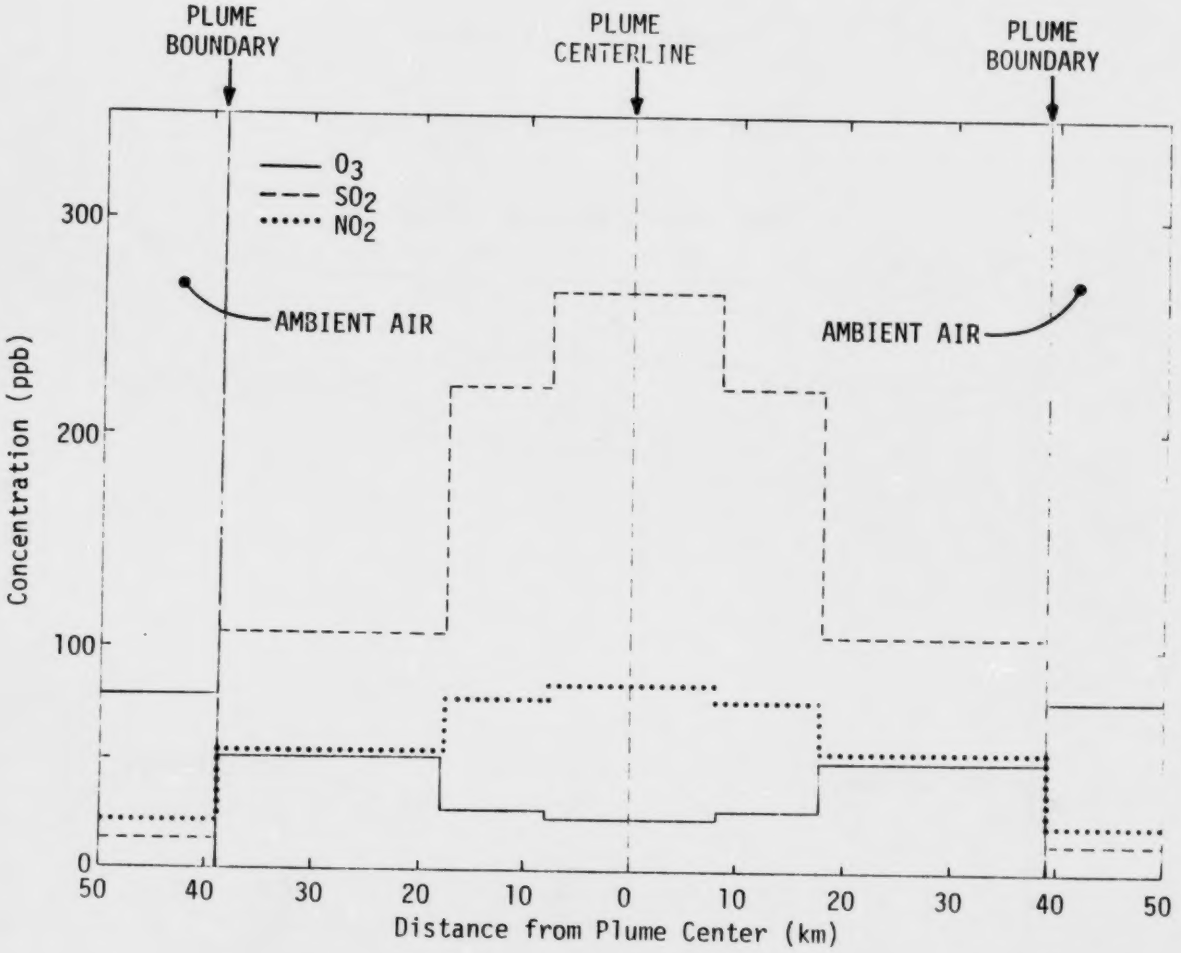

(a) 12 km Downwind of Labadie

Figure 15. Concentration profiles predicted by RPM-II with reduced plume dispersion rates for 30 July 1976.

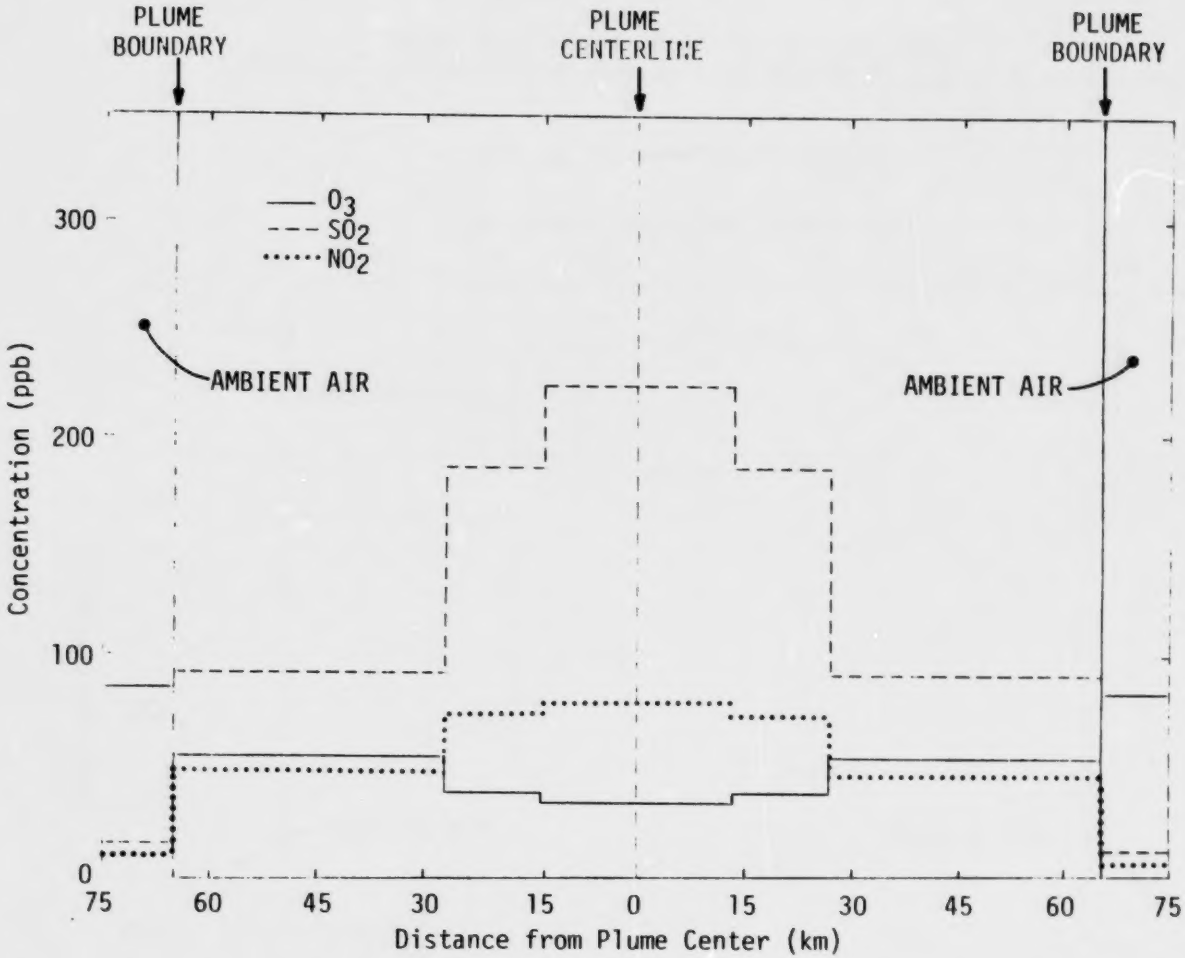

(b) 23 km Downwind of Labadie

Figure 15 (Concluded).

e. Situations Requiring a Sophisticated NO_2 Model

Because it is apparent from these discussions that, owing to their relatively simple treatment of chemistry, the simple models (i.e., TCM, OLM, and CNOM) may not be appropriate for use in situations in which hydrocarbon oxidation significantly influences NO_2 concentrations, it would be desirable to define concisely the character of the situations requiring more sophisticated models. On the basis of the simulations carried out in this study, however, it is clear that several parameters interact to determine plume ozone and NO_2 production rates. For example, we can examine the ratios of ambient reactive hydrocarbon concentrations to ambient NO_x concentrations used in these simulations to determine whether there is some critical value above or below which the production of plume ozone exceeds ambient oxone (net production of plume ozone is a good indicator of hydrocarbon oxidation influence on plume chemistry). Analyses of the numbers presented in Tables 3 and 5, which list the ambient hydrocarbon, ambient NO_x, the ambient O_3 concentration, and the measured and predicted plume O_3 concentrations for each scenario, indicate that there is no correlation between the ratio of ambient reactive hydrocarbons to NO_x or the absolute ambient reactive hydrocarbons concentration to the net production of ozone within the plume in these scenarios. We carried out similar analyses for dispersion rates and photolysis rates and found no critical values for these parameters, but we found that moderate dispersion and high photolysis rates are typical of (though neither necessary nor sufficient for) net plume ozone production. Therefore, a concise definition of conditions conducive to net plume ozone production is not possible on the basis of results derived from this study. Ozone production would appear to hinge generally on the existence of a sufficient amount of ambient hydrocarbons, solar insolation, and plume dispersion in combination. These findings are consistent with those of Keiffer et al. (1977) and Miller et al. (1978). Similarly, NO_2 production in plumes appears to be dependent on the combination of these three parameters as well as on the amount of NO_x emitted and in the ambient air. Further study might lead to a precise definition of conditions conducive to NO_2 and ozone production for general classes of situations.

2. Case Studies with Restricted Data Sets

The purpose of exercising the models with the restricted data sets was to compare the estimated degradation in model performance that could be expected when only limited data are available with performance given a complete data set. Unfortunately, a complete data set was not available for this study owing to the deficiencies in the data base discussed earlier; an accurate estimate of the degradation attributable to data limitations is accordingly, not possible. However, the comparison of the model predictions for restricted cases with those for the unrestricted cases (in which we adjusted dispersion rates and hydrocarbon concentrations) is useful, because it permits us to make a further assessment of how reasonable our dispersion estimates for the unrestricted cases may be.

The computed statistical parameters for NO_2 predictions of the models using the restricted data base are shown in Table 8. It is clear that the overall performances of all four models are inferior to performance with the unrestricted set but are still reasonably good. For example, the mean of the differences between RPM-II NO_2 predictions and observations is -9.2 ppb, the standard deviation is 30.31 ppb, and its correlation coefficient is 0.69 for the restricted set. The means of differences of all four models indicate that the models tended to underpredict NO_2 concentrations relative to their performances for the unrestricted cases. If we compare the plume dispersion parameters (plume widths and plume depths) used in the restricted and unrestricted cases, we find that the adjusted plume widths* generally are larger than the widths estimated from Pasquill-Gifford curves, and the adjusted plume depths* are generally smaller than the depths estimated from TVA curves (despite the 3000 m restriction we placed on plume depths estimated from TVA curves). The combined effect, however, is that the dispersion rates for the restricted cases are slightly larger, on the average, than those for the unrestricted cases. It is interesting to note that TCM tended to overpredict, even with the greater dispersion of the restricted cases.

---

* Plume areas were adjusted in the unrestricted case, and the adjustments to the areas were made by changing the plume widths only.

TABLE 8. COMPUTED STATISTICAL PARAMETERS FOR RPM-II, TCM, OLM, AND CNOM NO_2 PREDICTIONS FOR RESTRICTED CASES

	Models			
Statistics	RPM-II	TCM	OLM	CNOM
Mean Difference (ppb)	-9.20	2.63	-5.25	-7.75
Standard Deviation (ppb)	30.31	43.2	29.9	29.7
Correlation Coefficient	0.69	0.54	0.70	0.70

The NO and O_3 predictions of RPM-II for the restricted cases are not as good as those for the unrestricted cases. The mean of the differences between predictions and observations is -4.17 ppb for NO and -9.1 ppb for ozone. The correlation coefficients are 0.35 and 0.55 for O_3 and NO predictions, respectively. We cannot explain the significantly poorer performance of RPM-II for these species than for NO_2. However, because the wind speeds used in the restricted cases were estimated from measured surface winds--and these estimates are occasionally significantly different from measured winds at plume height, used in the unrestricted cases--the transit times to the aircraft traverse distances and the time-histories of sunlight exposure and ambient air entrainment in these restricted cases are occasionally inconsistent with actual plume conditions. These inconsistencies mean that RPM-II is not simulating the plume in conditions like the measurement conditions. This fact may explain in part the poorer performance of RPM-II in the restricted cases, but it does not fully explain why NO_2 predictions are so much better than NO and O_3 predictions. The simple models would not be as greatly affected by these inconsistencies because of their more simplified treatment of photochemistry, whereas RPM-II is most sensitive to them.

VI CONCLUSIONS

On the basis of a review and analysis of the MISTT data base and the comparison of RPM-II and simple plume model (TCM, OLM, and CNOM) predictions with plume concentration measurements made during the MISTT program, the following conclusions may be drawn:

> Validation of reactive plume models(including simple screening models)must await more accurate determination of input than was available in this study.

> RPM-II performed well when adjustments to input ambient hydrocarbon and plume dispersion rates were made to compensate for large uncertainties associated with the measurements of the parameters.

> The basic formulation of RPM-II appears to be sound and provides qualitatively accurate resolution of the spatial distributions of plume concentrations. RPM-II does appear to account qualitatively for both the chemical and physical phenomena governing O_3 and NO_2 formation in power plant plumes.

> The simple NO_2 models performed as well as RPM-II.

> Precise definition of conditions conducive to enhancement of plume NO_2 and ozone caused by hydrocarbon oxidation cannot be drawn from this study.

> The simple models' potential utility as screening procedures is not limited by the results of this study. Simple screening models appear to be sufficient for predicting peak ground-level NO_2 concentrations in most situations in which the peak occurs relatively close to the stack (less than 75 km). Based upon their relative performances, the total conversion method appears to be the most

conservative predictor (tending toward overprediction) of the three simple models tested, and the conservation of NO_x and oxidant method, which is the most complex, is least conservative.

VII RECOMMENDATIONS

Based on the experience gained during this study, and considering its findings, the following recommendations are made:

> Validation of sophisticated reactive plume models is required because of the growing demand for their usage in assessing short term ozone and NO_2 impacts of large point sources.

- However, validation of such models requires an extensive data base designed specifically to meet the input data and validation data needs of the models.
- Such a data base must include an accurate quantification of ambient hydrocarbons and plume dispersion rates (representative of appropriate averaging times) in addition to the other data collected in the MISTT study.

> Additional work is needed to develop new models, or extend existing models for practical use, that can account more directly for near-stack phenomena such as diffusion limiting of chemical reaction rates and nonuniform vertical plume concentration distributions. Validation of the new or extended models will also be required.

REFERENCES

Boris, J. P., and D. L. Book. 1973. Flux Corrected Transport. I. SHASTA, an Algorithm That Works. J. Comp. Phys. 11:38-69.

Calvert, J. G. 1976. Test of the Theory of Ozone Generation in Los Angeles Atmosphere. Environ. Sci. Technol. 10:248.

Cardwell, G. 1978. Regional Air Pollution Study (RAPS), Proposed Final Report. AMC7010.T0113PFR, Rockwell International, Air Monitoring Center, Creve Coeur, Missouri.

Carpenter, S. B., et al. 1971. Principal Plume Dispersion Models: TVA Power Plants. J. Air Pollut. Control Assoc. 21:491-495.

Coffin, D. L., and D. E. Gardner. 1972. Interaction of Biological Agents and Chemical Air Pollutants. Am. Occup. Hyg. 15:219-234.

Coffin, D. L., et al. 1968. Effect of Air Pollution on Alteration of Susceptibility to Pulmonary Infection. Proc. of Third Annual Conference on Atmospheric Contamination in Confined Space. Aerospace Medical Research Laboratory, pp. 71-80.

Csanady, G. T. 1973. Turbulent Diffusion in the Environment. D. Reidel, Dordrecht, Holland.

DeBower, K. K. 1976. A Method of Modeling Chemically Reactive Plumes. Thesis. Report No. 45 by Atmospheric Science Group. College of Engineering, University of Texas, Austin, Texas.

Ehrlich, R. 1966. Effects of Nitrogen Dioxide on Resistance to Respiratory Infection. Bact. Rev. 30:604-614.

Eschenroeder, A. Q. 1975. An Assessment of Models for Predicting Air Quality. ERTW-75-03, Environmental Science and Technology, Incorporated, Bedford, Massachusetts.

__________ 1972. Evaluation of a Diffusion Model for Photochemical Smog Simulation. EPA-R4-73-012, Environmental Protection Agency, Research Triangle Park, North Carolina.

Eschenroeder, A. Q., and J. R. Martinez. 1971. Further Development of the Photochemical Smog Model for the Los Angeles Basin. CR-1-191, General Research Corporation, Santa Barbara, California.

Gear, C. W. 1971. The Automatic Integration of Ordinary Differential Equations. Communications of the ACM. 14:176-190.

Gifford, F. A., Jr. 1961. Uses of Routine Meteorological Observations for Estimating Atmospheric Dispersion. Nuclear Safety. 2:47.

Hecht, T. A., J. H. Seinfeld, and M. C. Dodge. 1974. Further Development of a Generalized Kinetic Mechanism for Photochemical Smog. Environ. Sci. Technol. 8:327-339.

Hegg, D., et al. 1977. Reaction of Ozone and Nitrogen Oxides in Power Plant Plumes. Atmos. Environ. 11:521.

Keiffer, W. S., et al. 1977. Paper presented at 174th Annual Meeting, American Chemical Society, August 1977, Chicago, Illinois.

Killus, J. P., et al. 1977. Continued Research in Mesoscale Air Pollution Simulation Modeling--Vol. V: Refinements in Numerical Analysis, Transport, Chemistry, and Pollutant Removal. EF77-142, Systems Applications, Incorporated, San Rafael, California.

Liu, M. K., J. P. Killus, and P. M. Roth. 1977. A Study of the DEPICT Model. EF77-100R, Systems Applications, Incorporated, San Rafael, California.

Liu, M. K., D. A. Stewart, and P. M. Roth. 1978. An Improved Version of the Reactive Plume Model (RPM-II). Ninth NATO/CCMS International Technical Meeting on Air Pollution Modeling, 28-31 August 1978, Toronto, Canada.

Liu, M. K., M. A. Yocke, and P. M. Roth. 1978. Assessing the Potential Impact on Air Quality of Proposed PG&E Facilities in Northern California. Systems Applications, Incorporated, San Rafael, California.

Liu, M. K. et al. 1976. The Chemistry, Dispersion, and Transport of Air Pollutants Emitted from Fossil Fuel Power Plants in California: Data Analysis and Emission Impact Model. EF76-18R, Systems Applications, Incorporated, San Rafael, California.

Miller, D. F., et al. 1978. Ozone Formation Related to Power Plant Emissions. Science. 202:1186-1188.

Pasquill, F. 1976. Atmospheric Dispersion Parameters in Gaussian Plume Modeling. Part II. EPA-600/4-76-030b, U.S. Environmental Protection Agency, Research Triangle Park, North Carolina.

Peters, L. K., and L. W. Richards. 1977. Extension of Atmospheric Dispersion Models to Incorporate Fast Reversible Reactions. Atmos. Environ. 11:101-108.

Rasmussen, R. A., R. B. Chatfield, and M. W. Holdren. 1976. Hydrocarbon and Oxidant Chemistries Observed at a Site Near St. Louis. EPA Report under Contract 68-02-2254.

Riggan, W. B. 1976. Protocol for Studying Effects of Varying Patterns of Peak Exposures to NO_2 on Acute Respiratory Disease in the Los Angeles Basin. Environmental Protection Agency, Research Triangle Park, North Carolina.

Seinfeld, J. H., T. A. Hecht, and P. M. Roth. 1973. Existing Needs in the Experimental and Observational Study of Atmospheric Chemical Reactions: A Recommendations Report. R73-21, Systems Applications, Incorporated, San Rafael, California.

Shy, C. M., et al. 1970. The Chattanooga Schoolchildren Study: Effects of Community Exposure to Nitrogen Dioxide: I--Incidence of Acute Respiratory Illness, and II-- Methods, Description of Pollutant Exposures, and Results of Ventilatory Function Testing. J. Air Pollut. Control Assoc. 20:539, 582-588.

Taylor, G. H. 1977. Air Quality Impacts of Outer Continental Shelf Oil Development in the Santa Barbara Channel. Report P-5086, Environmental Research and Technology, Incorporated, Santa Barbara, California.

Tesche, T. W., et al. 1976. Determination of the Feasibility of Ozone Formation in Power Plant Plumes. EPRI EA-307, Electric Power Research Institute, Palo Alto, California.

Turner, D. B. 1971. Workbook of Atmospheric Dispersion Estimates. U.S. Department of Health, Education, and Welfare, Cincinnati, Ohio.

Turner, D. B. 1969. Workbook of Atmospheric Dispersion Estimates. 999-AP-26, U.S. Public Health Service, Cincinnati, Ohio.

Uthe, E. E., and W. E. Wilson. 1977. LIDAR Observations of the Density and Behavior of the Labadie Power Plant Plume. Proc. of 4th Joint Conference on Sensing of Environmental Pollutants. 6-11 November 1977, New Orleans, Louisiana.

Weber, A. H. 1976. Atmospheric Dispersion Parameters in Gaussian Plume Modeling. Part I. EPA-600/4-76-030a, U.S. Environmental Protection Agency, Research Triangle Park, North Carolina.

White, W. H. 1977. NO_x-O_3 Photochemistry in Power Plant Plumes: Comparison of Theory with Observation. Environ. Sci. Technol. 11:995-1000.

Whitten, G. Z., and H. Hogo. 1979. Air Quality Impacts of the Pacific Gas and Electric Power Plant in San Francisco. EF79-8, Systems Applications, Incorporated, San Rafael, California.

__________ 1977. Mathematical Modeling of Simulated Photochemical Smog. EPA-600/3-77-001, Environmental Protection Agency, Research Triangle Park, North Carolina.

Appendix A

AN IMPROVED VERSION OF THE REACTIVE PLUME MODEL (RPM-II) *

by

Mei-Kao Liu, Douglas A. Stewart, and Philip M. Roth
Systems Applications, Incorporated
950 Northgate Drive
San Rafael, California USA 94903

Abstract. A reactive plume model developed previously has been revised to consider concentration distributions across the plume. The model is composed of a fixed number of cells that can expand as the plume travels downwind. For an inert pollutant, there is no net flux across the cell boundaries. For background or reactive pollutants, net fluxes are calculated via equivalent diffusion coefficients. A more up-to-date kinetic module, the Carbon-Bond Mechanism, has been incorporated into the revised model to treat the reactions of hydrocarbons and oxides of nitrogen.

Introduction

Compared to emissions of pollutants from area or diffusive sources, emissions from large stationary or point sources, such as power plants, refineries, and other industrial facilities, possess distinct physical features that require special attention. From a theoretical point of view, the most prominent example is the characteristically different diffusive behavior of emissions from point and area sources. It can be demonstrated via statistical theory[1] that the diffusion of continuous emissions from a point source can be characterized by a dispersion coefficient that is initially proportional to time since emission and asymptotically proportional to the square root of that time. In the initial phase the diffusive property depends upon, among other variables, the histories of the individual fluid particles. Thus the diffusion of point source emissions is not amenable to the method commonly used for area sources, the Fickian diffusion treatment. Only at large diffusion times, when the effects of the type of emissions source on the fluid particles are greatly reduced, can the Fickian or K-theory approach be expected to be valid.

From a practical point of view, the most important difference between point and area source air quality modeling is the question of spatial resolution. Due to the disparity in the spatial scales appropriate to each, conventional grid models have difficulty in properly treating the transport and dispersion of emissions from a point source. This is probably the reason why Gaussian models have been used so extensively for point sources, despite their many known deficiencies.

---

* Paper presented at the Ninth NATO/CCMS International Technical Meeting on Air Pollution Modeling, 28-31 August, 1978, Toronto, Canada.

Rigorously, the use of Gaussian models is limited to inert and linearly reactive pollutants. Many problems unique to point source emissions, however, involve nonlinear chemical reactions. Because the emissions from power plants are rich in nitric oxide, which reacts with ozone, nitrogen dioxide is formed within the plume immediately downwind of a power plant while ozone is usually depleted.[2,3] This phenomenon is generally the result of complex photochemical reactions between the emitted nitric oxide and ozone and hydrocarbons entrained from the ambient air. Thus, for some point source problems, classical Gaussian models offer little help.

Many models have been developed to consider the nonlinear interactions of a plume with urban or rural air containing background concentrations of various pollutants. These models range from simple box-type models to complex grid models. A reactive plume model was developed a few years ago[4] to simulate the behavior of reactive pollutants in a plume from a single point source. This model is a moving parcel model based on simple mass balance for each pollutant species within a single well-mixed box. It treats chemical reactions using a detailed kinetic module. Provisions were also made for the model to accommodate variations in meteorological conditions and ambient pollutant concentrations. This model was applied to a number of power plants and refineries in the western United States, and the model predictions generally compared favorably with measurements. However, it was felt in these exercises that the use of a single well-mixed box in the model was rather restricting.[4] The objective of this paper is to describe an innovative approach aimed at removing this major restriction.

As a generalization of the single box concept in the original reactive plume model,[5] the revised model considers an array of well-mixed reactors or cells across the plume. Assume that the width and height of cell j can be described by two parameters:

$$w^j = w^j(s) \quad , \qquad \text{(A-1)}$$

$$h^j = h^j(s) \quad , \qquad \text{(A-2)}$$

where w^j denotes the width of cell j, h^j is the vertical thickness of the plume, and s represents the distance downwind of a point source measured along the plume axis. Based on a mass balance, the governing equation along a wind trajectory s can then be expressed as

$$\frac{dc_i^j}{dt} = \left(\frac{dc_i^j}{dt}\right)_{chem} - \left(\frac{1}{w^j} \cdot \frac{dw^j}{ds}\right) uc_i^j - \left(\frac{1}{h^j} \cdot \frac{dh^j}{ds}\right) uc_i^j \quad , \qquad \text{(A-3)}$$

$$i = 1, 2, \ldots, N; \qquad j = 1, 2, \ldots, M;$$

where c_i^j denotes the concentration of chemical species i in cell j, u is the wind speed along the plume trajectory, and t is time since emission. In the revised model, the total mass of each primary pollutant is initially divided equally among M cells. By allowing the volume of each cell to expand as dictated by atmospheric dispersion, cell boundaries can be viewed as impermeable for unreactive pollutants. Thus, only the diffusion of reactive and entrained pollutants must be parameterized. For example, within the framework of a Gaussian formulation and for an elliptically shaped plume, the radii (in transformed polar coordinates) of concentric rings containing equal pollutant masses can be shown to be[6]

$$r_j = \sqrt{2\ell n\left(\frac{M}{M - j}\right)} \quad , \tag{A-4}$$

where r_j is the radius of the j-th concentric ring, and σ_y and σ_z represent the horizontal and vertical dispersion coefficients for the plume. (The transformed polar coordinates are given by $r^2 = y^2/\sigma_y^2 + z^2/\sigma_z^2$.) Under plume trapping conditions, the width of the j-th cell in a rectangular-shaped plume can be found by solving the transcendental equation:

$$\frac{1}{2M} = \frac{\text{erf}\left(\frac{y_j}{\sqrt{2}\sigma_y}\right) - \text{erf}\left(\frac{y_{j-1}}{\sqrt{2}\sigma_y}\right)}{\left(\frac{y_j}{\sigma_y}\right) - \left(\frac{y_{j-1}}{\sigma_y}\right)} \quad , \tag{A-5}$$

where y_j is the width of the j-th cell. Equation (A-5) can be solved numerically via iterative schemes.

Horizontal Dispersion

One of the most important processes in the behavior of a plume from a large point source is horizontal dispersion. As shown in Figure A-1, the revised reactive plume model is composed of a fixed number of cells that can expand as they move downwind. For an inert species emitted from the source, the rates of expansion of these cells are determined by horizontal dispersion such that there is no net mass flux across cell boundaries. For a background or a reactive pollutant the Fickian diffusion approach is adopted: The flux across the interface between cells j and j+1 is assumed to be equal to the product of an equivalent diffusion coefficient K_j and the concentration gradient of the background or reactive species relative to that of an inert species. That is,

$$F_j = -K_j\left(\left.\frac{c}{y}\right|_j - \left.\frac{\tilde{c}}{y}\right|_j\right) \quad , \tag{A-6}$$

where c and $\tilde{c}$ denote the concentration distributions of the background or reactive pollutant and the inert species, respectively. The equivalent diffusion coefficient can be determined by considering the case of a constant background concentration c_B. Since, after each time step, c_B should be unchanged, a simple balance of mass fluxes for cell j yields

$$c_B\left(\frac{dy_j}{dt}\right) - c_B\left(\frac{dy_{j-1}}{dt}\right) = K_j\left(\left.\frac{\partial\tilde{c}}{\partial y}\right|_j\right) - K_{j-1}\left(\left.\frac{\partial\tilde{c}}{\partial y}\right|_{j-1}\right) \quad . \tag{A-7}$$

Assuming local symmetry at the centerline of the plume one may impose

$$K_0 = 0 \quad . \tag{A-8}$$

Then the equivalent diffusion coefficient K_j can be solved by using the recurrence formula in Eq. (A-7) and appropriate finite difference approximations.

Vertical Structure of the Plume

As shown in Figure A-2, the revised version of the reactive plume model is designed to estimate the averaged concentrations of reactive pollutants within the plume under limited mixing conditions. For computing ground-level concentrations, the model is thus applicable only at points downwind of the plume touch-down point (identified in Figure A-2 as TD). For example, if the Gaussian equation is used, the downwind distance of the maximum ground-level concentration can be obtained by setting

$$\frac{d}{dx}\left[\frac{Q}{\pi\sigma_y\sigma_z u}\, e^{-\left(\frac{H^2}{2\sigma_z^{\,2}}\right)}\right]_{y=0} = 0 \tag{A-9}$$

and assuming $\sigma_z = ax^b$ and $\sigma_y = dx^f$. In these expressions Q is the rate of emissions, H is the effective stack height, and a, b, d, and f are empirical coefficients. In this case the downwind distance of the maximum ground-level concentration is:

$$x_{max} = \left[\frac{bH^2}{a^2(b+f)}\right]^{1/2b} \qquad 1\ \text{km} < x < 10\ \text{km} \quad . \tag{A-10}$$

Thus, as shown in Figure A-3, the reactive plume model can be trivially modified for estimating the ground-level concentration of an inert species by assuming

$$c_{surface} = 0 \qquad \text{for } x < x_{max} \quad . \tag{A-11}$$

For reactive pollutants such as NO_2, the arithmetic is slightly more complicated because the downwind distance of the maximum ground-level concentration is given by an equation of the form

$$\frac{dc_{NO_2}}{dx} = \left|\left(\frac{dc_{NO_2}}{dx}\right)_{\text{chemical formation}}\right| - \left|\left(\frac{dc_{NO_2}}{dx}\right)_{\text{diffusion}}\right| = 0 \quad . \tag{A-12}$$

This expression can be evaluated numerically.

Kinetic Mechanism

Many applications of the reactive plume model require a kinetic mechanism describing pertinent chemical reactions. This mechanism must include a specification of the elementary kinetic steps and their associated rate constants.

Extensive efforts have been made in the past to develop a valid kinetic mechanism for photochemical smog, focusing primarily on systems of hydrocarbons and nitrogen oxides.[7] The revised version of the reactive plume model incorporates a recently developed kinetic module, the Carbon-Bond Mechanism (CBM).[8] This mechanism includes the latest information on more than 30 reaction steps to model chemical transformations in HC-NO_x-O_3 systems. A list of these steps and their associated rate constants appears in Table A-1. The CBM has been found to simulate the reactivities of hydrocarbon compounds in the atmosphere more accurately than the mechanism in the original reactive plume model.

In this preliminary study, the full Carbon-Bond Mechanism was used. Because of the computational burden, in future applications consideration will be given to the use of a simplified set of reactions that invokes the quasi-steady-state assumption for certain radicals.

Results and Discussion

The reactive plume model (RPM-II) described above was exercised for the hypothetical case of six horizontal cells used to simulate a symmetric Gaussian plume of NO emitted into an atmosphere containing low ambient concentrations of O_3 and HC. The results, which should be considered as preliminary, are reported here. In Figure A-4, the computed equivalent diffusion coefficients at the cell boundaries are plotted as a function of time and distance from the plume centerline. The calculated NO and O_3 concentrations are presented in Figures A-5 and A-6. The NO profiles appear to retain the Gaussian shape. In contrast, the ozone distribution shows that ozone is depleted within the plume initially and reformed at a later time. It is not clear, however, whether the slight ozone bulge at the middle two cells of the plume is real or an artifact as a result of numerical round-off errors. Further testing of this model is currently being carried out.

Acknowledgments

This work was supported in part by the Exxon Company U.S.A., Pacific Gas and Electric Company, and the U.S. Environmental Protection Agency (Contract DA-6-99-5212A).

TABLE A-1. CARBON-BOND MECHANISM*

Reaction	Rate Constant at 298K (ppm^{-1} min^{-1})	Activation Energy (K)
$NO_2 + h\nu \rightarrow NO + O$	Experimental	--
$O_3 \rightarrow O_3$	4.40×10^6	--
$O_3 + NO \rightarrow NO_2 + O_2$	2.39×10^1	1.45×10^3
$O_3 + NO_2 \rightarrow NO_3 + O_2$	4.80×10^{-2}	2.45×10^3
$O + NO_2 \rightarrow NO + O_2$	1.34×10^4	--
$O_3 + OH \rightarrow HO_2 + O_2$	7.70×10^1	1.0×10^3
$O_3 + HO_2 \rightarrow OH + 2O_2$	5.00	1.525×10^3
$NO_2 + OH \rightarrow HNO_3$	1.40×10^4	--
$CO + OH \rightarrow HO_2 + CO_2$	4.40×10^2	--
$NO + NO \rightarrow NO_2$	1.50×10^{-4}	--
$NO_3 + NO \rightarrow 2NO_2$	2.80×10^4	--
$NO_3 + NO_2 + H_2O \rightarrow 2HNO_3$	3.10×10^{-5}	-1.06×10^4
$HO_2 + NO \rightarrow NO_2 + OH$	1.20×10^4	--
$HO_2 + HO_2 \rightarrow$	1.50×10^3	--
$PAR + O \rightarrow MEO_2 + OH$	2.00×10^1	--
$PAR + OH \rightarrow MEO_2$	1.50×10^3	--
$OLE + O \rightarrow MEO_2 + ACO_3 + X$	2.70×10^3	--
$OLE + O \rightarrow CARB + PAR$	2.70×10^3	--
$OLE + OH \rightarrow RAO_2$	4.20×10^4	--
$OLE + O_3 \rightarrow CARB + CRIG$	8.00×10^{-3}	--
$OLE + O_3 \rightarrow CARB + MCRG$	8.00×10^{-3}	--
$ETH + O \rightarrow MEO_2 + HO_2 + CO$	6.00×10^2	--
$ETH + O \rightarrow CARB$	6.00×10^2	--

TABLE A-1 (Continued)

Reaction	Rate Constant at 298K ($ppm^{-1}min^{-1}$)	Activation Energy (K)
$ETH + OH \rightarrow RBO_2$	1.20×10^4	--
$ETH + O_3 \rightarrow CARB + CRIG$	2.40×10^{-3}	--
$ACO_3 + NO \rightarrow NO_2 + MEO_2 + CO_2$	3.80×10^3	--
$RBO_2 + NO \rightarrow NO_2 + 2CARB + HO_2$	1.20×10^4	--
$RAO_2 + NO \rightarrow NO_2 + 2CARB + HO_2$	1.20×10^4	--
$MEO_2 + NO \rightarrow NO_2 + CARB + MEO_2 + X$	$(1.2 \times 10^4)(A - 1)/A^{\S}$	--
$MEO_2 + NO \rightarrow NO_2 + CARB + HO_2$	$(1.2 \times 10^4)/A^{\S}$	--
$MEO_2 + NO \rightarrow$	1.00×10^3	--
$RBO_2 + O_3 \rightarrow 2CARB + HO_2$	5.0	--
$RAO_2 + O_3 \rightarrow 2CARB + HO_2$	2.00×10^2	--
$MEO_2 + O_3 \rightarrow CARB + HO_2$	5.0	--
$CARB + OH \rightarrow \alpha(HO_2 + CO) + (1- \alpha)(ACO_2 + X)$	$(2.4 - \alpha) \times 10^4$	--
$CARB + h\nu \rightarrow CO$	$\alpha\ K_f{}^{\dagger}$	--
$CARB + h\nu \rightarrow (1 + \alpha)HO_2 + (1- \alpha)(MEO_2 + X) + CO$	$\left(\frac{\alpha + 1}{2}\right) K_f{}^{\dagger}$	
$X + PAR \rightarrow$	1.00×10^5	--
$ACO_3 + NO_2 \rightarrow PAN$	2.00×10^3	--
$PAN \rightarrow NO_2 + ACO_3$	2.80×10^{-2}	1.25×10^4
$ACO_3 + HO_2 \rightarrow$	4.00×10^3	--
$MEO_2 + HO_2 \rightarrow$	4.00×10^3	--
$CRIG + NO \rightarrow NO_2 + CARB$	1.20×10^4	--
$CRIG + NO_2 \rightarrow NO_3 + CARB$	8.00×10^3	--
$CRIG + CARB$	2.00×10^3	--
$MCRG + NO \rightarrow NO_2 + CARB + PAR$	1.20×10^4	--

TABLE A-1 (Continued)

Reaction	Rate Constant at 298K ($ppm^{-1}min^{-1}$)	Activation Energy (K)
MCRG + NO_2 → NO_3 + CARB + PAR	8.00×10^3	--
MCRG + CARB →	2.00×10^3	--
CRIG → CO	6.70×10^2	--
CRIG →	2.40×10^2	--
CRIG → $2HO_2$ + CO_2	9.00×10^1	--
MCRG →	1.50×10^2	--
MCRG → MEO_2 + OH + CO	3.40×10^2	--
MCRG → MEO_2 + HO_2+ CO_2	4.25×10^2	--
MCRG → CARB + $2HO_2$ + CO	8.50×10^1	--
ARO + OH → HO_2 + 3Y	6.00×10^3	--
ARO + OH → HO_2 + BZA + X	1.60×10^3	--
ARO + OH → OH + BZA + W	1.50×10^4	--
W + CARB →	1.00×10^5	--
Y + NO → NO + CARB + PAR	3.00×10^1	--
Y + NO → NO_2 + AERO	1.50×10^1	--
Y + NO_3 → 2CARB	3.50×10^4	--
Y + O_3 → AERO	6.00×10^{-1}	--
BZA + OH → HO_2 + 3Y + CO	1.00×10^4	--
BZA → MEO_2 + HO_2 + 3Y	K_{BZA}††	--

TABLE A-1 (Concluded)

Reaction	Rate Constant at 298K ($ppm^{-1}min^{-1}$)	Activation Energy (K)
$SO_2 + OH \rightarrow HSO_5$	2.00×10^3	--
$HSO_5 + NO \rightarrow NO_2 + HSO_4$	8.00×10^2	--
$HSO_4 + NO_2 \rightarrow AERS + HNO_3$	1.00×10^4	--

---

* Units of min^{-1}.

† A = Average number of aledhyde formed per hydrocarbon oxidized.

§ α is the fraction of total aldehydes that represents formaldehyde and ketones. K_f is the aldehyde photolysis rate constant.

** $K_{BZA} = 100 \times \left(\frac{\alpha + 1}{2}\right) K_f$.

†† Species in the carbon-bond mechanism.

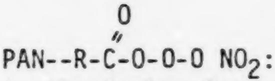

$PAN\text{--}R\text{-}\overset{O}{\overset{\|}{C}}\text{-}O\text{-}O\text{-}O\ NO_2$

> PAN--R-C-O-O-O NO_2: R is principally CH_3 ; mass balance in the Carbon-Bond Mechanism (CBM) assumes that R is CH_3 .

> OLE--$HCH{=}CH_2$: reacts with the propylene rate constant.

> CARB--HCHO: reacts as either formaldehyde or higher aldehydes depending on paramater α.

> PAR--CH_4: reacts as average paraffin or is brought in by χ for mass balance.

> ARO-- : reacts as substituted aromatic (e.g., toluene).

> ETH--C_2H_4: treated explicitly as ethylene.

> BZA-- 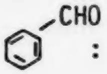 : minor compound in aromatics chemistry (mostly benzaldehyde).

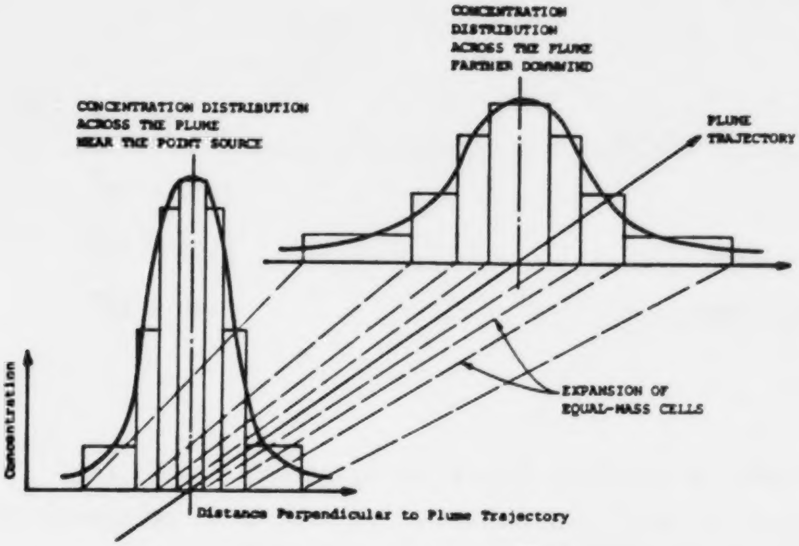
CONCENTRATION
DISTRIBUTION
ACROSS THE PLUME
FARTHER DOWNWIND
CONCENTRATION DISTRIBUTION
ACROSS THE PLUME
NEAR THE POINT SOURCE
PLUME
TRAJECTORY
EXPANSION OF
EQUAL-MASS CELLS
Concentration
Distance Perpendicular to Plume Trajectory

Figure A-1. Schematic of cell expansion as a function of downwind distance in the revised reactive plume model.

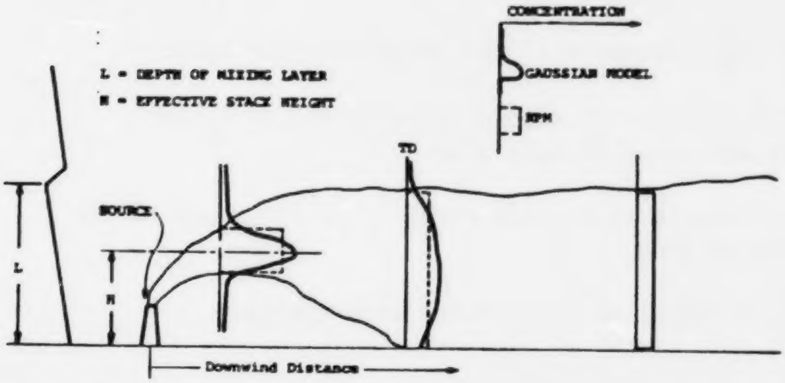
CONCENTRATION
GAUSSIAN MODEL
RPM
L = DEPTH OF MIXING LAYER
H = EFFECTIVE STACK HEIGHT
TD
SOURCE
L
H
Downwind Distance

Figure A-2. Vertical concentration distribution in the plume as a function of downwind distance. TD indicates point at which the plume touches the ground.

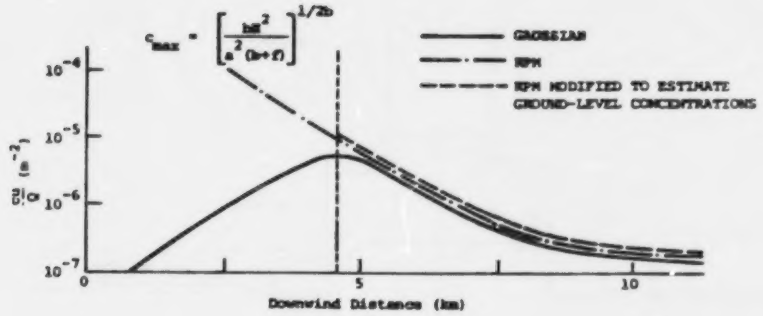

Figure A-3. **Plume centerline concentration as a function of downwind distance.**

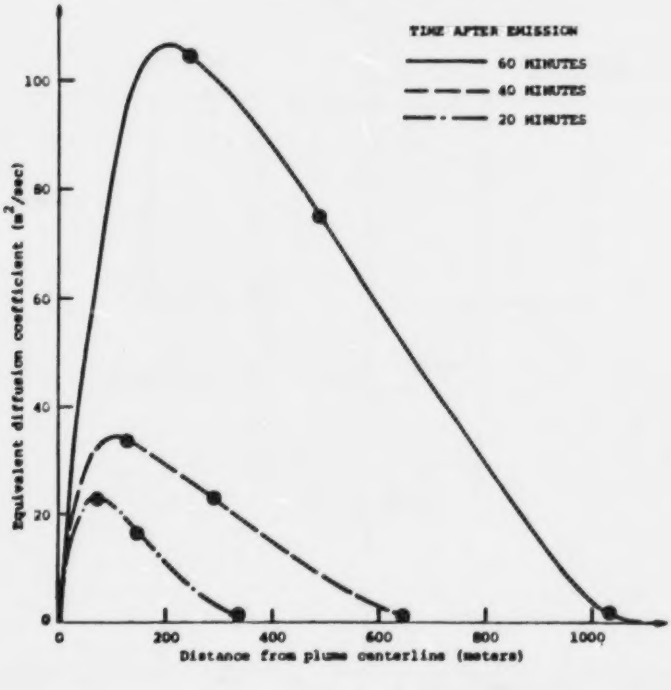

Figure A-4. **Equivalent diffusion coefficients as a function of time after emission and location.**

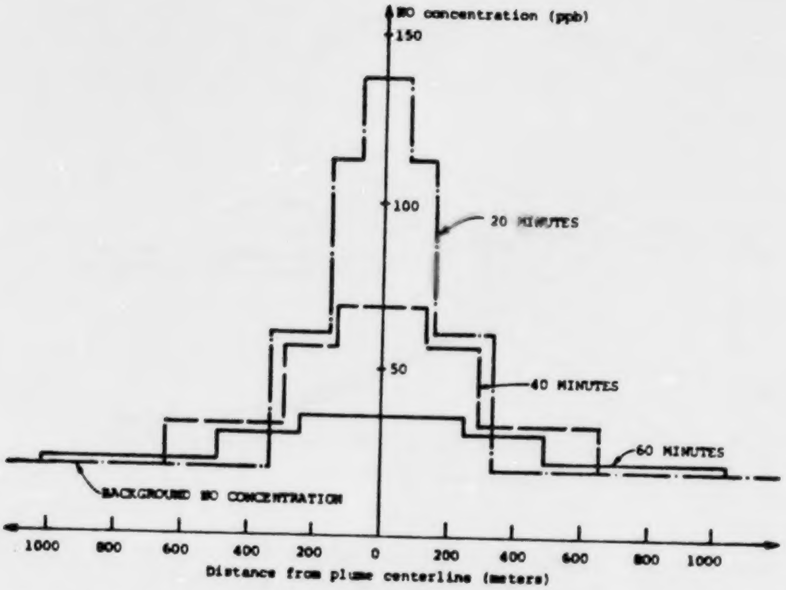

Figure A-5. Computed NO concentration as a function of time after emission and location.

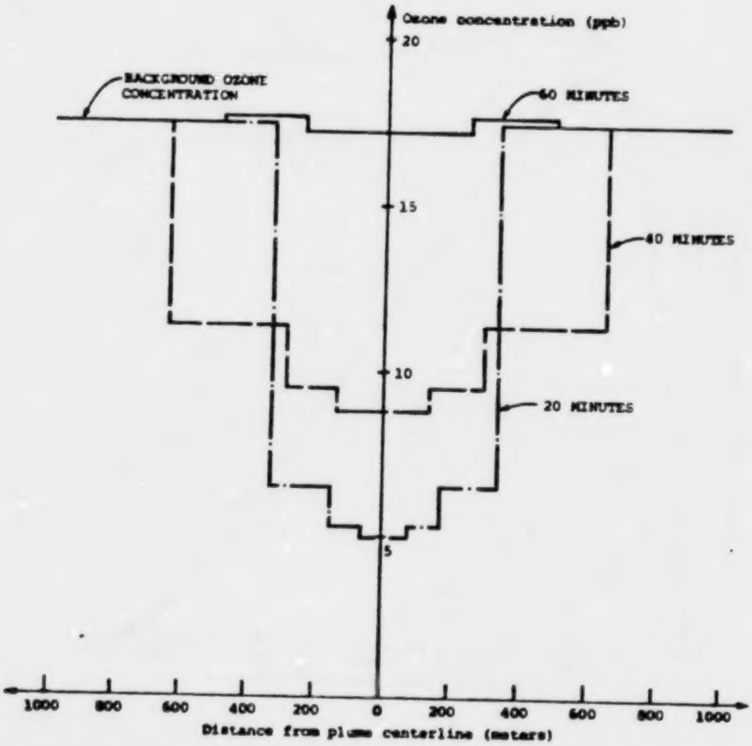

Figure A-6. Computed ozone concentration as a function of time after emission and location.

References

1. G. I. Taylor, "Diffusion by Continuous Movements," Proc. London Math. Soc., Vol. 2, No. 20, pp. 196-202, 1921.

2. D. D. Davis, G. Smith, and G. Klauber, "Trace Gas Analysis of Power Plant Plumes via Aircraft Measurements: O_3, NO_x, and SO_2 Chemistry," Science, Vol. 186, pp. 733-736, 1974.

3. O. T. Melo, "Nanticoke GS Brown Plume Study," Ontario Hydro Report No. 77-250-K, Toronto, Ontario, Canada, 1977.

4. M. K. Liu, "Development of a Mathematical Model for Simulating Power Plant Plumes," Fourth Int'l. Clean Air Congress, Tokyo, Japan, May 1977.

5. M. K. Liu, M. A. Yocke, and P. V. Mundkur, "Numerical Simulation of Reactive Plumes," 68th Meeting of Am. Inst. Chem. Engineers, Los Angeles, California, 17 November 1975; also Air Series, American Institute of Chemical Engineers, 1976.

6. J. Freiberg, "The Iron Catalysed Oxidation of SO_2 to Acid Sulfate in Dispersing Plumes," Atmos. Environ., Vol. 10, pp. 121-130, 1976.

7. T. A. Hecht, J. H. Seinfeld, and M. C. Dodge, "Further Development of a Generalized Kinetic Mechanism for Photochemical Smog," Environ. Sci. Technol., Vol. 8, pp. 327-339, 1974.

8. G. Z. Whitten and H. Hogo, "Mathematical Modeling of Simulated Photochemical Smog," EPA-600/3-77-001, Systems Applications, Incorporated, San Rafael, California, 1977.

Appendix B

RPM-I SENSITIVITY STUDY*

by

Thomas W. Tesche and Philip M. Roth

OVERVIEW

One of the objectives of this project was to determine the sensitivity of RPM predictions to changes in the various input parameters in order to gain insight into the response of the model. Quantification of the impact of certain variables (e.g. emissions, atmospheric stability, temperature) on model predictions can be used to infer conditions that might be conducive to ozone formation in plumes.

The discussion in this section begins with a consideration of what a sensitivity study is, how its results may be applied, and what limitations one must place on the interpretation of the results. Then, a qualitative discussion of the study methodology is presented in order to reveal the distinguishing features of the approach used in arriving at RPM sensitivities. Next, the results of the preliminary variable screening study are identified, followed by a determination of sensitivities of four key variables. Conclusions concerning these results are presented last.

Because the approach used in the sensitivity study involves certain statistical concepts that may be unfamiliar to some readers, we present the theoretical details and procedures of the sensitivity study and a glossary of terms in Appendix C entitled "A Study of the Sensitivity of the Reactive Plume Model: Theoretical Basis and Procedures." In this section we provide the reader with an overview of the study and a discussion of the meaning and use of the results.

METHODOLOGY OF THE SENSITIVITY STUDY

Use of a Sensitivity Study

Essentially, a model sensitivity study involves an examination of the impact on the magnitude of a model's predicted response of changes in the magnitude of each of the model's parameters and variables. By studying the impact of changes in key variables insight into the nature of the model can be obtained. Furthermore, if the model provides good agreement with the physical system it simulates, then knowledge of model sensitivities may be used to infer the impact on the physical environment arising from changes in meterological or emission conditions.

---

* Reprinted from Ogren, J. A., et al. (1976), "Determination of the Feasibility of Ozone Formation in Power Plant Plumes, "EPRI EA-307, Meteorology Research, Incorporated, Altadena, California, and Systems Applications, Incorporated, San Rafael, California.

There are several reasons for conducting a model sensitivity analysis. Once the most sensitive variables have been identified, it is possible, by examining their respective range of uncertainties (due to theoretical simplification or measurement inaccuracies), to identify those variables for which the range of uncertainty can be reduced. This has important economic significance for, as we shall see, the variable to which RPM is most sensitive is also the one which was least well determined in the present field programs.

If sensitivity and uncertainty measures are obtained for each variable, the product of these quantities allows one to rank variables in order of their effective impact on model predictions. If a variable is one for which some degree of control can be exercised (such as improved measurements of ambient pollutant concentration or solar radiation), the design of the field program can then be modified to provide the necessary detail. However, if the key variable is uncontrolable (such as atmospheric mixing) then the uncertainties might be reduced by means of further model refinement. These reductions in the uncertainties associated with the variables of highest sensitivity will reduce the resultant uncertainty in the model's prediction.

Concept of a Response Function and Sensitivity Surface

In this section, we present certain concepts relating to the design of a sensitivity study and to the interpretation of results derived from such an effort. The following geometrical argument may be of value in introducing these concepts. Assume that for the physical environment of a power plant plume, only two variables--χ_1 and χ_2--are necessary to completely describe the occurrence of ozone concentrations. In the physical system, the combination of these two variables in any number of ways could be described by a three-dimensional surface, referred to as the "ozone surface", that represents the ozone concentrations in the plume. Conceptually, such a surface is represented by the three-dimensional topography shown in Figure B-1.

If ozone generation were to occur in plumes it might be associated with those regions (peaks) on the ozone topography that extend above some level marking the boundary between "ozone formation" and "no ozone formation." The purpose of the field programs was to determine experimentally if peaks such as those in Figure B-1 exist in real plumes.

The sensitivity study seeks to examine the nature of the ozone surface in Figure B-1. However, because RPM approximates plume phenomena, the model cannot reproduce the exact features of the hypothetical ozone surface that is presented in Figure B-1. But, by running the model many times, with each run corresponding to different values of χ_1 and χ_2, the predicted ozone concentrations can be used to describe another surface that resembles the ozone surface in Figure B-1. We call this the "response surface". The analytic function that describes this surface is called the "response function". Later, it will become apparent that it is the response function describing the RPM response surface that is of major concern in the sensitivity study. Due to the model's limitations the response surface that one can construct on the basis of RPM simulations will be different from the ozone surface in Figure B-1. The extent of this difference between the ozone and response surfaces is a measure of the model's validity.

From a sensitivity analysis one can determine the direction along the response surface of the greatest change in predicted ozone concentrations as a result of variation in any one of the variables. If the model closely represents the physical system, an identification of the "peaks" on the response surface may lead to an identification of those points on the ozone surface that correspond to ozone generation in plumes.

Summary of the Steps in the Sensitivity Study Methodology

In this section we describe the general steps taken in the determination of RPM sensitivities. Basically, the steps include:

- Selection of variables believed to be important in contributing to RPM ozone predictions
- Screening of variables to identify those of lesser importance which may be eliminated from further analysis

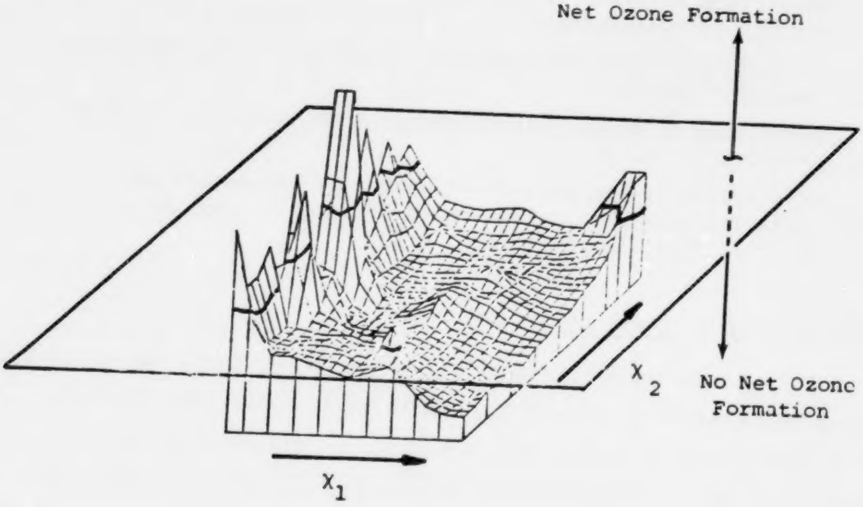
Net Ozone Formation
No Net Ozone Formation
X_2
X_1

Figure B-1. Schematic representation of a hypothetical ozone surface describing concentration in a power plant plume as a function of two variables.

- Tentative postulation of the general nature of the response function
- Selection of a simulation plan to vary model inputs that is compatible with the anticipated nature of the response function
- Simulation of hypothetical plumes using RPM for all sets of inputs specified by the simulation plan
- Regression analysis of the model predictions for the purpose of constructing the response function
- Evaluation of the accuracy and limitations of the resultant response function.
- Repetition of the foregoing steps if the response function proves inadequate
- Computation of RPM sensitivities to the parameters and variables under consideration by differentiating the response function.

Selection of Sensitivity Study Variables

The first step in the study involves determination of those variables and parameters believed to be significant in terms of model sensitivities. For lack of a more rigorous method for selecting the sensitivity variables, it is necessary to rely upon experience in air quality modeling and a physical understanding of plumes. Frequently more variables are initially considered than are either practical or necessary. Thus, one task in the sensitivity study involves screening of the variables to determine if some may be eliminated from consideration without significantly affecting the results of the study.

Eleven variables were identified that have (or may have) an important influence on the potential formation of ozone in a power plant plume. These variables and their assumed ranges are presented in Table B -1. Discussion of the variables and the rationale for the selection of suitable ranges for each variable is given in Appendix C . For the present, it is sufficient to say that the ranges chosen represent common but not necessarily extreme values. Strictly speaking, the model's sensitivity must be expressed in terms of the variation of the individual variables about some point within their respective ranges. Thus, baseline conditions were estimated for each variable; they are presented in Table B -2.

The eleven sensitivity variables were non-dimensionalized to avoid consideration of their units. In addition, the variables were scaled on the basis of

Table B-1

FACTORS IN THE POTENTIAL FORMATION OF OZONE IN POWER PLANT PLUMES

No.	Description	Symbol	Typical Range	Units
1	Reactivity of Ambient Hydrocarbon Mixture	R	$6500 \le x_1 \le 10{,}300$	min^{-1}
2	Ambient Ozone Concentration	O_3	$0.05 \le x_2 \le 0.10$	ppm
3	Ambient NO_x Concentration	bNO_x	$0.02 \le x_3 \le 0.05$	ppm
4	Ambient Reactive Hydrocarbon Concentration	RHC	$0.1 \le x_4 \le 2.0$	ppm (by volume)
5	Effective Plume Dispersion Parameter	P	$0.89 \le x_5 \le 1.3$	dimensionless
6	Mean Wind Speed	U	$3.25 \le x_6 \le 5.75$	meters/sec
7	Effective NO_2 Photolysis Rate	k_1	$0.1 \le x_7 \le 0.26$	min^{-1}
8	Absolute Ambient Humidity	w	$2000 \le x_8 \le 32{,}000$	ppm H_2O
9	Initial RPM NO_x Concentrations	pNO_x	$0.270 \le x_9 \le 1.08$	ppm
10	Ambient Atmospheric Temperature	T	$288.7 \le x_{10} \le 308.2$	°K
11	Initial RPM SO_2 Concentrations	SO_2	$0.05 \le x_{11} \le 0.5$	ppm

Table B-2

RPM SENSITIVITY STUDY INPUTS CORRESPONDING TO "BASELINE" CONDITIONS

Species	Ambient Concentrations (ppm)	Initial Conditions (ppm)
NO	0.0057	0.435
NO_2	0.0298	0.2175
O_3	0.075	0.010
Paraffins	0.5933	0.050
Olefins	0.0767	0.010
Aldehydes	0.0767	0.010
Aromatics	0.3003	0.030
SO_2	0.030	0.275

$k_1 = 0.18\ \text{min}^{-1}$

Wind Speed = 4.75 $\text{meters}\cdot\text{sec}^{-1}$

Initial Plume Width = 300 meters

Initial Plume Thickness = 137 meters

their assumed ranges so that when model sensitivities are computed later, they are not influenced by differences in the magnitudes of the ranges.

Specifically, each of the variables in Table B-1 was normalized by its half range, X_{HR}, and centered about the midpoint, X_0, of the range. Mathematically,

$$\chi_i = \frac{X - X_0}{X_{HR}} \qquad \text{(B-1)}$$

If X takes on a high value, X_{High}, and a low value, X_{Low}, then

$$X_{HR} = \frac{X_{High} - X_{Low}}{2} \qquad \text{(B-2)}$$

and

$$X_0 = \frac{X_{High} + X_{Low}}{2} \qquad \text{(B-3)}$$

The result was a new set of sensitivity variables, $\chi_1, \chi_2, \cdots \chi_{11}$. Table B-3 provides a list of the new variables χ_i and their relationship to the original variables X_i, the model inputs to RPM.

Selection of the Form of the Response Function

For a given variable, we are particularly interested in knowing the variation in the model's response due to slight excursions of the input variable about some reference (or baseline) value in that variable's range. We initially confine the study to a limited region of the response surface discussed in the previous section. Then, knowledge of the rate of change of the model's response with respect to any variable provides a measure of the model's sensitivity to that variable.

If the range of the model's response is sufficiently restricted, due to prudent selection of the variable ranges, then a multivariate Taylor series expansion may provide an adequate approximation to the true, but unknown, functional relationship between the RPM response and the input variables. Essentially, the series expansion approximates the form of the response surface in the local region of interest. Because of the limited variable ranges under consideration, only the first derivative terms in the expansion

Table B-3

NORMALIZED VARIABLES USED IN THE REACTIVE PLUME MODEL SENSITIVITY STUDY

Normalized Sensitivity Variable	Description	Normalized Value
X_1	Reactivity of the Hydrocarbon Mixture	$X_1 = \frac{x_1 - 8399.0}{950.0}$
X_2	Ambient Ozone Concentration	$X_2 = \frac{x_2 - 0.075}{0.0125}$
X_3	Ambient NO_x Concentration	$X_3 = \frac{x_3 - 0.035}{0.0075}$
X_4	Ambient Reactive Hydrocarbon Concentration	$X_4 = \frac{x_4 - 1.05}{0.475}$
X_5	Effective Plume Dispersion Parameter	$X_5 = \frac{x_5 - 1.095}{0.1025}$
X_6	Mean Wind Speed	$X_6 = \frac{x_6 - 4.5}{1.25}$
X_7	Effective NO_2 Photolysis Rate	$X_7 = \frac{x_7 - 0.18}{0.04}$
X_8	Absolute Ambient Humidity	$X_8 = \frac{x_8 - 17000.0}{7500.0}$
X_9	Initial RPM NO_x Concentration	$X_9 = \frac{x_9 - 0.6525}{0.225}$
X_{10}	Ambient Atmospheric Temperature	$X_{10} = \frac{x_{10} - 298.4}{9.75}$
X_{11}	Initial RPM SO_2 Concentration	$X_{11} = \frac{x_{11} - 0.275}{0.1125}$

need to be retained; higher order terms can be neglected. Later in the analysis, after the sensitivities are known for the local region of interest, it is possible to expand the range of the variables to examine more of the "topography" of the response surface. This broader examination of the model's response permits one to test the range of variables over which the assumed Taylor series relationship is valid. It also points out when additional terms in the response function need to be included.

The Simulation Plan

Having identified the variables and the form of the response function to be tentatively entertained, it is next necessary to develop a plan for selecting the settings of the variables. Classically, the design of many sensitivity studies has been based on varying one variable at a time, holding all others constant, and then examining the system's response to changes in the selected variable. However, this one-variable-at-a-time methodology has drawbacks. It is inefficient in situations where many variables must be analyzed or where important interactions among variables are suspected. It can also be expensive in terms of computer costs. Inasmuch as these drawbacks to the one-variable-at-a-time approach are present in this study, we selected a simulation plan that optimizes the amount of information obtainable. The methodology we have chosen involves varying all variables at the same time. However, due to the nature of the design, it is possible to estimate the importance of each variable and to examine synergisms (interactions) among variables--something that is lacking in the one-variable-at-a-time approach. The interested reader is referred to Appendix C where the features of the simulation plan are described.

The nature of the plan is based largely upon the form of the response function that is tentatively entertained. Depending upon the number of variables under consideration and the extent to which variable interactions and nonlinearities are suspected to occur, the plan is structured so as to permit these features of the system to be revealed clearly and economically. If the results of preliminary studies indicate that the form of the response function is inappropriate, the simulation plan may be revised in order to provide for the appropriate computer simulations necessary for determining nonlinearities and interactions. The method one employs in revising the plan is given in Appendix C.

Evaluation of the Ozone Response Function

Once the simulation plan has been specified, inputs for a number of RPM simulations are prepared. Each of the sensitivity variables is set at either a high or low value depending upon what is prescribed by the plan. After the RPM simulations are performed, predicted plume ozone concentrations are recorded. Regression analysis is then used to determine the ozone response function which relates predicted RPM ozone concentrations to the variables under consideration. Finally, to test the adequacy of the ozone response function, additional RPM simulations are made. The values of the variables used in this extra set of simulations are then input to the response function to test its accuracy relative to the independent RPM predictions.

The generality of the response function for describing the features of the response surface may be examined, in part, by performing simulations in which the variables assume values outside the range for which they were originally used in generating the response function. The extent to which the response function agrees with RPM predictions based upon this wider range of variation provides a good indication of the range over which the response function gives a good description of the RPM response surface.

Procedure for Estimating Sensitivities

After the response function is determined, tested, and its range of application established, model sensitivities can be calculated. The model's response, η, is expressed in Taylor series form in terms of the variables χ_i. By differentiating the response function with respect to a given variable χ_i, one obtains a direct measure of the model's sensitivity to variations in χ_i. Note that the first derivative

$$\left.\frac{\partial \eta}{\partial \chi_i}\right|_{\chi_0}$$

is evaluated at the reference point (midpoint) of the variable's range.

VARIABLE SCREENING EXERCISE

A preliminary screening study of the eleven non-dimensional variables identified in Table B-3 was carried out for the purpose of identifying those variables that might be eliminated from further consideration. Screening was necessary in order to reduce the number of simulations to a manageable level. (To thoroughly investigate all possible combinations of the eleven variables, each of which may assume a high or low value, 2^{11} or 2048 simulations would be required.) We first examined the "main effect" of each variable with respect to the model's response.

The Taylor series expansion for a function of eleven variables in which only a constant and the main effects are retained has the form

$$\eta = b_0 + b_1\chi_1 + b_2\chi_2 + \ldots b_{11}\chi_{11} \qquad \text{(B-4)}$$

where η = the predicted response

b_i = main effect coefficients (parameters) in the regression equation, i=1,2,...11

χ_i = values of the eleven variables.

The form of Equation (B-4) implies that the response function is adequately described in terms of the sum of eleven main effects. Interactions among variables (e.g., $\chi_i\chi_j$) are neglected. Strictly speaking, to determine the validity of retaining only main effects, it is necessary to test the function by comparing it with the results of many RPM simulations in which the eleven variables are set at different values within their respective ranges. Because such a test involves a large number of computer runs, it was not employed in this study. For the present, we assume that the form of Equation (B-4) is sufficiently representative of the true and unknown response function that the equation can be used to screen certain variables from further study. In a later section we present graphical results that corroborate this assumption. For the present, however, we note that the range of validity of the response function given by Equation (B-4) is uncertain.

To use Equation (B-4) in evaluating the main effects of the eleven variables, a simulation plan was formulated; it is described in Appendix C. On the basis of the plan, thirty-two RPM simulations were carried out. In each simulation the variables were set to either a high or low value, as prescribed by the plan, and held constant for a six-hour simulation time. The six-hour period represents downwind travel distances of between 70 and 125 km (44-77 mi) depending upon the value of the wind speed (see Table B-1).

Next, the thirty-two predicted results were fitted by linear regression to Equation (10-4), yielding the following equation:

$$\begin{aligned}\eta = 112.9 - 1.688\ \chi_1 + 8.00\ \chi_2 + 4.625\ \chi_3 + 7.813\ \chi_4 \\ - 2.062\ \chi_5 + 0.0\ \chi_6 + 10.81\ \chi_7 - 2.188\ \chi_8 \\ + 1.563\ \chi_9 - 1.625\ \chi_{10} - 0.625\ \chi_{11}\end{aligned} \qquad (B-5)$$

where the variables χ_i are listed in Table 10-3.

In evaluating the regression relation of Equation (B-5) some variables, such as χ_7, χ_2, χ_4, and χ_3, have relatively large coefficients whereas others such as χ_6, χ_{11}, and χ_9 have smaller coefficients. The question might be raised: Can this information alone be used to indicate the relative sensitivity of RPM predictions due to the different variables? This does not appear to be the case. Equation (B-5) is a linear equation; the interactions between variables do not appear in the equation, except perhaps implicitly in the coefficients b_i. To assess the importance of a given variable, it is necessary to know not only what its main effect is, i.e., the effect of changes in a variable all by itself, but also the contribution it makes to the ozone prediction when varied in conjunction with the other variables. (We expand upon this concept in more detail in Appendix C.)

For the purpose of variable screening, Equation (B-5) is a very useful result. If the coefficients in the regression are rank-ordered and plotted on half-normal probability paper, as in Figure B-2, all of the coefficients, except four, fall very close to a straight line passing through the origin. The four outliers correspond to the NO_2 photolysis rate, and background concentrations of ozone, hydrocarbons, and NO_x. Daniel$^{(B-1)}$ discusses in detail the significance that is attached to variables whose coefficients lie on the straight line. Essentially, this result suggests that the impact of the main effects of the remaining seven variables on model predictions is unimportant relative to the four outliers. Based on this result, seven of the original variables were screened out of the analysis and the sensitivity study was redirected to focus on the four outliers--k_1, O_3, NO_x, and RHC.

It should be emphasized that screening of the seven variables was based solely upon the main effects of the eleven variables. If large interactive

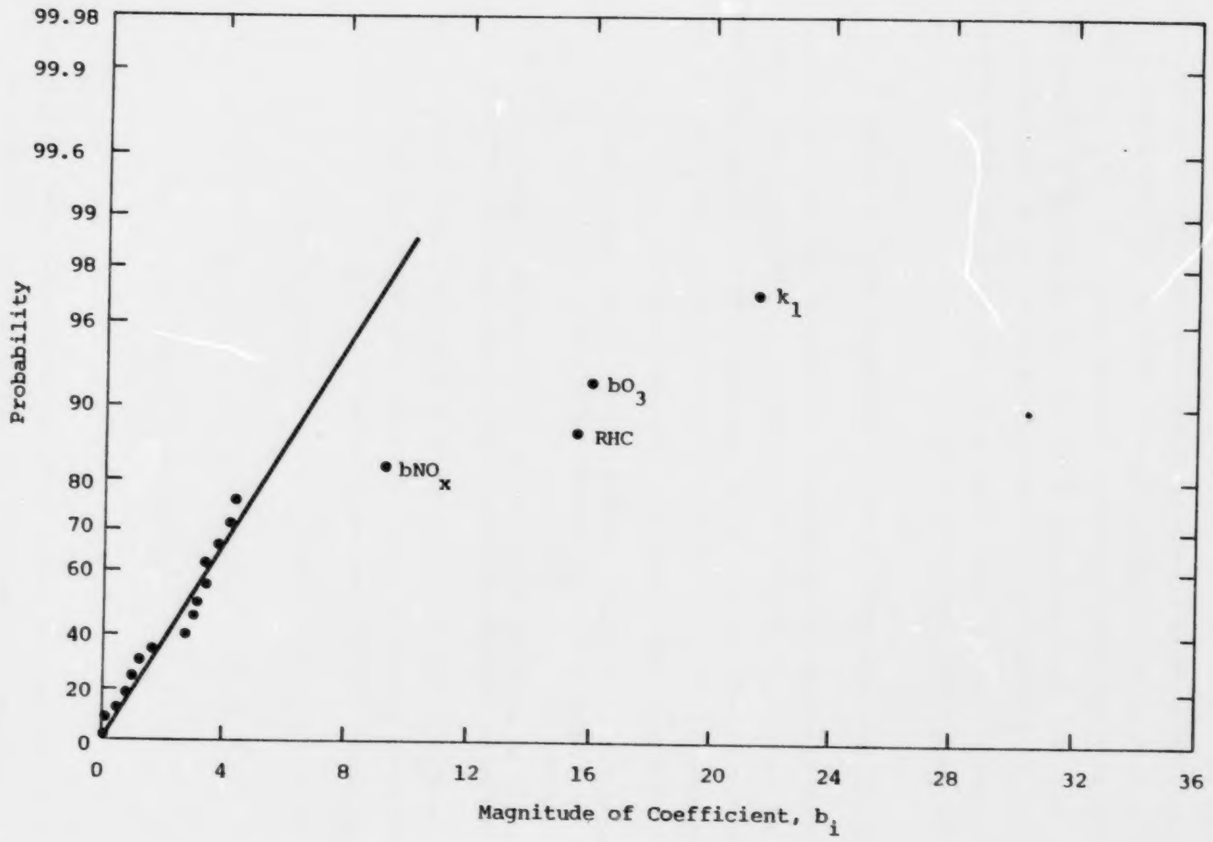

FIGURE B-2. HALF-NORMAL PLOT OF THE COEFFICIENTS IN THE REGRESSION EQUATION (B-5) effects between the seven variables, or between one of the seven and one of the four outlying variables exist, then elimination of some of the variables may not be justified. But the scope of the sensitivity study was such that some screening was necessary. Consequently, if some of the seven variables have important effects on RPM predictions that are not manifest in the main effects alone, then these interactive effects will be confounded to an unknown extent with the sensitivities we compute for k_1, O_3, NO_x, and RHC in the next section. In view of the uncertainties concerning the possible importance of interactions among the eleven variables, we do not attempt to infer relationships that may exist between the variables and ozone formation based upon the main effect estimates alone.

DETERMINATION OF RPM SENSITIVITIES TO THE REMAINING FOUR VARIABLES

After narrowing the scope of the sensitivity study to include only four variables, an important attribute of the simulation plan originally formulated for examining main effects became apparent. We discovered that further use could be made of the first thirty-two sensitivity simulations. In particular the results of the simulations could be used to:

- Thoroughly investigate the sensitivity of RPM predictions to variations in k_1, and background O_3, NO_x, and RHC concentrations.
- Provide an estimate of the error introduced as a result of eliminating the remaining seven variables from consideration.

Under the assumption that the four variables previously identified can be used to adequately replicate RPM ozone predictions after six hours, the following nonlinear equation was entertained:

$$\begin{aligned}\eta = b_0 &+ b_2\chi_2 + b_3\chi_3 + b_4\chi_4 + b_7\chi_7 + b_{23}\chi_2\chi_3 + b_{24}\chi_2\chi_4 \\ &+ b_{27}\chi_2\chi_7 + b_{34}\chi_3\chi_4 + b_{37}\chi_3\chi_7 + b_{47}\chi_4\chi_7 + b_{234}\chi_2\chi_3\chi_4 \\ &+ b_{237}\chi_2\chi_3\chi_7 + b_{247}\chi_2\chi_4\chi_7 + b_{347}\chi_3\chi_4\chi_7 \\ &+ b_{2347}\chi_2\chi_3\chi_4\chi_7 \quad .\end{aligned} \tag{B-6}$$

Note that this equation represents a Taylor series expansion in which second and higher derivatives are excluded, but the first-order interactions between the variables are retained. Using a least squares regression technique, the coefficients in Equation (B-6) were evaluated based on the results of the thirty-two simulations. They are presented in Table B-4. The constant term, b_0, was determined to be 0.113 ppm.

Table B-4

VARIABLES AND COEFFICIENTS IN THE OZONE RESPONSE FUNCTION

Ozone Response Function	
Variable(s)	Coefficient
X_2	8.0
X_3	4.625
X_4	7.813
X_7	10.810
X_2X_3	-0.125
X_2X_1	-0.9375
X_2X_7	-2.063
X_3X_4	1.438
X_3X_7	1.938
X_4X_7	0.625
$X_2X_3X_4$	01.57
$X_2X_3X_7$	-2.06
$X_2X_4X_7$	1.63
$X_3X_4X_7$	0.63
$X_2X_3X_4X_7$	0.5

Because Equation (B -6) contains all possible first-order combinations of variables χ_2, χ_3, χ_4, and χ_7, differentiation of the equation with respect to any variable provides a measure of the sensitivity associated with that variable. These derivatives are presented in Table B -5. An important result was obtained from this exercise. Variable χ_7, the NO_2 photolysis rate, appeared, on the basis of its coefficient in Equation (B -5), to be the most important variable from the sensitivity standpoint. However, when the interactive effects among variables are taken into account χ_4, the background concentration of reactive hydrocarbons, replaced χ_7 as the most sensitive variable. In Table B -5 the relative sensitivity of the four variables is calculated.

Accuracy and Limitations of the Ozone Response Function

The response function given by Equation (B-6) was determined on the basis of thirty-two RPM simulations in which the eleven variables were varied independently of each other. Every variable was constrained to assume either a high $(X = X_{High})$ or a low $(X = X_{Low})$ value according to the ranges specified in Table B-1. Defining α as

$$\alpha = \chi_i = \frac{X - X_0}{X_{HR}} , \qquad (B-7)$$

it is clear that the simulations were based on variable inputs to RPM corresponding to values of α (or χ_i) equal to ±1. Thus, a response function has been constructed based on RPM predictions resulting from the variables χ_2, χ_3, χ_4, and χ_7 set at values of $\alpha = \pm 1$.

Table B -5

DERIVATIVES OF THE OZONE RESPONSE FUNCTION

Variable	χ_i	$\frac{d\eta}{d\chi_i}$	Relative Sensitivity*
Background Ozone	χ_2	6.51	49%
Background NO_x	χ_3	8.52	64%
Reactive Hydrocarbons	χ_4	13.27	100%
NO_2 Photolysis Rate	χ_7	12.01	91%

*Based on the sensitivity measure for reactive hydrocarbons.

The points $\alpha = \pm 1$ define a region on the response surface. To test the accuracy of the response function within this region for which it was developed and to examine the validity of the function for variable ranges greater than those corresponding to $\alpha = \pm 1$ (that is, outside of the original region), a number of additional RPM simulations were performed for values of α equal to -2.0, -1.4, -0.5, 0.0, 0.5, 1.4, and 2.0. In Table B -6, a comparison is given between RPM predictions at eleven points on the response surface and the predicted ozone concentrations given by the response function. Based upon the test results, the ozone response function provides excellent agreement with RPM six-hour ozone predictions out to at least $\alpha = \pm 1.4$. At $\alpha = \pm 2.0$ and presumably beyond, agreement is generally poor. Thus the response function is not generally valid for the entire response surface, but appears to be quite accurate in the region close to the point corresponding to baseline conditions.

The remaining portion of this chapter is devoted to an interpretation of the sensitivity results and an assessment of their generality. We conclude with an identification of additional analyses that can potentially extend the utility and accuracy of the present sensitivity estimates.

ASSESSMENT OF RESULTS

From the RPM sensitivity study it was possible to estimate the contribution made by the main effects of the eleven original variables. Furthermore, a complete exploration of all of the first order interactions among the four variables with the largest main effects--k_1 and background concentrations of O_3, NO_x, and RHC--was accomplished. With these results a response function relating RPM ozone predictions to the four variables was developed. Based on the magnitude of the first derivatives of the response function, the model's most sensitive variables are:

1) Background Reactive Hydrocarbon Concentrations
2) NO_2 Photolysis Rate
3) Background NO_x Concentrations
4) Background Ozone Concentrations

It should be noted that the above four variables are not directly related to power plant emissions or plume characteristics. This suggests that the primary source of ozone predicted in the plume in the sensitivity study is the

Table B-6

ACCURACY OF THE OZONE RESPONSE FUNCTION

Variable Settings, α	Ozone Response		
	y_{RPM} (ppm)	η_{ozone} (ppm ± 0.003)(3)	Error(1)
-2.0(2)	0.037	0.063	70%
-1.4	0.069	0.078	13%
-1.0	0.082	0.089	9%
-0.5(2)	0.102	0.101	1%
-0.5	0.097	0.101	4%
0.0	0.113	0.113	--
0.5(2)	0.129	0.125	3%
0.5	0.129	0.125	3%
1.0	0.144	0.140	3%
1.4	0.157	0.154	2%
2.0(2)	0.161	0.186	16%

(1) The Error is defined as % Error = $\frac{y_{RPM} - \eta}{y_{RPM}} \times 100\%$.

(2) In these simulations, all eleven variables were set to a common value of α. In the remaining simulations, χ_2, χ_3, χ_4, and χ_7 were given a common value of α; the remainder were set at $\alpha = 0$.

(3) The estimated error in the response function estimates is based upon errors introduced as a result of neglecting seven of the original eleven variables. This error is discussed in Appendix C.

entrainment of reactive pollutants from the background air. Thus, it appears that the sensitivity study results are more reflective of the sensitivity of RPM's kinetic mechanism to variations in model inputs than of the possibility that ozone is likely to form in plumes. A brief discussion of these results follows.

Response Function

The response function developed in this study is significant in that it permits an evaluation of RPM's sensitivity to key variables. Knowledge of these sensitivities can then be used to direct further model refinements and as an aid in planning field experiments. Strictly speaking, the response function is not a prognostic tool. Certain simplifications made in developing the function preclude it from being used to predict whether or not ozone will form in plumes. These simplifications include:

- The use of constant ambient pollutant concentrations.
- The use of constant solar radiation levels.
- The use of constant wind speeds and dilution rates.

Also, the function is based on computed ozone concentrations at the end of a fixed period of time--six hours. Nevertheless, the response function does shed light on the sensitivity of the kinetic mechanism to variations in input parameters.

Reactive Hydrocarbons

The concentration of background reactive hydrocarbons is the variable to which RPM predictions are most sensitive. This result has two implications. First, those geographical regions for which background hydrocarbon levels are high will most likely have a higher potential for ozone formation in plumes. Second, due to the high sensitivity of RPM to hydrocarbon concentrations, future plume studies investigating the question of ozone formation must provide for hydrocarbon sampling.

From the preliminary results of the variable screening exercise and from past experience with the kinetic mechanism, it appears that the most important measurement is the total mass of non-methane hydrocarbons (TNMHC). Although knowledge of the hydrocarbon distribution (i.e., the amount of each species present) is useful, the kinetic mechanism is less sensitive to uncertainties in individual or lumped species concentrations than it is to the mass of TNMHC.

NO_2 Photolysis

The importance of the NO_2 photolysis rate revealed in this study is in qualitative agreement with past results. In particular, previous sensitivity studies involving mesoscale photochemical air pollution models$^{(B-2)}$ have shown that k_1 was the most sensitive of the kinetic variables studied. These results suggest that if ozone is generated in plumes during certain conditions, it would most likely occur during periods of strong solar insolation--the summer months. The potential for formation would also be greater in the lower latitudes.

Nitrogen Oxides

The third most important variable is background NO_x concentrations. Regardless of whether they derive from power plants, smelters, or traffic emissions, atmospheric nitrogen oxides play an essential role in plume photochemistry. Obviously, with larger NO_2 concentrations, a concomitant increase in ozone can be expected. Therefore, potential ozone production problems might be more likely in the vicinity of large urban centers or industrial parks where NO_x emissions are greatest than in rural areas where NO_x concentrations are very low.

An interesting feature in Figure B-2 is that the main effect of power plant NO_x emissions (pNO_x) is only one-third of the main effect for background NO_x, and that pNO_x ranks ninth in order of main effect. Does this imply that stack emissions of NO_x are insignificant relative to the other variables? To answer this question, two points must be considered.

First, power plants are known to be important contributors to the overall atmospheric NO_x burden. Nitrogen oxides ranked third in order of sensitivity. Second, it is instructive to consider the total mass of NO_x contributed by the power plant relative to the amount of NO_x entrained by the atmosphere. An RPM simulation was carried out based upon baseline conditions ($\alpha = 0$) given in Table B-2. A passive tracer, equal in magnitude to the background level of NO_x, was entrained by the plume as it dispersed downwind. The dispersion rate corresponded to neutral stability conditions. During the initial stages of rapid plume dilution the concentration of tracer in the plume reached 90 percent of the background value after only 14 km (23 mi). Furthermore, at the end of six hours, the total mass of tracer entrained by the plume was approximately sixty-four times the mass of NO_x used as the initial condition.

The present results suggest that the potential for ozone formation in a given plume is more dependent upon the background NO_x than the mass of nitrogen oxides emitted from the stack. However, before ruling out the importance of NO_x emissions it would be necessary to investigate the chemistry occurring in the plume at times earlier than six hours. An examination of the temporal changes in the background atmosphere and how these changes affect the present results might also be of value. (Recall that the background concentrations and radiation levels were held constant during each simulation.)

Ozone Background Concentrations

In this study, the sensitivity of RPM predictions to variations in background ozone concentrations was found to be approximately one-half that due to reactive hydrocarbons. It is not surprising that the model is sensitive to background ozone; a considerable amount of ozone can be entrained as the plume expands. A simple experiment was performed to determine if the large main effect in Equation (B-5) is primarily due to the influence of entrained background ozone rather than to ozone formed within the plume. The main effects were re-computed, based upon the difference between predicted plume ozone concentrations and the ambient value that was assumed fixed. This analysis indicated that the regression coefficient for background ozone was reduced from 8.0 to approximately 5.0, ranking background ozone concentrations third rather than second in order of main effects. From this result we conclude that if conditions are favorable to the occurrence of high background levels of ozone, they are likely to be favorable to ozone production in the plume as well.

SUMMARY

The goal of the sensitivity study was to explore the impact on the model's response due to variations in key input parameters and variables. In general, this goal has been achieved.

Application of the sensitivity analysis described in this report is not typical of most model sensitivity studies. The methods used for the design and evaluation of the sensitivity program were possible primarily due to the ease with which the model can be employed and the modest costs of computer simulations. However, because the sensitivity study was brought to a conclusion primarily due to time and economic constraints rather than the attainment of results conclusively delineating RPM's sensitivity, the results of the present study are regarded as an intermediate step. We believe that further exploration of the sensitivity approach outlined in this chapter (and in Appendix C) is warranted. The rewards of continued study would be a clearer identification of those conditions under which ozone might be likely to form in plumes. Also, avenues of model refinement and program design could be explored.

To extend the results of the present study, the following improvements to the present methodology should be considered.

- Incorporation of the temporal variation in k_1
- Variation in the ambient pollutant concentrations to reflect background emissions and reactions
- Re-evaluation of the adequacy of the hydrocarbon reactivity index
- Reduction of the number of original variables under consideration (if possible)
- Consideration of special combinations of key variables, such as very high background hydrocarbon concentrations and very low background NO_x levels.

In Appendix C, we outline some ideas on how a more complete description of RPM's sensitivity might be achieved.

REFERENCES

B-1 Daniel, C., "Use of Half-Normal Plots in Interpreting Factorial Two-Level Experiments," Technometrics, Vol 1, No. 4, November, 1959.

B-2 Reynolds, S. D., et al., "Development and Refinement of the SAI Urban Airshed Model," Final Report under EPA Contract No. 68-02-1237 (4 volumes), Systems Applications, Inc., San Rafael, California, 1975.

Appendix C

A SENSITIVITY STUDY OF THE REACTIVE PLUME MODEL (RPM-I)--THEORETICAL BASIS AND PROCEDURES*

by

Thomas W. Tesche and Philip M. Roth

OVERVIEW

This appendix presents the theoretical basis of the RPM sensitivity study and a more detailed discussion of the procedures used in arriving at RPM sensitivities. Because certain terminology may be unfamiliar to some readers, a glossary of terms is given at the end of the appendix to facilitate a better understanding of the approach. (When these terms first occur in the text, they are italicized.) Throughout the appendix frequent reference is made to the discussion and certain tables and figures in Appendix B. Thus, a review of Appendix B is recommended prior to the reading of this appendix.

In this appendix we begin with a discussion of the selection of eleven variables and parameters considered in the sensitivity study. Then, we present the theoretical basis for obtaining the *response function*, which relates predicted ozone concentrations to the variables. Next, the statistical concepts associated with the simulation plan are introduced, followed by the variable screening exercise and evaluation of the response function. The appendix concludes with suggested avenues by which the use of a statistically designed sensitivity study might be of further value.

SELECTION OF SENSITIVITY STUDY VARIABLES

We identify eleven variables believed to have an influence on RPM predictions of ozone concentrations in a power plant plume. In Table B-1 the variables and their typical ranges are presented. In the following subsections, brief discussions relating to the eleven original variables and parameters are given. The rationale for the selection of suitable ranges for each variable will be expanded upon in a later portion of this appendix.

---

* Reprinted from Ogren, J. A., et al. (1976), "Determination of the Feasibility of Ozone Formation in Power Plant Plumes, "EPRI EA-308, Meteorology Research, Incorporated, Altadena, California, and Systems Applications, Incorporated, San Rafael, California.

X_1--Reactivity

The reactivity of a given hydrocarbon mixture has direct bearing on the potential amount of ozone formed and also on the rate at which secondary pollutants, including ozone, are formed. Ideally, one would like to define an index that is uniquely representative of a hydrocarbon mixture's reactivity under a wide range of conditions. Unfortunately, attempts to define a comprehensive reactivity index have been unsuccessful to date. As a result, a number of indices for hydrocarbon reactivity have been advanced by different investigators(C-1,C-2).

Despite the inherent difficulties in attempting to define a reactivity index, some objective measure of a hydrocarbon mixture's capacity for promoting ozone formation is needed. Because hydrocarbon-hydroxyl reactions are known to proceed much more rapidly than reactions of hydrocarbons with O or O_3, we defined the reactivity of a hydrocarbon mixture as

$$R = \frac{\sum_{i=1}^{4} k_i \bar{P}_i}{\sum_{i=1}^{4} \bar{P}_i} \qquad \text{(C-1)}$$

where

$\bar{P}_i$ = mass fraction of the i-th hydrocarbon group

k_i = effective reaction rate of the i-th hydrocarbon group with hydroxyl radicals

1 = olefins
2 = paraffins
3 = aldehydes
4 = aromatics

The basis for determining a suitable range of hydrocarbon reactivities is the detailed Atmospheric Hydrocarbon Concentration Study by the California Air Resources Board(C-5). Nonmethane hydrocarbons through C_{10} were analyzed at several stations, including:

- El Monte, ARB Laboratory
- Downtown Los Angeles, APCD station
- Banning, CALTRANS facility
- Palm Springs, APCD station

during pre-dawn, peak traffic, and peak oxidant hours at each site.

To determine the effective reactivity of a hydrocarbon mixture it is necessary to compute lumped rate constants, k_i, for each of the four hydrocarbon groupings. One approach involves weighting the rate constant of each species by its initial mole fraction and then summing over all species in the group to obtain an effective rate constant (C-3). However, this technique ignores the temporal variation of hydrocarbon concentrations. In reality, as the reactions proceed, the more reactive species are depleted at a faster rate. Once the reactive species are completely oxidized, the rate of oxidation of the less reactive species is substantially reduced. Consequently, the linear summation method consistently overpredicts the overall reaction rate. This difficulty was circumvented by employing a parametric scheme first introduced by Hecht et al. (C-4) that explicitly treats the temporal variation of the species mixture within each hydrocarbon group.

Analysis of the ARB data led to the reactivity indices given in Table C-1. Although the atmosphere in Los Angeles is generally considered to be more "reactive" than locations such as Banning or Palm Springs, from Table C-1 the rural stations are associated with larger reactivity indices than Los Angeles. This result is due principally to the higher hydrocarbon concentrations and lower computed rate constants for Los Angeles than for Banning or Palm Springs.

Table C-1

REACTIVITY INDICES BASED UPON ARB ATMOSPHERIC HYDROCARBON DATA,
AVERAGING INTERVAL: JUNE-SEPTEMBER, 1974

Location	Time of Day	Reactivity Index
Palm Springs	1400-1700	10,300
Banning	0600-0900	10,300
Los Angeles APCD	0600-0900	6,500
El Monte	0600-0900	9,780
El Monte	1100-1400	10,200

It is necessary to avoid too strict an interpretation of the reactivity indices inasmuch as they are subject to the following assumptions:

- Aldehyde and olefin concentrations are assumed to be similar at all locations mentioned (due to a paucity of aldehyde data).
- The hydrocarbon concentrations do not reflect an instantaneous sampling, but rather represent mean values averaged over a four-month period.
- The reactivity index is based on the reaction

$$HC + OH\cdot \rightarrow RO_2^{\cdot} + H_2O \qquad (C-2)$$

whereas, in actuality, several radicals are in competition in the hydrocarbon oxidation reactions.

Despite these limitations, the reactivities at Palm Springs (10,300) and Los Angeles (6,500) were used because it is felt that they do represent a useful range in the hydrocarbon mixture composition throughout a rural-metropolitan region. It is clear, however, that they do not represent extreme conditions. In Table C-2, estimated hydrocarbon splits for the four groups are presented for the high and low reactivity indices.

Table C-2

RELATIVE CONCENTRATIONS OF HYDROCARBON GROUPS
IN MIXTURES WITH VARIOUS REACTIVITY INDICES

Hydrocarbon Group	Relative Concentration by Volume (percent)	
	Low Reactivity Index	High Reactivity Index
Olefins	9.6	5
Paraffins	53.9	59
Aldehydes	9.6	5
Aromatics	26.9	31
Total	100.0	100

X_2, X_3, X_4--Ambient Pollutant Concentrations

Variables 2, 3, and 4 are the ambient concentrations of O_3, NO_x, and reactive hydrocarbons. The ranges reported for these pollutants represent reasonable but not necessarily extreme values. To provide separate values for background NO_2 and NO as required by RPM, we invoked the quasi-steady state assumption that

$$[O_3] \approx \frac{k_1}{k_3} \cdot \frac{[NO_2]}{[NO]} \qquad (C-3)$$

which is generally valid in the atmosphere except in the later stages of photochemistry$^{(C-7)}$ or close to emission sources. The ratio k_1/k_3 is assumed equal to 1/70.

X_5, X_6--Effective Plume Dispersion

As an approximation, the cross-sectional geometry of a plume may be described by a rectangular element given by the expressions

$$w = c_1 x^{P_1} \qquad (C-4)$$

$$h = c_2 x^{P_2} \qquad (C-5)$$

where:

w = plume width
h = plume thickness
c_1, c_2 = stability-dependent coefficients
P_1, P_2 = stability-dependent exponents
x = downwind distance.

Equations (C-4) and (C-5) may be combined to approximate the cross-sectional area of the rectangular plume,

$$A = cx^{P} \qquad (C-6)$$

where $c = (c_1) \cdot (c_2)$ and $P = P_1 + P_2$.

The dilution rate of the plume, as observed from the coordinate system moving with an air parcel, is proportional to the spatial derivative of the cross-sectional area, or

$$\text{dilution} \propto \frac{dA}{dX} = cpX^{P-1} \qquad \text{(C-7)}$$

On the other hand, the dilution rate with respect to an inertial (Eulerian) reference system is given by the time derivative of the cross-sectional area, or

$$\text{dilution} \propto \frac{dA}{dt} = cpX^{P-1} \frac{dx}{dt} = cvpx^{P-1} \qquad \text{(C-8)}$$

where v is the mean wind speed. Thus, plume dispersion is a function of an effective dispersion exponent, P, and, depending on the choice of coordinate systems, it may also be a function of wind speed. Although RPM embodies a semi-Lagrangian coordinate system, we elected to retain the wind speed as a variable in the initial phase of the sensitivity study to see what effect, if any, wind speed has on ozone predictions. The wind speed range is based on typical wind speeds observed during the field programs. The composite exponent P was derived from diffusion rate estimates made by N. E. Bowne for dispersion over rural terrain(C-6).

X_7--NO_2 Photolysis Rates

For the six hour simulations used in the sensitivity study, it is obvious that the photolysis rate for NO_2 will have temporal variation. However, to avoid the complexity introduced by including temporal variations in k_1, we elected to use constant photolysis rates that are slightly less than the peak rate expected during any six hour daylight period.

X_8--Absolute Humidity

Absolute humidity is included as a variable in the sensitivity study primarily because of the suggestion that the potential for ozone formation in plumes is greater under high humidity conditions$^{(C-8)}$. The absolute water content in the atmosphere, w, is given by

$$w = 0.622\left[\frac{P_{sat}}{P - P_{vap}}\right]\cdot RH \qquad (C-9)$$

where

P_{sat} = saturation vapor pressure
P_{vap} = actual vapor pressure
P = absolute pressure
RH = relative humidity.

At one atmosphere, the absolute humidity varies between approximately 2000 and 32000 ppm water, depending on the existing relative humidity and ambient temperature. Consequently, a variety of temperature-relative humidity conditions can be treated with the single variable, w.

X_9--NO_x Emissions

Generation of oxides of nitrogen (NO_x) from power plants arises primarily due to the high (1500-2000°C) furnace temperatures. NO, the major constituent at the stack, is formed by reaction of atmospheric N_2 and O_2. Typically, about 95 percent of the NO_x emissions are NO. As the material is transported downwind, NO is converted to NO_2 by reaction with ambient O_3. In some plumes this conversion is roughly 50 percent complete after 12 to 60 minutes$^{(C-8)}$; however, in reviewing the aerometric data from the Four Corners study, it appeared that roughly 25 percent conversion of NO to NO_2 occurred within the first 5 km (3 mi). Thus, for initial NO_x conditions used in the sensitivity study, we assumed that $[NO_2] = \frac{1}{3}[NO]$ at the initial condition location of 1.0 km (0.62 mi).

X_{10}-- Absolute Temperature

Ambient temperatures are included in the sensitivity study because chemical reactions with nonzero activation energies have temperature dependent rate constants, k, given by the Arrhenius relation

$$k = k_0 e^{-E_A/RT} \tag{C-10}$$

where

k_0 = rate constant at a reference temperature
T = temperature
R = ideal gas constant
E_A = activation energy.

To study the influence of temperature variations on ozone concentrations, the reaction rates in the kinetic mechanism were computed for each of the ambient temperatures investigated in the study.

X_{11}--SO_2 Initial Conditions

Sulfur dioxide was included as a variable in the sensitivity study primarily because it has been suggested that sulfur oxides may play a role in ozone generation(C-8) and because it is a variable over which the power plant operator can exercise some degree of control. The range selected for SO_2 initial conditions is reflective of near stack SO_2 concentrations measured during the Four Corners program.

In review, eleven variables have been identified as having potentially important impacts on RPM predictions. The next topic to be considered involves how these eleven variables may be functionally related. Thus, we next present in the following section the general theory upon which the entire sensitivity study is based.

THEORETICAL CONSIDERATIONS

The Response Function

The goal of the sensitivity study is to determine RPM model sensitivities to variations in the magnitude of its input variables and parameters. This task is greatly facilitated if it is possible to determine a functional relationship between the set of input variables and the model's response. That is,

$$\eta = f(\vec{x},\vec{\beta}) \tag{C-11}$$

where η is the anticipated response of RPM, $\vec{x}$ is a 1 x k vector of controlled variables or parameters, $x_1, x_2 \ldots x_k$, and $\vec{\beta}_p$ is a p x 1 vector of parameters

$\beta_1, \beta_2, \ldots \beta_p$. Clearly, the sensitivity of the RPM's response to a given variable x_i is determined by the partial derivative of Equation (C-11) with respect to a given variable x_i. Because such a functional relationship is very useful in obtaining model sensitivities, this section is devoted to a theoretical discussion of the existence and form of the RPM response function.

In Appendix B the concept of a response function was introduced. Basically, Equation (C-11) represents the response function relating RPM predictions and inputs. Evaluation of the function over the ranges of each of the input variables leads to what is known as the *response surface*. It is unlikely that one can ever determine precisely the nature of the function (Equation C-11) that describes the true RPM response over the wide range of variables in RPM. However, often an adequate representation of the function can be made with an empirical expression that approximates the behavior of RPM's response. By examining the response of RPM over some region in the space of the input variables (hereafter referred to as *variable space*), it may be possible to obtain an empirical approximation to the true response function through the use of certain common statistical techniques. However, first it is necessary to "tentatively entertain" the form that the empirical expression has.

The basic model equation we begin with is

$$y = \eta + \varepsilon \qquad \text{(C-12)}$$

where

y = the actual RPM Prediction for a given *setting* of the variables

η = the response given by the empirical expression to be developed

ε = the error between the RPM prediction and the approximated response.

For laboratory or industrial experiments in which experimental error is often a concern, the magnitude of the error, ε, is of practical importance because it tends to obscure a clear determination of the extent to which the observation, y, and the response, η, agree. Because in the present study we are concerned with computer experiments, the only error present involves machine truncation error which is unimportant. Therefore, the quantity ε in this investigation provides a direct comparison of the degree to which the empirical response function η agrees with actual RPM predictions, y.

Approximating Polynomials

We assume that RPM predictions can be approximated by the function η where

$$\eta = f(x_1, x_2, x_3 \cdots x_k) \tag{C-13}$$

Performing a *multivariate* Taylor Series expansion about $\vec{x}_0 = (x_{01}, X_{02}, x_{03}, \cdots x_{0k})$, the midpoint in the ranges of the variables, gives

$$\begin{aligned} \eta = \eta_0 &+ (x_1 - x_{01})\frac{\partial f}{\partial x_1}\bigg|_{\vec{x}_0} + (x_2 - x_{02})\frac{\partial f}{\partial x_2}\bigg|_{\vec{x}_0} + \cdots + \\ &\tfrac{1}{2}(x_1 - x_{01})^2 \frac{\partial^2 f}{\partial x_1^2}\bigg|_{\vec{x}_0} + \cdots + (x_1 - x_{01})(x_2 - x_{02})\frac{\partial^2 f}{\partial x_1 \partial x_2}\bigg|_{\vec{x}_0} + \cdots \end{aligned} \tag{C-14}$$

This expansion about x_0 may be rewritten more compactly as

$$\begin{aligned} \eta = \beta_0 &+ \beta_1\chi_1 + \beta_2\chi_2 + \cdots + \beta_k\chi_k + \beta_{11}\chi_1^2 + \beta_{22}\chi_2^2 + \cdots + \beta_{kk}\chi_k^2 + \\ &\beta_{12}\chi_1\chi_2 + \beta_{13}\chi_1\chi_3 + \cdots \end{aligned} \tag{C-15}$$

where the variables χ_i have been nondimensionalized as described in Appendix B.

The response relationship of Equation (C-15) is very general. Depending upon which of the infinite number of terms in the Taylor Series expansion one wishes to retain, the resulting expression can be simple or complex.

The form of the empirical expansion tentatively entertained as a suitable approximation to the response function will largely determine the nature of the simulation plan to be selected and the amount of effort involved in evaluating the coefficients in the response function. Perhaps the simplest form of Equation (C-15) is

$$\eta = \beta_0 + \beta_1 x_1 + \beta_2 x_2 + \dots + \beta_k x_k \qquad \text{(C-16)}$$

where this function represents a planar surface in *k-dimensional space*. Note that Equation (C-16) is a linear model equation exhibiting the properties of additivity and homogeneity. Additivity means that if a variable x_1 produces an effect η_i when used alone, and variable x_2 produces an effect η_2 when used alone, then x_1, x_2 used together produce the effect $\eta_1 + \eta_2$. Homogeneity implies that if a variable x_1 produces an effect η_1, then for any real number λ, λx_1 produces an effect $\lambda\eta_1$. For some physical systems a model such as Equation (C-16) may be satisfactory. However for other systems, where nonlinearities are known or suspected to exist, it may be inadequate. If this is the case, additional terms are retained in Equation (C-15).

For example, if, on the basis of past experience or theoretical arguments, interactions among variables are known to occur, thus producing synergistic effects, certain cross-product terms may be retained in the Taylor Series resulting in a model equation of the form

$$\eta = \beta_0 + \beta_1 x_1 + \beta_2 x_2 + \dots + \beta_k x_k + \beta_{12} x_1 x_2 + \beta_{13} x_1 x_3 + \dots \qquad \text{(C-17)}$$

If, on the other hand, certain variables are known to produce non-linear effects on the predicted response, then the following equation might be entertained:

$$\begin{aligned} \eta = {} & \beta_0 + \beta_1 x_1 + \beta_2 x_2 + \dots + \beta_k x_k \\ & + \beta_{11} x_1^2 + \beta_{22} x_2^2 + \dots + \beta_{kk} x_k^2 \end{aligned} \qquad \text{(C-18)}$$

Collectively, Equations (C-16) to (C-18) represent polynomial forms of response functions of increasing compexity. In general, one would select the functional form believed to be most appropriate and then structure a simulation plan around that model equation. After the parameters in the equation have been estimated, the response function is tested. Should it prove inadequate, the model's form is altered as appropriate and further experimentation is carried out. Thus, the construction of a suitable response function may be iterative in nature, involving stages of simulation plan design, conduct of the experiment, analysis of the results, and conjecture over the appropriateness of the current model.

Evaluation of the Parameters in the Response Function

Once the tentative form of the response function is specified, a set of procedures called the simulation plan is formulated to provide the information necessary for determining the parameters in the function. Essentially, this information consists of a number of RPM simulations in which the variable settings $\chi_1, \chi_2, \ldots \chi_p$ and the computed RPM ozone predictions $y_1, y_2, \ldots y_N$ are recorded. If the response function is linear with respect to the parameters, i.e.

$$\frac{\partial f(\vec{\chi},\vec{\beta})}{\partial \beta_i} = f_i'(\vec{\chi}) \qquad i = 1,2,\ldots p$$

then the parameters may be determined by the method of least squares$^{(C-9)}$. On the other hand, if any of the p derivatives just identified or $\chi_1, \chi_2, \ldots \chi_p$ is dependent on $\vec{\beta}$, the response function is non-linear in the parameters and nonlinear parameter estimation techniques must then be employed$^{(C-10)}$. In this study we confine our attention only to those cases in which the response function under consideration is linear in the parameters.

To describe how the parameters are estimated by the least squares method consider the following example. Suppose the simple model equation

$$\eta = \beta_0 + \beta_1\chi_1 + \beta_2\chi_2 + \beta_3\chi_1\chi_2 \qquad \text{(C-19)}$$

is tentatively under consideration. If we define the (4 x 1) vector $\vec{X}_i = (1, \chi_1, \chi_2, \chi_1\chi_2)$ and the (4 x 1) vector $\vec{\beta}$ as

$$\vec{\beta} = \begin{bmatrix} \beta_0 \\ \beta_1 \\ \beta_2 \\ \beta_3 \end{bmatrix}$$

then the response function may be written in vector form as

$$\eta_i = \vec{X}_i \cdot \vec{\beta} \qquad \text{(C-20)}$$

To estimate the vector $\vec{\beta}$, use is made of the numerous RPM simulation results based on the simulation plan. For the present, assume that m simulations with RPM were made yielding a (m x 1) vector of results

$$y = \begin{bmatrix} y_1 \\ y_2 \\ y_m \end{bmatrix} \qquad m > 4$$

It is not possible, with a limited number of simulations, to determine $\vec{\beta}$ in Equation (C-20) precisely. However it is possible to approximate $\vec{\beta}$ with another vector $\vec{b}$ called the *parameter estimates*. Rewriting Equation (C-20) in terms of the computed RPM observations $\vec{y} = (y_1, y_2 \ldots y_m)$ and the parameter estimates gives

$$y_i = \vec{X}_i \cdot \vec{b} \qquad \text{(C-21)}$$

If m simulations are performed the results can be expressed compactly as

$$\vec{y} = (X) \cdot \vec{b} \qquad \text{(C-22)}$$

where (X) is the matrix composed of the m vectors $\vec{X}_i$, each one representing a unique combination of variable settings as prescribed by the experimental design. Solving for the least squares estimates of the parameters gives

$$\vec{b} = [(X)^T (X)]^{-1} \cdot (X)^T \vec{y} \qquad \text{(C-23)}$$

Thus, the parameter estimates b_0, b_1, b_2, b_3 may be substituted into Equation (C-19) to give the empirical response function

$$\eta = b_0 + b_1 X_1 + b_2 X_2 + b_3 X_1 X_2 \qquad \text{(C-24)}$$

The accuracy and suitability of the response function can then be tested by comparing the response function predictions with an additional, independent set of RPM predictions.

THE SIMULATION PLAN

Factorial Design

The simulation plan (or experimental design) is a key element in the sensitivity study. As we discussed in Appendix B, the plan prescribes the variable settings for each of the many computer simulations to be performed. If the plan is carefully laid out, a considerable amount of useful information can be obtained. In particular, a good plan may "stress" a candidate response function by making it difficult to fit the data. Furthermore, by careful observation of the behavior of the response function over the ranges of the independent variables, possible corrections to a deficient function might be made, i.e. retention of cross product or higher order terms. On the other hand, a poorly chosen plan may make the results of the computer simulations essentially worthless, regardless of how clever an analysis is subsequently performed.

For these reasons, we chose to use *factorially designed experiments* as the basis for the sensitivity study. The underlying theory and rationale for factorial experiments are extensively reported elsewhere(C-11,C-12,C-13). Here we only summarize the basic concepts.

If each of the eleven variables or *factors* is assigned high and low values (levels) then a complete experiment, thoroughly exploring the influence of all factors on the response η, would require 2^{11} or 2048 computer simulations. This is called a *two-level* factorial experiment. To reduce the number of simulations to a manageable level, only a fraction of the 2^{11} experiments are made at first. Thus, the study begins with a *fractional factorial experiment.* The advantages of fractional designs are that:

- Estimates of the *main effects* of each variable can be obtained independently.
- The magnitude of *two factor* and higher order variable interactions may be inferred independently of the main effects of the variables (and where desirable, of each other).
- Given prior knowledge of the physical system, certain variable interactions can be neglected.
- "Screening" is possible in order to reduce the number of variables under consideration.
- The designs can be constructed so as to be evolutionary in the sense that a clearer picture of RPM's response evolves as succeeding experiments are conducted.
- Parameter estimation can be greatly facilitated.

Screening Experiment

One major consideration in designing sensitivity experiments is to ascertain if the variables under initial consideration may be reduced in number. The advantages of such a reduction are immediately apparent--far fewer runs are required to evaluate the coefficients in a tentative response function. It is likely that within the set of eleven variables there exists a subset of variables which are most important. In this study, it is not immediately obvious that such a subset exists. To determine if some variables could be screened the model given by Equation (C-16) was selected. This model explicitly relates only the effect of each of the eleven variables to the predicted response η. Any interaction effects between variables (i.e. two factor, three factor or higher interactions) are obscured in the parameters $\beta_0, \beta_1 \dots \beta_k$ of the model. Fortunately, fractional factorial designs are helpful in identifying the important variables in a large group of variables and also in revealing the magnitudes of some factor interactions.

The 2^{11-6} Design

The design (or plan) selected for use in variable screening is a 2^{11-6} fractional factorial*. The attractiveness of this design is that it permits estimation of the eleven main effects independent of two factor interactions with a minimum number of runs. Further, many (but not all) of the two factor interactions can be estimated as well. As a result, because the complete factorial design is not used, considerable *confounding* will occur with the 2^{11-6} fractional.

In Table C-3, the *design matrix* for a 2^{11-6} fractional factorial design is given. Plusses and minuses in the table refer to RPM input variable settings $x_1, x_2, x_3 \dots x_{11}$ corresponding to the normalized variable settings of $\pm\chi_1, \pm\chi_2 \dots \pm\chi_{11}$. For example, run number 1 in Table C-1 stipulates that $\chi_1 = -1$. From Table B-3 χ_1 is defined as

$$\chi_1 = \frac{x_1 - 8399.}{950.} \qquad \text{(C-25)}$$

---

[*] A 2^{11-6} fractional factorial design is a $\frac{1}{2^6}$ fraction of a 2^{11} design, comprising 2^5 or 32 computer simulations.

Table C-3

DESIGN MATRIX FOR A 2^{11-6} FRACTIONAL FACTORIAL EXPERIMENT

Run No.	I	1	X_2	X_3	X_4	X_5	(124) X_6	(235) X_7	(123) X_8	(234) X_9	(345) $X_{(10)}$	(125) $X_{(11)}$
1	+	−	−	−	−	−	−	−	−	−	−	−
2	+	+	−	−	−	−	+	−	+	−	−	+
3	+	−	+	−	−	−	+	+	+	+	−	+
4	+	+	+	−	−	−	−	+	−	+	−	−
5	+	−	−	+	−	−	−	+	+	+	+	−
6	+	+	−	+	−	−	+	+	−	+	+	+
7	+	−	+	+	−	−	+	−	−	−	+	+
8	+	+	+	+	−	−	−	−	+	−	+	−
9	+	−	−	−	+	−	+	−	−	+	+	−
10	+	+	−	−	+	−	−	−	+	+	+	+
11	+	−	+	−	+	−	−	+	+	−	+	+
12	−	+	+	−	+	−	+	+	−	−	+	−
13	+	−	−	+	+	−	+	+	+	−	−	−
14	+	+	−	+	+	−	−	+	−	−	−	+
15	+	−	+	+	+	−	−	−	−	+	−	+
16	+	+	+	+	+	−	+	−	+	+	−	−
17	+	−	−	−	−	+	−	+	−	−	+	+
18	+	+	−	−	−	+	+	+	+	−	+	−
19	+	−	+	−	−	+	+	−	+	+	+	−
20	+	+	+	−	−	+	−	−	−	+	+	+
21	+	−	−	+	−	+	−	−	+	+	−	+
22	+	+	−	+	−	+	+	−	−	+	−	−
23	+	−	+	+	−	+	+	+	−	−	−	−
24	+	+	+	+	−	+	−	+	+	−	−	+
25	+	−	−	−	+	+	+	+	−	+	−	+
26	+	+	−	−	+	+	−	+	+	+	−	−
27	+	−	+	−	+	+	−	−	+	−	−	−
28	+	+	+	−	+	+	+	−	−	−	−	+
29	+	−	−	+	+	+	+	−	+	−	+	+
30	+	+	−	+	+	+	−	−	−	−	+	−
31	+	−	+	+	+	+	−	+	−	+	+	−
32	+	+	+	+	+	+	−	+	+	+	+	+

Substituting $\chi_1 = -1$ into (C-25) results in a hydrocarbon reactivity index of R = 7449. Consequently, for this run the amount of reactive hydrocarbons (specified by χ_4 as a "low" value) is apportioned among the olefin, paraffin, aldehyde, and aromatic groupings so as to yield a mixture reactivity of R = 7449. Note that column I corresponds to the parameter estimate β_0 in Equation (C-15). With this 2^{11-6} design all main effects are unconfounded with two factor interactions. This is easily verified by forming the product of elements in any two columns and comparing the result with any third column. The product column and any third column will contain elements of opposite sign indicating that confounding does not occur.

The ability of the 2^{11-6} design to provide independent estimates of the eleven main effects is based upon a "foldover" feature of the design. Basically, the 32 rows in Table C-3 can be separated into two matrices that are mirror images of each other. That is, one matrix is merely the negative of the other. Considering one of the two matrices for the moment, with the 16 RPM simulations estimates of the main effects of the eleven variables can be made but they will be confounded with two factor and higher order interactions. However, identical confounding occurs with the other matrix. Thus if both of the 16 run matrices are used separately to estimate the parameters in Equation (C-22) it is then possible to subtract out the effects of the two factor and higher order interactions and obtain independent estimates of the eleven main effects. (The interested reader is referred to Box and Hunter (C-14) for a more complete discussion of foldover designs.)

From Table C-3, it can be shown that the main effects of variables 6, 7, 8, 9, 10 and 11 are confounded with the effects of three factor interactions in the following manner.

6 = 124
7 = 235
8 = 123
9 = 234
(10) = 345
(11) = 125

This can be determined in the same fashion that confounding between two factor interactions was checked.

In sum, confounding means that the "6" effect, an estimate of the parameter β_6 in Equation (C-15) is, in actuality, an estimate of $\beta_6 + \beta_{124} \pm$ higher order interactions. Likewise, the parameters corresponding to the two factor interactions in Equation (C-15), i.e. $\beta_{12}X_1X_2$, $\beta_{13}X_1X_3$, are also confounded with each other in the 2^{11-6} fraction factorial design. For completeness the two factor confounding patterns for a 2^{11-6} design are presented in Table C-4.

It should be pointed out that the confounding patterns can be intentionally chosen so that only those factors thought to be unimportant are confounded with the important factors. However, in the present situation with eleven variables it is very difficult to construct optimum confounding relationships.

SCREENING EXPERIMENT

Based on the 2^{11-6} fractional design, thirty-two RPM simulations were carried out. The predicted ozone concentrations after six hours are listed in Table C-5.

To estimate the magnitude of the main effects of variables $X_1 \ldots X_{11}$ and the two-factor interaction patterns $P_1 \ldots P_{15}$, the algorithm outlined by Box and Hunter (C-14) was used. The estimate of the main effect of variable X_1 is obtained by taking the sum of products between the elements of the observation vector

$$\vec{y} = \begin{bmatrix} y_1 \\ y_2 \\ \vdots \\ y_{32} \end{bmatrix}$$

and the corresponding elements of column i in the design matrix (Table C-3) and dividing this product by N/2 where N = 32. Mathematically,

$$\text{Effect}_i = \frac{2}{N} \sum_{j=1}^{N} y_i X_{ij} \qquad \text{(C-26)}$$

To estimate the magnitude of two factor interaction effects, the following formula was used.

Table C-4

TWO-FACTOR CONFOUNDING PATTERN FOR A 2^{11-6} FRACTIONAL FACTORIAL DESIGN

Pattern	Confounding Relationship
P_1	$X_1X_2 + X_4X_6 + X_3X_8 + X_5X_{11}$
P_2	$X_1X_3 + X_2X_8 + X_6X_9 + X_7X_{11}$
P_3	$X_1X_4 + X_2X_6 + X_8X_9$
P_4	$X_1X_5 + X_2X_{11} + X_7X_8$
P_5	$X_1X_6 + X_2X_4 + X_3X_9 + X_7X_{10}$
P_6	$X_1X_7 + X_5X_8 + X_3X_{11} + X_6X_{10}$
P_7	$X_1X_8 + X_2X_3 + X_5X_7 + X_4X_9$
P_8	$X_1X_9 + X_3X_6 + X_4X_8 + X_{10}X_{11}$
P_9	$X_1X_{10} + X_9X_{11} + X_6X_7$
P_{10}	$X_1X_{11} + X_2X_5 + X_3X_7 + X_9X_{10}$
P_{11}	$X_2X_7 + X_3X_5 + X_4X_{10} + X_8X_{11}$
P_{12}	$X_2X_9 + X_3X_4 + X_5X_{10} + X_6X_8$
P_{13}	$X_2X_{10} + X_4X_7 + X_5X_9$
P_{14}	$X_3X_{10} + X_4X_5 + X_6X_{11} + X_7X_9$
P_{15}	$X_4X_{11} + X_5X_6 + X_8X_{10}$

Table C-5

PREDICTED RPM OZONE CONCENTRATIONS
AFTER A SIX-HOUR SIMULATION

Run No.*	Ozone Concentration (ppm)
y_1	0.083
y_2	0.080
y_3	0.135
y_4	0.122
y_5	0.116
y_6	0.113
y_7	0.122
y_8	0.102
y_9	0.097
y_{10}	0.099
y_{11}	0.115
y_{12}	0.129
y_{13}	0.140
y_{14}	0.135
y_{15}	0.132
y_{16}	0.121
y_{17}	0.105
y_{18}	0.095
y_{19}	0.101
y_{20}	0.102
y_{21}	0.089
y_{22}	0.084
y_{23}	0.129
y_{24}	0.119
y_{25}	0.123
y_{26}	0.117
y_{27}	0.115
y_{28}	0.112
y_{29}	0.097
y_{30}	0.101
y_{31}	0.148
y_{32}	0.140

---

[*] The run number corresponds to the variable settings identified in Table C-3.

$$\text{Effect}_{mn} = \frac{2}{N} \sum_{j=1}^{N} y_j \chi_{mj} \chi_{nj} \qquad \text{(C-27)}$$

where χ_{mj} and χ_{nj} represent the columns of pluses and minuses associated with variables χ_m and χ_n in Table C-3.

From inspection of the design matrix in Table C-3, it is clear that application of Equation (C-27) to variables $\chi_1\chi_2$ yields the same two factor interaction estimate as the estimates for $\chi_4\chi_6$, $\chi_3\chi_8$, and $\chi_5\chi_{11}$. Thus, the effects of the foregoing two factor interactions are confounded. To determine the magnitude of the effects of the collective interactions (given by patterns P_1, P_2 ... P_{15}), Equation (C-27) was applied to the two factor interaction patterns in Table C-4. The results of these computations, as well as the estimates of the main effects of the eleven variables computed from Equation (C-26), are listed in Table C-6. These results are presented in descending order of magnitude.

Qualitatively, the magnitude of each effect is related to the degree to which that effect can "explain" the predicted RPM ozone concentration. From Equation C-5, it would appear at first glance that k_1 and background ozone, reactive hydrocarbon, and nitrogen oxides concentrations are most significant with respect to predicted plume ozone levels. To investigate this possibility further, the half-normal plot in Figure C-2 was constructed. The interpretation of Figure C-2 was that the estimated effects of the four outlying variables do not possess the same distributional form as the others and that they should be investigated further, separate from the remaining seven. We expand upon this analysis of Figure C-2 briefly.

The general use of half-normal plots in analyzing two-level factorial experiments was first introduced by Daniel(C-15). Here we are concerned only with half-normal plots as applied to two-level fractional factorial designs. In particular, we wish to use half-normal plots as an aid in determining which (if any) of the estimates of main effects and two factor interactions given in Table (C-4) represent real effects and which ones are either spurious, or within the level of uncertainty (noise level) of the computer simulations.

Table C-6

MAIN EFFECT AND TWO-FACTOR INTERACTION ESTIMATES FOR A 2^{11-6} FRACTIONAL FACTORIAL DESIGN

Main Effects Or Two-Factor Inter-Action Pattern*	Magnitude of Effect
X_7 - k_1	21.62
X_2 - O_3	16.0
X_4 - RHC	15.62
X_3 - bNO_x	9.25
X_8 - W	-4.38
X_5 - P	-4.13
P_{11}	-4.13
P_{10}	3.88
X_1 - R	-3.38
X_{10} - T	-3.25
X_9 - pNO_x	3.13
P_9	3.13
P_3	3.0
P_2	-2.88
P_{12}	2.88
P_5	-1.88
P_{15}	-1.88
X_{11} - SO_2	-1.25
P_4	-1.25
P_{13}	1.25
P_8	-1.00
P_{14}	1.08
P_1	0.88
P_6	0.50
P_7	-0.25
X_6 - U	0.0

---

*The two factor interaction patterns are identified in Table C-2.

The fact that some estimated effects *(estimates)* resulting from a two-level factorial analysis are large compared with others, does not, of itself, mean that real effects actually exist. Even in *null experiments*, i.e., experiments on factors which have no real effects, it will often be found that the largest estimate evaluated is several times larger than the average level of all the estimates. When the estimates are judged on the basis of size alone therefore, there is a distinct possibility that what is merely a large error may be wrongly thought to be a real effect. What is needed in such situations is a way of deciding whether large estimates are measures of real effects or are just large errors.

When the estimates of main effects in Table C-6 are plotted on half-normal paper (Figure B-2) most of them lie on a line passing through the origin; four do not. Unless most of the effects are real, the smaller estimates in a half-normal plot should "point towards the origin." This is because the smaller estimates are usually estimates of experimental error (or in the present situation, model uncertainties) and should lie on some theoretical half-normal line passing through the origin. If the smaller effects do not cluster about such a line this suggests that most of the effects are real, in which case the experiment is far from null, and half-normal plotting is not of value in variable screening.

However, if some of the larger estimates are due to real effects this is usually quite clear because these estimates will not be close to the line but will fall below and off to the right of it. This is, in fact, observed in Figure B-2. This behavior suggests that the main effects of the four outliers--k_1, bNO_x, RHC, and O_3--are real, and that the remaining seven main effects are representative of normally distributed random errors$^{(C-15)}$. The conclusion that the remaining seven effects are really no different from an error distribution does not mean that they have no influence on RPM predictions. It is possible that some of the variable ranges selected may have been too narrow to permit a noticeable main effect. In this regard, the hydrocarbon reactivity index is one possibility. But based upon the present results, the main effects of the four outliers appear to be real while the others do not. This conclusion, then, is the basis for the more detailed examination of the four variables that we describe next.

ANALYSIS OF FOUR VARIABLES

The sensitivity study was redirected to consider four variables--k_1, bNO_x, RHC, and O_3--in greater detail, including a closer examination of the effects of variable interactions. Because some of the two factor interaction patterns in Table C-6 have larger estimated effects than the main effects of certain variables alone, an analysis of the interaction among the four variables was deemed worthwhile. Thus, to investigate variable interactions, Equation (B-6), was selected as a tentative response function because it includes all possible first order combinations of the variables X_2, X_3, X_4, X_7.

Having selected a tentative model equation, the next step involved the specification of an appropriate simulation plan. To evaluate the coefficients of Equation (B-6), a minimum of 2^4 or 16 computer runs was required. In reviewing the 2^{11-6} design in Table C-1, it became apparent that by rearranging the 32 rows in a specific manner, two complete, and identical 2^4 factorial designs could be obtained. This fortuitous result meant that:

- It would not be necessary to perform additional RPM simulations; advantage could be taken of the previous computer runs.
- With two separate designs it would be possible to estimate the errors associated with the elimination of the other seven variables from consideration.

The only difference between the two 2^4 designs is that the variable settings are different for the seven variables eliminated from further study. In other words, the original 32 computer runs can be rearranged into sixteen pairs where the variable settings for X_2, X_3, X_4, and X_7 of each pair are the same, but that the settings for the remaining seven variables are not. This circumstance permits an evaluation of the effect of considering only four of the original eleven variables.

In Table C-7 the pair of 2^4 factorial designs is presented. The original run numbers corresponding to the 2^{11-6} design matrix in Table C-3 are given in column (1). The variable settings for the main effects are presented in columns (2) to (5); the corresponding two, three, and four factor interactions, in columns (6) to (16) are determined by multiplying the appropriate plus and minus sign in columns (2) to (5). The original RPM predictions are given in column (17), and in column (18) the mean value of each pair of runs is given.

Table C-7

THE 2^4 FACTORIAL DESIGN MATRIX WITH ESTIMATED STANDARD DEVIATIONS

Run No.	Main Effects				Two-Factor Interactions						Three Factor Interactions				Four Factor Interaction	y_i	Mean y_i	Standard Deviation S_i
	2	3	4	7	23	24	27	34	37	47	234	237	247	347	2347	(ppb)	(ppb)	(ppb)
(1)	(2)	(3)	(4)	(5)	(6)	(7)	(8)	(9)	(10)	(11)	(12)	(13)	(14)	(15)	(16)	(17)	(18)	(19)
y_{16}	-	-	-	-	+	+	+	+	+	+	-	-	-	-	+	89.	84.5	6.36
y_{31}	-	-	-	-	+	+	+	+	+	+	-	-	-	-	+	80.		
y_{22}	+	-	-	-	-	-	-	+	+	+	+	+	+	-	-	101.	101.5	0.71
y_8	+	-	-	-	-	-	-	+	+	+	+	+	+	-	-	102.		
y_{19}	-	+	-	-	-	+	+	-	-	+	+	+	-	+	-	89.	86.5	3.54
y_4	-	+	-	-	-	+	+	-	-	+	+	+	-	+	-	84.		
y_7	+	+	-	-	+	-	-	-	-	+	-	-	+	+	+	112.	107.0	7.07
y_{29}	+	+	-	-	+	-	-	-	-	+	-	-	+	+	+	102.		
y_{18}	-	-	+	-	+	-	+	-	+	-	+	-	+	+	-	97.	98.0	1.41
y_9	-	-	+	-	+	-	+	-	+	-	+	-	+	+	-	99.		
y_5	+	-	+	-	-	+	-	-	+	-	-	+	-	+	+	115.	113.5	2.12
y_{26}	+	-	+	-	-	+	-	-	+	-	-	+	-	+	+	112.		
y_{14}	-	+	+	-	-	-	+	+	-	-	-	+	+	-	+	97.	99.0	2.83
y_{27}	-	+	+	-	-	-	+	+	-	-	-	+	+	-	+	101.		
y_{28}	+	+	+	-	+	+	-	+	-	-	+	-	-	-	-	132.	126.5	7.78
y_1	+	+	+	-	+	+	-	+	-	-	+	-	-	-	-	121.		
y_{17}	-	-	-	+	+	+	-	+	-	-	-	+	+	+	-	103.	98.0	7.07
y_{12}	-	-	-	+	+	+	-	+	-	-	-	+	+	+	-	93.		
y_{11}	+	-	-	+	-	-	+	+	-	-	+	-	-	+	+	125.	123.5	2.12
y_{30}	+	-	-	+	-	-	+	+	-	-	+	-	-	+	+	122.		
y_{10}	-	+	-	+	-	+	-	-	+	-	+	-	+	-	+	118.	115.5	3.54
y_{21}	-	+	-	+	-	+	-	-	+	-	+	-	+	-	+	113.		
y_{25}	+	+	-	+	+	-	+	-	+	-	-	+	-	-	-	129.	124.0	7.07
y_2	+	+	-	+	+	-	+	-	+	-	-	+	-	-	-	119.		
y_{13}	-	-	+	+	+	-	-	-	-	+	+	+	-	-	+	123.	120.0	4.23
y_{23}	-	-	+	+	+	-	-	-	-	+	+	+	-	-	+	117.		
y_{20}	+	-	+	+	-	+	+	-	-	+	-	-	+	-	-	115.	127.0	16.97
y_3	+	-	+	+	-	+	+	-	-	+	-	-	+	-	-	139.		
y_{24}	-	+	+	+	-	-	-	+	+	+	-	-	-	+	-	140.	137.5	3.54
y_6	-	+	+	+	-	-	-	+	+	+	-	-	-	+	-	135.		
y_{15}	+	+	+	+	+	+	+	+	+	+	+	+	+	+	+	148.	144.0	5.66
y_{32}	+	+	+	+	+	+	+	+	+	+	+	+	+	+	+	140.		

To quantify the uncertainties involved with deleting the seven variables, variances and standard deviations of each pair of simulation results were computed. Then the sixteen variance estimates were combined to provide a pooled standard deviation of 0.006 ppm for the entire set of 32 computer simulations. This result suggests that the uncertainties involved in eliminating the seven variables from the response function are smaller than the uncertainties inherent in RPM's prediction of ozone concentrations.

Because the evaluation of the response function based on the 2^4 design, computation of model sensitivities, and discussion of the results are presented in Appendix B we do not repeat that discussion here. Instead, we consider ways in which the present study can be improved by further experimentation.

Additional Sensitivity Analyses

In identifying how the present sensitivity study methodology can be extended it is useful at this point to comment on the rationale behind the selection of the variable ranges chosen in Table B-1. Suppose that RPM ozone predictions were a function of only one variable, and further, that the response could be graphically described by curve number 1 in Figure C-1.

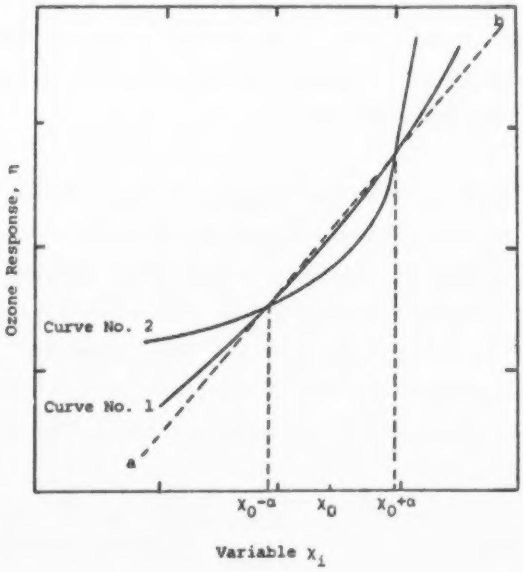

Figure C-1. Hypothetical RPM Response as a Function of One Variable

Within the range of $\alpha=\pm1$ RPM's response might be approximated well by a linear response function as indicated by the Line a-b. Beyond $\alpha=\pm1$, the linear approximation would begin to fail. However, if curve number 2 represented the true RPM response, then interpolation between the two observational points $\alpha=\pm1$ and extrapolation beyond them will be seriously in error. Thus, depending upon the nature of RPM's response to variations in the variable space, a linear approximation may or may not be appropriate.

In the present sensitivity study, there was no reason to believe that the RPM ozone response function is linear in all eleven variables throughout the entire variable space. Consequently, in prescribing the high and low ranges for each variable, it was necessary to ensure that if the tentative response function proved inadequate due to quadratic effects, experimental points beyond $\alpha=\pm1$ could be chosen that met the following criteria.

- The expanded range was still within physical reality.
- The expanded range was not so great as to unduly stress RPM's predictive capability.

An additional consideration involves the nature of fractional factorial designs. Inasmuch as the magnitude of the variable interactions tend to decrease relative to main effects as the variable range is decreased, a narrower range might lead to a better separation between main effects and factor interactions. However, as the range decreases, so does the magnitude of all of the effects*, so that eventually the effects are of the same order of magnitude as experimental error (or in this case, the uncertainties in RPM). Thus, a tradeoff exists between variable range and the ability to resolve main effects from confounding interactions.

With these considerations in mind the ranges cited in Table B-3 were chosen. While they certainly do not reflect extreme conditions (note that these ranges are contained within the typical ranges given in Table B-1) they are sufficiently wide to enable an inspection of RPM sensitivity over practical range of conditions. It is evident from the good agreement in Table B-6 between the response function and RPM predictions within the region of space defined by $\alpha=\pm1.4$ that the first order model given by Equation C-16 is quite satisfactory. Beyond $\alpha=\pm1.4$, the agreement begins to deteriorate.

---

*From Equations (C-26) and (C-27) it is apparent that as the range of the input variables decreases, so will the range in predicted RPM responses y_i.

If, in the future, one is interested in extending the range over which the response function is suitable (and hence in extending the range over which RPM sensitivities are known), additional terms will have to be retained in the Taylor Series expansion. In particular, second order (quadratic) effects may be important beyond $\alpha = \pm1.4$.

If an expanded domain in variable space were to be considered, a new simulation would have to be structured so as to accommodate the search for quadratic and higher order effects. (A summarization of second and third order designs that address this problem is given by Hill and Hunter$^{(C-16)}$.) With judicial selection of appropriate fractional factorial designs, the results of individual fractional experiments may be reviewed sequentially and used to redirect further experimentation. This would enable one to explore the regions beyond $\alpha=\pm1.4$ and to progressively determine a more suitable form for the RPM response function. If a more general function were determined, then the sensitivities obtained from it would reflect RPM sensitivities to a wider range of model inputs than is currently possible with Equation (B-6). Because the potential for ozone appears to be more closely associated with extreme conditions in a variable's range rather than the more common values, continued sensitivity analysis may shed further light on those conditions under which ozone formation might occur in a power plant plume.

REFERENCES

C-1 Wilson, K. W., Doyle, G. J., "Investigation of Organic Solvents," Final Report, EPA Contract CPA 22-69-125, September (1970).

C-2 Levey, A., Miller, S. E., and Scofield, F., "The Photochemical Smog Reactivity of Solvents," in "Proceedings of the Second International Clean Air Congress," H. M. Englund and W. T. Berry (eds.), Academic Press, New York, 1971.

C-3 Jackson, M. W. (1963), "Effects of Some Engine Variables and Control Systems on Composition and Reactivity of Exhaust Hydrocarbons," SAE Prog. in Technol., Vehicle Emissions, Vol. 12, Part II (Selected SAE Papers, 1963-1966), pp. 241-267 (1967).

C-4 Hecht, T. A., et al., "Mathematical Simulation of Smog Chamber Photochemical Experiments," Report R74-9, Systems Applications, Incorporated, San Rafael, California, November 1974.

C-5 Mayrsohn, H., et al., "Atmospheric Hydrocarbon Concentrations: June-September, 1974," State of California Air Resources Board, April 1975.

C-6 Bowne, N. E. (1974), "Diffusion Rates," J. Air Poll. Control Assoc., Vol. 24, No. 9.

C-7 Wark. K., Thermodynamics, McGraw-Hill Book Co., New York, New York, (1966) pg. 337.

C-8 Klauber, G., "Airborne Field Study of Power Plant Plumes: O_3, NO_x, and SO_2 Chemistry," Ph. D. Dissertation, The John Hopkins University, 1975.

C-9 Draper, N. and Smith, H., Applied Regression Analysis, John Wiley and Sons, Inc., New York, New York, January 1967.

C-10 Bard, Y., Nonlinear Parameter Estimation, Academic Press, New York, New York, 1974.

C-11 Hunter, W. G., and Hoff, M. E., (1967), "Planning Experiments to Increase Research Efficiency," Industrial and Engineering Chemistry, Vol. 59, No. 3.

C-12 Hunter, J. S., (1960), "Some Applications of Statistics to Experimentation," Chemical Engineering Program Symposium Series 56, No. 31, p. 10.

C-13 Davies, O. L., The Design and Analysis of Industrial Experiments, Hafner Publishing Company, New York, (1960).

C-14 Box, G. E. P., and Hunter, J. S., (1961), "The 2^{K-P} Fractional Factorial Designs, Part 1," Technometrics, Vol. 3, No. 3.

C-15 Daniel, C., "Use of Half-Normal Plots in Interpreting Factorial Two-Level Experiments," Technometrics, Vol. 1, No. 4, November 1959.

C-16 Hill, W. J., and Hunter, W. G., "A Review of Response Surface Methodology: A Literative Survey," Technometrics, Vol. 8, No. 4, November 1966.

GLOSSARY FOR APPENDIX C

Confounding--In a complete factorial design all of the main effects and interactions are estimated independently. However, in a fractional factorial design, in which only a part of the complete factorial design is carried out, the number of effects which can be estimated independently is correspondingly smaller. In this case, the estimate of a main effect is derived in the same manner as certain interactions. These estimates are identical and indistinguishable. It is in this sense that main effects and factor interactions are said to be confounded.

Confounding Pattern--This is merely an identification of those main effects and factor interactions that are mutually confounded.

Design Matrix--A convenient mathematical expression containing the basic features of the simulation plan, i.e., the variation and range of each of the factors under consideration and the nature of the response function tentatively entertained.

Estimate--The numerical value of a main effect or factor interaction.

Simulation Plan--A formalized set of procedures which dictate the manner in which a series of experiments is to be conducted. For each experiment, the plan prescribes the value each factor is to assume.

Factor--Quantities commonly referred to as variables or parameters that are responsible for changes in RPM predictions. Factors might include such things as wind speed, temperature, activation energies, etc.

Factorially Designed Experiments--A factorial experiment studies the effect on some observable quantity (e.g. ozone concentrations) of varying two or more factors, such as wind speed, temperature, hydrocarbon concentrations, etc. A series of values or levels of each factor is chosen, and certain combinations of the levels of the factors are investigated with respect to the observed quantity. The particular combinations of the factor levels chosen and the order in which they are tested is prescribed by the experimental design. In a complete factorial design all combinations of all levels of all the factors are tested. In a two-level factorial design, the factors take on only "high" or "low" values.

Fractional Factorial Design--A simulation plan in which only a fraction of a complete factorial is run.

Interaction--An interaction between two factors means that a change in response between levels of one factor is not the same for all levels of the other factor.

k-dimensional space--A variable space defined by k variables.

Main Effect--The difference between the means of the observed quantity (the response) for all levels of one factor, averaged over all levels of the other factor.

Multivariate--With respect to analytic functions, multivariate means that the function is expressed in terms of a number of independent variables.

Null Experiment--An experiment in which the factors investigated have no influence whatever upon the system or model response.

Parameter Estimates--Estimates of the coefficients associated with the factors in the response function based upon least squares or nonlinear parameter estimation techniques.

Response--The numerical result of an observation made with a particular combination of factor (or variable) settings.

Response Function--An analytic relationship between an observed response and two or more factors that determine the magnitude of the response. Because the true or precise relationship between response and factors is never known, the response function represents an approximation to the unknown function.

Response Surface--The surface in k-dimensional space (where k equals the number of factors) generated by evaluation of the response function for every conceivable combination of the values of the factors.

Replicate--The repetition of an experiment or procedure.

Sensitivity--A measure of the magnitude of the response of a system or model to changes in the magnitude of any one of the input variables or factors. Sensitivities may be computed by computing the partial derivatives of the response function with respect to the various factors.

Setting--The particular value of a factor (a variable or parameter) within its range that is used for a given experiment.

Two Factor Interactions--Interactions among two factors. (See Interactions.)

Variable Space--The conceptual region defined by the ranges of the various factors. For example, two-dimensional space might be characterized by a flat surface; three-dimensional space is contained within a cube. If temperature were a fourth variable, the three-dimensional geometry and spatial temperature field would characterize four-dimensional space. If the temperature field varied with time--a fifth variable--five-dimensional variable space can be envisioned.